

AN ABSTRACT OF THE DISSERTATION OF

Timothy E. Link for the degree of Doctor of Philosophy in Environmental Sciences presented on October 2, 2001. Title: The Water and Energy Dynamics of an Old-Growth Seasonal Temperate Rainforest.

Redacted for Privacy

Abstract approved:


Michael H. Unsworth / Danny Marks

In the Pacific Northwest (PNW), concern about the impacts of climate and land cover change on water resources, flood-generating processes, and ecosystem dynamics emphasize the need for a mechanistic understanding of the interactions between forest canopies and hydrological processes. A detailed measurement and modeling program during the 1999 and 2000 hydrologic years characterized hydrological conditions and processes in a 500-600 year old Douglas fir-western hemlock seasonal temperate rainforest. The measurement program included sub-canopy arrays of radiometers, tipping bucket rain gauges, and soil temperature and moisture probes, to supplement a vertical temperature and humidity profile within the forest canopy. Analysis of the precipitation interception characteristics of the canopy indicated that the mean direct throughfall proportion was 0.36, and the mean saturation storage was 3.3 mm. Evaporation from small storms insufficient to saturate the canopy comprised 19% of the net interception loss, and canopy drying and evaporation during rainfall accounted for 47% and 33% of the net loss, respectively. Results of the measurement program were used to modify the Simultaneous Heat and Water (SHAW) model for forested systems. Changes to the model include improved representation of interception dynamics, stomatal conductance, and within-canopy energy transfer processes. The

model effectively simulated canopy air and vapor density profiles, snowcover processes, throughfall, soil water content profiles, shallow soil temperatures, and transpiration fluxes for both a calibration period and for an uncalibrated year. Soil warming at bare locations was delayed until most of the snowcover ablated due to the large heat sink associated with the residual snow patches. During the summer, simulated evapotranspiration decreased from a maximum monthly mean of 2.17 mm day⁻¹ in July to 1.34 mm day⁻¹ in September, as a result of declining soil moisture and net radiation. Our results indicate that a relatively simple parameterization of the SHAW model for the vegetation canopy can accurately simulate seasonal hydrologic fluxes in this environment. Application and validation of the model in other forest systems will establish similarities and differences in the interactions of vegetation and hydrology, and assess the sensitivity of other systems to natural and anthropogenic perturbations.

© Copyright by Timothy E. Link
October 2, 2001
All Rights Reserved

The Water and Energy Dynamics of an Old-Growth Seasonal Temperate Rainforest

by
Timothy E. Link

A DISSERTATION

submitted to

Oregon State University

in partial fulfillment of
the requirements for the
degree of

Doctor of Philosophy

Presented October 2, 2001
Commencement June 2002

Doctor of Philosophy dissertation of Timothy E. Link presented on October 2, 2001.

APPROVED:

Redacted for Privacy

Co-Major Professor, representing Environmental Sciences

Redacted for Privacy

Co-Major Professor, representing Environmental Sciences

Redacted for Privacy

Head of Environmental Sciences Program

Redacted for Privacy

Dean of the Graduate School

I understand that my thesis will become part of the permanent collection of Oregon State University libraries. My signature below authorizes release of my thesis to any reader upon request.

Redacted for Privacy

Timothy E. Link, Author

ACKNOWLEDGEMENTS

Support for this research was provided by the Western Regional Center (WESTGEC) of the National Institute for Global Environmental Change (NIGEC), the U. S. Forest Service (USFS), and the Agricultural Research Service (ARS), Northwest Watershed Research Center. I am particularly grateful to the U. S. Environmental Protection Agency (USEPA), Western Ecology Division who provided office and computing facilities for the duration of this research.

I would like to thank Richard Cuenca, Larry Boersma, and Dan Luoma, for comments on the draft of this dissertation. I am particularly indebted to Mike Unsworth, Danny Marks, and Gerald Flerchinger for unsurpassed academic guidance, moral support, and for their extensive comments during the preparation of this manuscript. Shaun Kelly, Mark Seyfried, and John Selker were extremely helpful, and provided many valuable suggestions on the field component of this research. Mark Murdock, Dan Golub, and Richard Keim all deserve a special thanks for field assistance. In particular, thanks are due to Mark Van Scoy who helped out in frequently cold and soggy conditions, and who always made the extra effort in the most inclement conditions to collect high-quality data. The WRCCRF staff, Tom King, Trevor Newton, Dave Braun, Dave Shaw, Mark Creighton, Annie Hamilton, and Ken Bible kept the onsite activities running smoothly during the past three years.

Many thanks to a dear friend of the family, Elizabeth Thatcher who provided encouragement and support through all the years of my educational endeavors. The extended Kammerzell family, Sam, Oliver, Kip, and Quixote provided undying moral

support and were always a willing to listen to the finer details of hydrologic science.

To my parents, Kathy Gerlach Link and James Link, I owe you the most for your continued support, encouragement and faith, and for understanding why I've been home so few times over the past six years. Finally, I am the most deeply indebted to Sharyl Kammerzell for her love, understanding, and willingness to endure this extended graduate school career.

CONTRIBUTION OF AUTHORS

Drs. Mike Unsworth and Danny Marks provided extensive comments and suggestions for manuscripts that comprise Chapters 2, 3, and 4. Dr. Gerald Flerchinger assisted with the modifications to the SHAW model presented in Chapter 4, and provided many helpful suggestions for the improvement of the associated manuscript.

TABLE OF CONTENTS

	<u>Page</u>
1. INTRODUCTION	1
1.1 Water Resources and Climate.....	3
1.2 Land Management and Hydrology	5
1.3 Interaction of Water and Carbon Dynamics	6
1.4 Role of Intensive Measurements and Model Development.....	7
1.5 Dissertation Structure	10
2. CANOPY CHARACTERISTICS AND CLIMATE CONDITIONS AT THE WIND RIVER CANOPY CRANE RESEARCH FACILITY, CARSON WASHINGTON, 1998-2000	12
2.1 Abstract.....	13
2.2 Introduction.....	14
2.3 Methods	17
2.3.1 Site Description.....	17
2.3.2 Data Collection	21
2.4 Results and Discussion	30
2.4.1 Climate.....	30
2.4.2 Hydrology and Soil Conditions	46
2.5 Conclusions.....	53
2.6 Acknowledgements.....	54
3. THE INTERCEPTION DYNAMICS OF A SEASONAL TEMPERATE RAINFOREST	55
3.1 Abstract.....	56
3.2 Introduction.....	57

TABLE OF CONTENTS (CONTINUED)

	<u>Page</u>
3.3 Methods and Materials.....	62
3.3.1 Site Description.....	62
3.3.2 Throughfall Measurements	65
3.3.3 Meteorological Data Collection.....	66
3.3.4 Methods for Calculation of Interception Parameters.....	67
3.3.5 The Gash Analytical Model.....	72
3.4 Results and Discussion	75
3.4.1 During Event Climate and Precipitation Variability.....	75
3.4.2 Throughfall and Interception Loss.....	80
3.4.3 Canopy Interception Parameters.....	85
3.5 Testing a Simple Analytical Model	92
3.5.1 Model Application	92
3.5.2 Model Results and Discussion.....	93
3.6 Conclusions.....	97
3.7 Acknowledgements.....	98
4. SIMULATION OF WATER AND ENERGY FLUXES IN AN OLD GROWTH SEASONAL TEMPERATE RAINFOREST USING THE SIMULTANEOUS HEAT AND WATER (SHAW) MODEL.....	99
4.1 Abstract.....	100
4.2 Introduction.....	101
4.3 Methods	104
4.3.1 Site Description.....	104
4.3.2 Data Collection and Instrumentation	106
4.3.3 SHAW Model Developments	111
4.3.4 Model Parameterization.....	118
4.4 Results and Discussion	125
4.4.1 Within Canopy Air Temperature and Vapor Density	125
4.4.2 Snow Processes.....	128

TABLE OF CONTENTS (CONTINUED)

	<u>Page</u>
4.4.3 Soil Water Content.....	129
4.4.4 Soil Temperature.....	134
4.4.5 Evaporation and Transpiration.....	136
4.4.6 Simulated Energy and Water Fluxes	141
4.5 Summary and Conclusions	145
4.6 Acknowledgements.....	146
5. CONCLUSIONS.....	148
5.1 Summary	148
5.2 Future Directions	152
BIBLIOGRAPHY	158

LIST OF FIGURES

<u>Figure</u>	<u>Page</u>
1.1. Distribution of Douglas fir in the U. S.....	9
2.1. Location of the T. T. Munger Research Natural Area and the Wind River Canopy Crane Research Facility (WRCCRF).	18
2.2. Location of climate and soil monitoring equipment at the WRCCRF.....	20
2.3. Mean climate conditions at OPENSTA, STA70 and STA02, 1998 - 2000.	31
2.4. Comparison of hy 1999 and hy 2000 temperature and precipitation to long-term means.....	34
2.5. Air temperature differences between the WRCCRF climate stations.	39
2.6. Above- and below-canopy solar and thermal radiation.	44
2.7. Precipitation intensity, snow depth, soil moisture, water table elevation and streamflow at WRCCRF, hy1999 - 2000.	47
2.8. Spatial variation in 0-40 cm soil moisture at the WRCCRF.....	49
2.9. Temporal variation of soil water content profiles during the summer drydown period, hy2000.	50
3.1. Schematic throughfall sampling scheme. 1 tipping bucket precipitation gauge was randomly located within each 25 m quadrat. The diameter of the 2.3 ha crane circle is 200 m.....	66
3.2. Example event plot of data used to determine canopy direct throughfall proportion and saturation storage capacity.. Linear regressions are fit to a scatterplot of throughfall versus gross precipitation, by optimizing the fit of equations (3.1) and (3.2).....	68
3.3. Canopy saturation storage capacity estimated using the minimum method.	70
3.4. Detailed meteorological data for a precipitation event with low evaporation (Event 30).....	76
3.5. Detailed meteorological data for a precipitation event with relatively high evaporation (event 15).	77

LIST OF FIGURES (CONTINUED)

<u>Figure</u>	<u>Page</u>
3.6. Frequency distribution of the gauge catch expressed as a percentage of the gross rainfall, for all events exceeding 10 mm.	84
3.7. Frequency distribution of the direct throughfall proportion computed for all events.	86
3.8. Temporal variation in the canopy saturation storage capacity. Error bars are determined by propagation errors associated with the parameters p , P_s , and E/R , determined by the optimization technique.	88
3.9. Variability of canopy saturation storage capacity within the WRCCRF crane circle.	90
4.1. Conceptual diagram of the Simultaneous Heat and Water (SHAW) model.....	112
4.2. Scatterplot of relative canopy conductance vs. vapor pressure deficit. Individual data points were derived from EC measurements of total ecosystem water flux. The solid line is a plot of (4.2).	116
4.3. Measured and modeled within canopy air temperature profiles. Data are from a diurnal cycle during cloudless midsummer conditions.	126
4.4. Measured and modeled 0-30 cm soil water content.....	130
4.5. Measured and modeled deep soil water content.	131
4.6. Measured and modeled 15 cm soil temperature trends.....	135
4.7. Measured and simulated ensemble-averaged ecosystem water flux.....	138

LIST OF TABLES

<u>Table</u>	<u>Page</u>
2.1. WRCCRF instrumentation summary.....	22
2.2. Potential evapotranspiration computation results	42
3.1. Literature values of conifer canopy storage capacities (<i>S</i>)	59
3.2. WRCCRF mean climate conditions, 1999 and 2000.....	64
3.3. Precipitation and interception summary	81
3.4. Detailed interception summary, 2000	82
3.5. Saturation storage derivation.	87
3.6. Gash analytical model performance.....	94
4.1. Model driving data hierarchy.....	110
4.2. SHAW model parameterization.....	119
4.3. Measured and modeled snowcover variables, 2000	129
4.4. Model fitting statistics.....	133
4.5. Throughfall and interception summary.....	137
4.6. Mean daily evapotranspiration results.	140
4.7. Simulated mean monthly energy flux summary.	142
4.8. SHAW monthly water flux summary	143
5.1. Summary of the predicted changes in temperature and precipitation in the PNW, year 2025.....	155

LIST OF NOTATION

E	Evaporation rate (mm hr^{-1})
E_s	Evaporation rate when canopy is saturated (mm hr^{-1})
E_t	Transpiration rate (mm hr^{-1})
E_t'	Transpiration rate corrected for energy-balance closure (mm hr^{-1})
E/R	Ratio of evaporation to rainfall under saturated canopy conditions (dimensionless)
G	Soil heat flux (W m^{-2})
H	Sensible heat flux (W m^{-2})
I_{net}	Net interception loss (mm)
I_c	Interception loss during canopy wetting for $P_G < P_s$ (mm)
I_w	Interception loss during canopy wetting for events $P_G \geq P_s$ (mm)
I_s	Interception loss during saturated canopy conditions (mm)
I_a	Interception loss during canopy drying (mm)
K_{sat}	Saturated hydraulic conductivity (m s^{-1})
P_G	Gross precipitation (mm)
P_s	Precipitation required to saturate the canopy (mm)
P_N	Net throughfall (mm)
R_L	Thermal ($3.5\text{--}100\ \mu\text{m}$) radiation (W m^{-2})
R_n	Net radiation (W m^{-2})
R_s	Solar ($0.28\text{--}3.5\ \mu\text{m}$) radiation (W m^{-2})
S	Saturation storage of the canopy (mm)
S_c	Saturation storage per unit leaf area (mm m^{-2})
S_o	Above-canopy solar radiation (W m^{-2})
S_f	Below-canopy solar radiation (W m^{-2})
T_a	Air temperature ($^{\circ}\text{C}$)
T_c	Canopy temperature ($^{\circ}\text{C}$)
T_g	Soil temperature ($^{\circ}\text{C}$)
T_L	Adiabatic lapse rate ($9.8\ ^{\circ}\text{C km}^{-1}$)
T_l	Leaf temperature ($^{\circ}\text{C}$)
c_p	Specific heat of air ($\text{J kg}^{-1}\ \text{K}^{-1}$)
d	Zero plane displacement (m)
$g_{a,H}$	Aerodynamic conductance for heat (m s^{-1})
g_{am}	Aerodynamic conductance for momentum (m s^{-1})
g_{aw}	Aerodynamic conductance for water vapor (m s^{-1})
g_c	Canopy conductance (m s^{-1})
g_s	Stomatal conductance (m s^{-1})
k	Von Kármán constant (0.4, dimensionless)
p	Direct throughfall proportion (dimensionless)
p_t	Proportion of precipitation diverted to stemflow (dimensionless)
u	Wind velocity (m s^{-1})

LIST OF NOTATION (CONTINUED)

u^*	Friction velocity (m s^{-1})
u_{dir}	Wind direction ($^\circ$)
u_{max}	Maximum wind velocity (m s^{-1})
z_c	Canopy height (m)
z_s	Sensor measurement height (m)
$z_{0,M}$	Roughness length for momentum (m)
$z_{0,H}$	Roughness length for heat (m).
Δ	Slope of the saturation vapor pressure/temperature curve ($\text{Pa } ^\circ\text{C}^{-1}$)
Ω	Foliage clumping factor (dimensionless)
Ψ_c	Critical leaf water potential (Pa)
Ψ_e	Pore air-entry potential (Pa)
Ψ_l	Leaf water potential (Pa)
α	Albedo (dimensionless)
β	Bowen ratio (dimensionless)
δe	Vapor pressure deficit (Pa)
γ	Psychrometric constant ($\text{Pa } ^\circ\text{C}^{-1}$)
κ	Extinction coefficient (dimensionless)
λ	Latent heat of vaporization (J kg^{-1})
ρ_a	Density of air (kg m^{-3})
ρ_b	Bulk density (g cm^{-3})
ρ_v	Vapor density (kg m^{-3})
θ	Soil water content (vol vol^{-1})
θ_{sat}	Saturated soil water content (vol vol^{-1})
τ_b	Transmissivity of the canopy to direct radiation (dimensionless)
τ_d	Transmissivity of the canopy to diffuse radiation (dimensionless)
AMBD	Absolute mean bias difference
BDOR	Meteorological station at Bonneville Dam, Cascade Locks, Oregon
DALR	Dry adiabatic lapse rate
EC	Eddy covariance
LAI	Leaf Area Index ($\text{m}^2 \text{m}^{-2}$)
ME	Model efficiency
OPENSTA	Open site meteorological station
PNW	Pacific Northwest
RH	Relative humidity (%)
RMBD	Root mean bias difference
RMSD	Root mean square difference
SHAW	Simultaneous Heat and Water Model
STA02	2.0 m meteorological station

LIST OF NOTATION (CONTINUED)

STA10	12 m meteorological station
STA20	23 m meteorological station
STA40	40 m meteorological station
STA60	57 m meteorological station
STA70	68 m meteorological station
STA85	85 m meteorological station
SWE	Snow water equivalent
TDR	Time domain reflectometry
WRCCRF	Wind River Canopy Crane Research Facility
WRRS	Wind River Ranger Station meteorological station

THE WATER AND ENERGY DYNAMICS OF AN OLD-GROWTH SEASONAL TEMPERATE RAINFOREST

Chapter 1

1. INTRODUCTION

Hydrological processes in the near surface environment are strongly influenced by the presence of vegetation. Evaporation and transpiration of water by vegetation are major components of the hydrological balance of land surfaces, accounting for approximately 61% of gross precipitation on a global basis [Maidment, 1993]. Forest canopies intercept a large portion of the incident precipitation, ranging from approximately 10% to 40% of the annual water balance, depending on canopy and environmental conditions [Dingman, 1994]. Interception losses reduce the net precipitation, or throughfall (P_n) below forest canopies, and can lead to evaporation fluxes that exceed transpiration in wet environments [Calder, 1976]. In some regions, interception of fog water is an additional source of precipitation, increasing soil water content during dry conditions, and possibly contributing to streamflow [Harr *et al.*, 1982]. Transpiration rates for forests under well-watered conditions typically range from 2 to 12 mm day⁻¹, depending on canopy and climate conditions [Jones, 1992]. In regions characterized by seasonal or transient snowcover, forest canopies alter the interception characteristics and snow surface energy balance relative to open sites. Open areas may develop deeper snowpacks which ablate more rapidly due to increased radiative and turbulent energy fluxes relative to forested areas [Link and Marks, 1999; Marks *et al.*, 1998].

The impacts of vegetation on the individual components of the hydrologic balance varies based on a wide range of physical factors, including aspect, elevation, soil properties, season, climate regime, and biological factors such as stand height, density, age, species composition, and leaf area index. Research in forested environments is confounded by the difficulty of accurately measuring hydrologic fluxes, characterizing the biophysical properties of forest stands, and controlling for the high degree of spatial heterogeneity in canopy structure. These research issues must be surmounted if we are to gain an accurate mechanistic understanding of how vegetated systems both control hydrologic fluxes, and respond to environmental conditions. An understanding of hydrological processes at the stand level is necessary to scale processes up to the basin, landscape, and ultimately regional scale, to develop a more complete understanding of how vegetation controls surface energy and mass fluxes.

Questions regarding the interactions of vegetation and hydrology are particularly important in the Pacific Northwest (PNW) region of the United States. The region has lowlands with predominantly urban and agricultural land uses, and forested uplands where a large proportion of the land is dedicated to intensive timber management. The Mediterranean climate in the PNW is characterized by cool, wet winter conditions, and warm, dry summer conditions. During the summer, when evapotranspiration exceeds precipitation, water resource demands are augmented by seasonal snowmelt and stored supplies. Competing resource demands of timber production, high-quality municipal water supplies for a rapidly growing population, plentiful irrigation supplies, and survival of endangered species, set against a backdrop of a potentially

changing climate have raised a number of questions regarding the impact of vegetation on hydrological processes in this region.

1.1 Water Resources and Climate

The population of the Pacific Coast region of the U. S. is expected to increase by 52% between 1995 and 2040, causing a proportional increase on the demand for public water supplies [*Brown, 2000*]. Water resources in the region are currently being stretched by competing demands for irrigation, public supplies, and instream flows for endangered species. Although future demand increases may be partially offset by a decline in the irrigation sector, impacts of climate change may effectively reduce future water supplies in the region.

Results of general circulation model (GCM) simulations incorporating increased CO₂ and other greenhouse gases in the atmosphere suggest that the future climate in the PNW will be characterized by increased temperatures and precipitation [*Hamlet and Lettenmaier, 1999; Miles et al., 2000*]. Warmer temperatures will result in a greater proportion of winter precipitation occurring as rain, rather than snow, with a subsequent reduction in the seasonal snow covered area [*McCabe and Wolock, 1999*]. Although precipitation is expected to increase, much of the increase is predicted to occur during the winter months, when a precipitation surplus already exists. Consequently, the seasonal hydrograph is expected to increase in magnitude, and shift forward in time, thereby decreasing regional water resources during the months of precipitation deficit [*Hamlet and Lettenmaier, 1999*].

The potential impacts of such climate change illustrates the need to more completely understand the interactions of vegetation and hydrology in the PNW. A large portion of the snowcover that supplies water resource demands in the PNW develops in the upland forested areas. Improved knowledge of snowcover processes in this environment is needed to improve modeling tools to test hypotheses regarding the impact of climatic variability on the production of snowmelt. This knowledge will lead to improved real-time process models and will increase the effectiveness of regional water management to more optimally meet resource demands.

An improved understanding of forest hydrology, in particular of the interception and water-use of vegetation is also needed to assess how climate change may alter the individual components of the hydrologic balance. Future conditions are expected to be warmer, which should increase the evaporative demand in the early spring and summer. Vegetation responds to both environmental vapor deficits and extreme temperatures by reducing stomatal aperture, and thereby reducing transpiration losses [Jarvis, 1976]. Conversely, increased ambient CO₂ may produce an increase in leaf area, which would be expected to increase both interception and transpiration fluxes. However, denser foliage structure might increase canopy airspace vapor densities, which would produce a negative feedback by decreasing the vapor gradient, and hence evapotranspiration (ET) losses. It has been suggested that transpiration may be a conservative flux due to counteracting mechanisms such as these [Roberts, 1983]. The mechanistic controls on evaporative fluxes therefore need to be explored in greater detail. Hydrologic research spanning multiple years and encompassing a range

of climatic conditions can yield important insights into the impacts of future conditions on hydrological processes.

1.2 Land Management and Hydrology

The influences of land management practices, principally logging and roading, on stream discharge in the PNW have sparked heated debate [e.g. *Jones and Grant, 1996; Jones and Grant, 2001; Thomas and Megahan, 1998; Thomas and Megahan, 2001*]. Many studies of the effects of logging on catchment hydrology indicate increased water yield and low flows in the 4-8 year period following logging, attributed to decreased ET [*Harr et al., 1982; Hicks et al., 1991; Keppeler and Ziemer, 1990*]. In the watersheds that initially exhibited increased water yields following logging, yield was observed to eventually decrease below predicted values based on control treatments. Decreases were attributed to the regrowth of species in the riparian zone which increased ET fluxes within these watersheds [*Harr and McCorison, 1979*].

A number of paired, small basin studies also identified an increase in small (i.e. <1 year return interval) peak flows following logging [*Harr et al., 1975; Jones and Grant, 1996; Thomas and Megahan, 1998; Wright et al., 1990; Ziemer, 1981*]. In contrast, other studies in the PNW observed reduced water yields and peak flows immediately following logging, which were hypothesized to result from decreased fog drip and reduction of intercepted snow loads [*Harr, 1982; Harr and McCorison, 1979*]. The impacts of logging on large peakflows and on peakflows from large basins remains a topic of debate with differing conclusions arising from different data

processing procedures and applications of statistical techniques [*Jones and Grant, 1996; Thomas and Megahan, 1998*].

Part of the difficulty in deciphering the impacts of management practices on peak flows, is that a number of interacting hydrological processes may be affected. For example, the volume and timing of peak flows are a function of the size, intensity, duration, and other characteristics of a precipitation event, canopy characteristics, antecedent moisture conditions, location and properties of forest roads, and soil compaction resulting from harvest activities. Long-term statistical evaluation of peak flows is further complicated by spatial and temporal variability of watershed properties as a result of growth and succession. Furthermore, long-term statistical analyses of large basin hydrology are complicated by climate fluctuations, which may mask the hydrologic signal generated by changing land cover [*Bowling et al., 2000*]. The differing conclusions and complications identified with the statistical techniques illustrates the need for the improved process models to accurately simulate the interactions of vegetation and hydrology.

1.3 Interaction of Water and Carbon Dynamics

Soil water content and temperature are major factors influencing the carbon exchange of forested ecosystems through their influence on the CO₂ exchange of the canopy, soil heterotrophic and autotrophic respiration, fine root turnover and decay of woody debris [*Waring and Running, 1998*]. In most forests of the PNW, the onset of soil- and within-canopy air temperature warming, and the concomitant uptake of CO₂ is controlled by the timing of the seasonal snowcover ablation. The interception

characteristics of canopies are important for CO₂ dynamics, because transpiration and CO₂ uptake will be reduced during periods when the foliage is wetted. Interception losses also reduce the amount of water available for root extraction, and may impose limits on CO₂ uptake during dry periods characterized by small precipitation events. During warm and dry conditions, forests may cease to be a sink for carbon, and may become a CO₂ source due to respiration fluxes equaling or exceeding photosynthetic uptake [Bazzaz, 1996]. An understanding of the ecological processes controlling carbon fluxes also requires a mechanistic understanding of the processes controlling water and energy fluxes. An improved knowledge of the interactions between hydrological and ecological processes is critical to assess the potential effects of climate change on forested ecosystems.

1.4 Role of Intensive Measurements and Model Development

Physically-based numerical modeling is a powerful technique that can be used to improve our understanding of the mechanisms that control hydrologic fluxes in forested environments. Numerical models can be used to estimate fluxes that are particularly difficult to measure, explore the sensitivity of fluxes to climatic variables, and test hypotheses regarding the impacts of vegetation on the hydrologic system. The development of robust numerical models can be confounded in forested environments by a lack of adequate knowledge of the biophysical characteristics of the system. As a result, the estimation of model parameters can cause counteracting and conflicting errors that may still produce a reasonable simulation of a system variable, but lead to erroneous conclusions. The potential for errors such as these underscores

the importance of fully validating process models that simulate a number of coupled hydrological and physical processes.

The establishment of intensive research sites is particularly useful to address questions concerning the interactions between hydrology, climate, and vegetation by integrating research from a variety of related disciplines [e.g. *Sellers et al.*, 1995; *Sellers et al.*, 1992] . The range and detail of data originating from concerted research efforts at intensive sites is particularly valuable for process model development. Intensive investigations permit accurate model parameterizations to be completed, allowing a more thorough evaluation of the numerical representation of processes within the model, rather than relying on the manipulation of poorly quantified parameters to calibrate and validate models. Data collected at such sites can also be used to increase the utility of process models by fully validating the individual processes simulated. Once we are confident in our ability to accurately simulate a given system, physical models may be used to explore the sensitivity of a system to biophysical and climatic perturbations.

The Wind River Canopy Crane Research Facility (WRCCRF) is a 4 ha intensive research facility focused on hydrological and ecological processes, located in the Cascade Mountains of southern Washington, U. S. A. Vegetation at the site consists of a Douglas Fir – western hemlock canopy about 65 m high, and more than 450 years old [*Shaw et al.*, in review]. Douglas-fir ecosystems are widely distributed in the western U. S., and represent a major land cover class in the Cascade and Coast ranges of the PNW (Figure 1) [*Little*, 1971]. The canopy cover at WRCCRF is a relatively extreme size and age end-member for forests in the region and is particularly

important for the assessment of the hydrologic functioning of undisturbed ecosystems prior to human management.

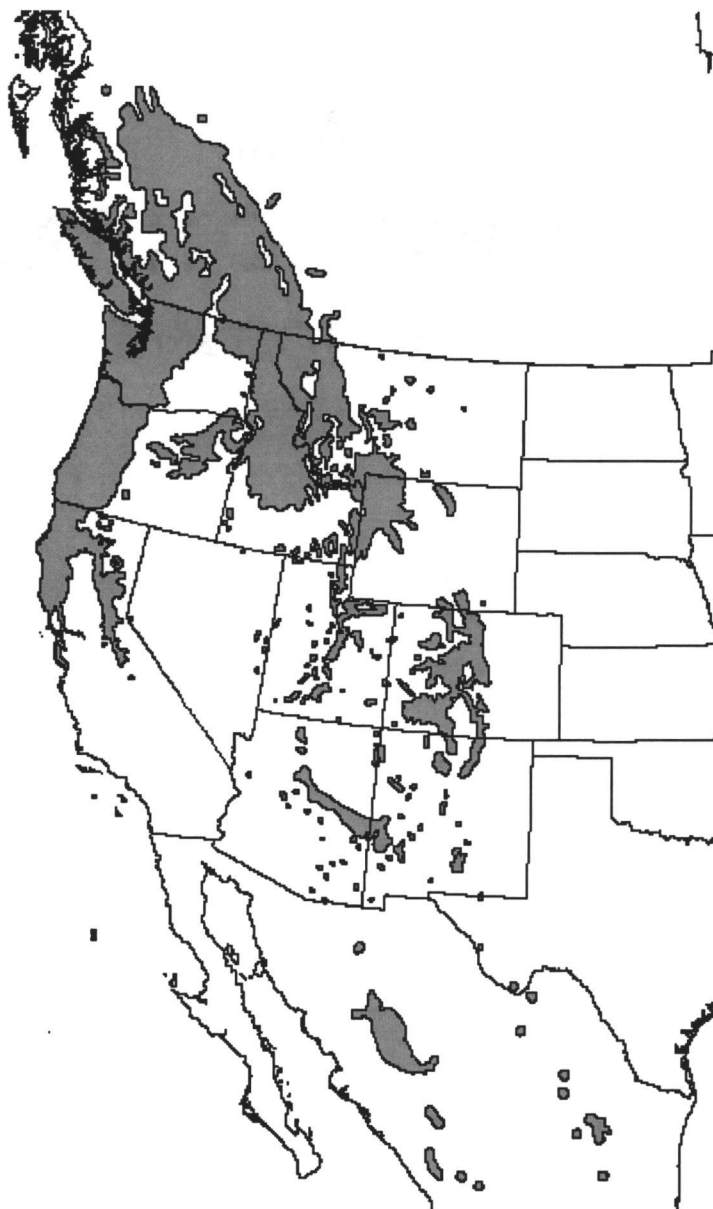


Figure 1.1. Distribution of Douglas fir in the U. S.

A Liebherr 550HC tower crane is installed in the center of the plot, and is used for canopy access and as a platform for microclimate sensors. The site was selected as

an Ameriflux research site in 1998, for intensive measurements of CO₂ and water fluxes, and associated hydrological and ecological processes [*Baldocchi et al.*, in press]. The site is an ideal location for investigations of forest hydrology and model development due a preponderance of both meteorological flux and scalar data collected at a variety of locations throughout the canopy. In addition, canopy access provided the crane has permitted the intensive characterization of the stand. The research site therefore presents a unique opportunity for hydrological model development given the wide range of existing data for model parameterization and validation. The site also creates opportunities for comparisons between hydrological models and the water balance components of models that simulate the interactions of ecological and hydrological processes [e.g. *Kaduk et al.*, in review; *Williams et al.*, 2001].

1.5 Dissertation Structure

The objective of this dissertation is to explore the surface hydrology at WRCCRF for the 1999 and 2000 hydrologic years through complementary measurement and modeling programs.

Chapter 2 presents a characterization of the canopy and climate conditions at the site for the period from August 1998 through December 2000. This chapter discusses the climatic differences between the study period and the long-term mean, and assesses implications of differences in microclimate over the forest and at a nearby open site. A detailed description of the instrumentation used for the core meteorological measurements is provided. The chapter also presents details and

results of supplemental hydrologic data that were collected throughout the 4 ha site for model parameterization and validation. Despite the small spatial extent of the site, considerable variation in soil water content and snow cover were observed.

A detailed analysis of dynamics of canopy precipitation interception is presented in Chapter 3. Interception losses, the mean canopy direct throughfall proportion, and the canopy saturation storage capacity are determined. A simple analytical model [Gash, 1979] is used to assess the components of net interception loss.

Chapter 4 presents results from an improved version of the Simultaneous Heat and Water (SHAW) model [Flerchinger and Saxton, 1989], used to simulate mass and energy-fluxes at the WRCCRF site. In particular, the interception characteristics of the canopy, the stomatal conductance routine, and the formulation of energy transfer processes within the canopy were modified to more accurately simulate transfer processes between the forest and the atmosphere.

Chapter 5 presents a summary of the methods and key findings of this investigation. Future research directions to further improve our understanding of the factors controlling hydrologic fluxes in forested systems are discussed. Areas for additional research include a more thorough evaluation of interception at various levels in the canopy, detailed evaluation of simulated within-canopy conditions, and complete sensitivity analysis of the system to climatic conditions and site parameterization using the SHAW model.

**2. CANOPY CHARACTERISTICS AND CLIMATE CONDITIONS AT THE
WIND RIVER CANOPY CRANE RESEARCH FACILITY, CARSON
WASHINGTON, 1998-2000**

Timothy E. Link
Danny Marks
Mike Unsworth

For submittal to the Journal of Hydrometeorology

2.1 Abstract

Climate and hydrologic conditions are presented for an old-growth seasonal temperate rainforest in the Cascade Mountains of southern Washington, U.S.A. during the 1999 and 2000 hydrologic years. The 1999-2000 period was characterized by average precipitation volumes, but slightly warmer winter temperatures which caused a greater proportion of the precipitation to occur as rain, rather than snow. Air temperatures in an open field near the site were observed to be 0.6 °C cooler and exhibit greater diurnal variation than temperatures measured above the forest canopy. Use of open station temperature and humidity data to estimate potential evapotranspiration resulted in a -13.2% annual difference compared to when above canopy data are used. Mean air temperatures below the forest canopy were 0.6 °C cooler than in the open, and exhibited higher humidity, and a nearly constant wind velocity of 0.3 m s⁻¹. Shallow soil moisture (0-40 cm) within the 4 ha site varied considerably, ranging from 12% to 40% vol vol⁻¹ between the maximum and minimum differences. Soil water content in the 90 – 120 cm layer was found to stay relatively wet, even late in the season, with values ranging from 26% to >40%. Soil temperatures were found to be relatively constant across the site, with vertical differences resulting from variable damping depths caused by soil water content variations. Variations in climate and hydrologic conditions indicate that researchers must consider the range of variation when scaling up studies completed within the site to the stand scale, and when extrapolating process knowledge gained at this site to other sites in the region.

2.2 Introduction

In this paper we present results of detailed forest and soil microclimate analyses from the Wind River Canopy Crane Research Facility (WRCCRF), an old-growth temperate rainforest stand in the Cascade Mountains in southern Washington, USA. The WRCCRF is an AmeriFlux site, for the study of forest carbon dynamics in an old-growth conifer ecosystem. The uptake and release of CO₂ by ecosystems is strongly controlled by temperature and soil moisture conditions, therefore an understanding of the processes affecting these variables is essential to understanding the dynamics of CO₂ exchange. An understanding of forest microclimates is also important from a management perspective, to evaluate the processes that buffer late-successional ecosystems from catastrophic change, so that these processes can be maintained in managed systems [*National Research Council, 2000*].

Local climate, soil moisture, and vegetation conditions strongly affect hydrological and ecological processes, including the surface energy balance, precipitation interception, snowcover deposition and ablation, transpiration, CO₂ assimilation by vegetation, decay of organic debris, and respiration. In areas that experience snow deposition, soil warming and the onset of growth in the spring is delayed until the snowcover has completely ablated [*Waring and Running, 1998*]. Climate conditions are particularly important in transient snow zones such as at the WRCCRF where small interannual variations can result in drastically different snowcover and soil temperature dynamics between years.

Under dry conditions, soil water content (θ) affects ecosystem processes by limiting transpiration and CO₂ uptake by vegetation. Warm temperatures can result in

greater CO₂ release by soil, root, and above ground respiration, and may cause forested systems to change from a net CO₂ sink to a net CO₂ source. Studies of coupled hydrological and ecosystem processes require basic meteorological data, which vary between years, between the location where data are collected and the system of interest, and within a given ecosystem. An understanding of the range of variation of the processes affected is important for inter-site and inter-year comparisons, and to interpret the results of detailed process studies.

Many hydrological and ecological field studies occur over a relatively short duration, lasting from 2 to 3 years, however ecosystem structure reflects long term climate conditions. Different measurement techniques used to quantify biophysical processes may integrate over a range of time periods. For example, net ecosystem exchange of CO₂ determined by eddy covariance techniques will integrate the period for which the instrumentation was operational, whereas detailed forest inventory techniques for carbon budgeting integrate processes roughly occurring over the past 0-100 years [Harmon *et al.*, in review]. Understanding how climate conditions occurring during brief field measurement periods relate to long-term conditions is important to evaluate whether measured biophysical fluxes are representative of long term mean conditions.

Hydrological and ecological investigations frequently use numerical models that require standard climate data (e.g. radiation, air temperature, relative humidity, and wind speed) to simulate the processes of interest. Many soil-vegetation-atmosphere models require climate data representative of conditions above a particular vegetation canopy [e.g. Flerchinger *et al.*, 1996b; Kaduk *et al.*, in review; Williams *et al.*, 1998],

however climate data are typically collected in open areas over bare ground or short grass covers [Tanner, 1990; WMO, 1996]. Other process-specific models require climate conditions at the snow or soil surface under vegetation canopies [e.g. Marks *et al.*, 1999], and necessitate the adjustment of open-site meteorological data for below-canopy conditions [Link and Marks, 1999]. The development of canopy correction algorithms and assessment of model performance necessitates the evaluation of the effect of vegetation covers on climate conditions both above and below a range of canopies.

Climate and soil moisture conditions also vary strongly within a forest stand as a result of heterogeneous vegetation and soil characteristics [Chen *et al.*, 1993; Chen *et al.*, 1999]. Researchers frequently attempt to scale temperature and moisture-dependent process measurements taken at relatively small scales (e.g. soil respiration $\sim 10^{-1} \text{ m}^2$; sap flux $\sim 10^1 \text{ m}^2$) up to the stand scale, to compare the results to other techniques that sample larger areas (e.g. eddy covariance $\sim 10^3 \text{ m}^2$). The development of effective sampling schemes, interpretation of within site data, and evaluation of potential errors associated with scaling data up to the stand level can be aided by an understanding of the range and patterns of variability of soil conditions within a stand.

The objective of this study was to provide a detailed description of climate and soil conditions at the WRCCRF during the 1999 and 2000 hydrological years, to better understand the results of detailed process-based research conducted at the site.

Specifically, we: 1.) Present meteorological datasets for the 1999 and 2000 hydrologic years (hy) at the WRCCRF, and a characterization of the canopy and soils at the site for use in the development and validation of simulation models; 2.) Assess

the differences in climate for hy1999 and hy2000 relative to long term conditions; 3.) Quantify the differences in meteorological conditions at an open site over short grass relative to conditions above the forest canopy, and assess the differences in estimated evaporation using the two datasets; 4.) Describe the differences in meteorological conditions at the open site relative to conditions below the forest canopy; 5.) Discuss the characteristics of the forest canopy at WRCCRF relative to other forest canopies; and 6.) Assess the spatial patterns and range of variation in soil moisture and temperature conditions within the WRCCRF site.

2.3 Methods

2.3.1 Site Description

The WRCCRF is located within the T. T. Munger Research Natural Area, near Carson, Washington at 45° 49' N latitude, 121° 57' W longitude, at an elevation of 367.5m amsl (Figure 2.1). The facility is located on an alluvial fan sloping gently from the southwest to the north, with a total relief across the study area of approximately 10 m. A small, ephemeral creek runs through the northern portion of the site into a perennial wetland approximately 100 m to the east of the site. Soils at the site are classified as medial, mesic, Entic Vitrandis. The soils are deep, well drained, medium textured, and originated from relatively recent (~3,500 to 12,000 years before present) volcanic airfall tephra [*Shaw et al.*, in review].

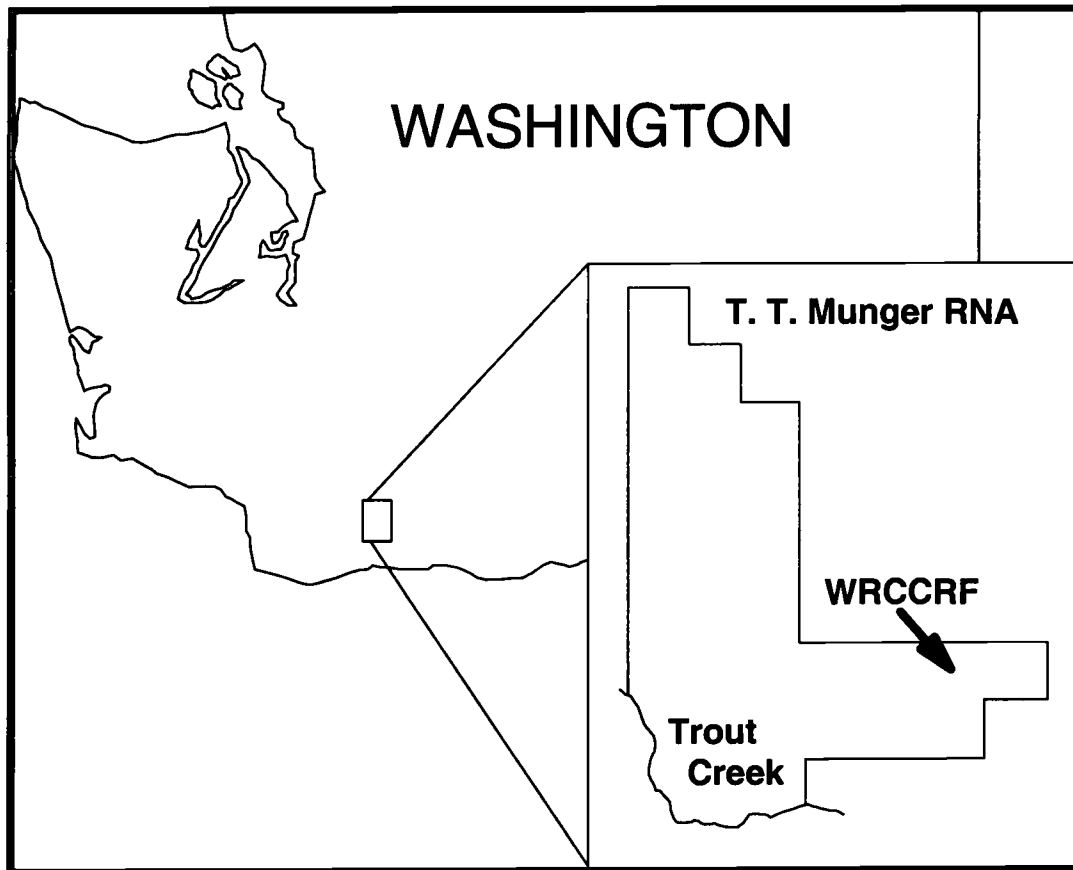


Figure 2.1. Location of the T. T. Munger Research Natural Area and the Wind River Canopy Crane Research Facility (WRCCRF).

Vegetation at the site is composed of a 500-600 year old Douglas fir (*Pseudotsuga menziesii*)/western hemlock (*Tsuga heterophylla*) forest. The canopy height is approximately 60 m, with the tallest trees reaching 65 m [Ishii *et al.*, 2000]. The canopy exhibits many old-growth characteristics, including a high degree of spatial heterogeneity in species and canopy depth, a multi-layered canopy, and high degree of biodiversity in the plant community [Franklin and Waring, 1980]. Dominant understorey species include vine maple (*Acer circinatum*), salal (*Gaultheria shallon*), Oregon grape (*Berberis nervosa*) and vanilla leaf (*Achlys triphylla*). A high diversity of non-vascular plants are present in the canopy, dominated by lichens in the

mid and upper canopy and bryophytes in the lower canopy. The presence of canopy epiphytes is important from a hydrological perspective, because these species may increase the precipitation interception capacity of the forest canopy [*Unsworth et al.*, in review]. The leaf area index (LAI) of the site was determined to be 8.6 ± 1.1 using the vertical line intercept method [*Thomas and Winner, 2000*]. The physical setting and ecological characteristics of the WRCCRF are described in detail by *Shaw et al.* [in review].

The WRCCRF study area consists of a 4 ha plot divided into four 1 ha quadrants which are each sub-divided into sixteen 25m x 25m sub-sections (Figure 2.2). An 85 m Liebherr 550 HC tower crane with a jib height of 74.5 m and range of 87 m is installed in a canopy gap at the center of the 4 ha plot. The rotation of the jib inscribes a 2.3 ha circle within the research plot. The crane provides 3-dimensional access to the forest canopy via a gondola suspended from the jib and provides a platform for above- and within-canopy micrometeorological measurements. Detailed process-level research is focused within the 2.3 ha crane circle, therefore additional below-canopy micrometeorological and soil measurements were conducted in the same area to provide spatially consistent data sets.

A large artificial clearing is located approximately 500 m south of the research site. The clearing is characterized by mixed grass cover which typically senesces in mid to late summer depending on climate conditions. A supplemental meteorological station is located on a small rise near the middle of the clearing, approximately 1.5 km south of the tower to provide backup data in the event of data loss from the above canopy installation.

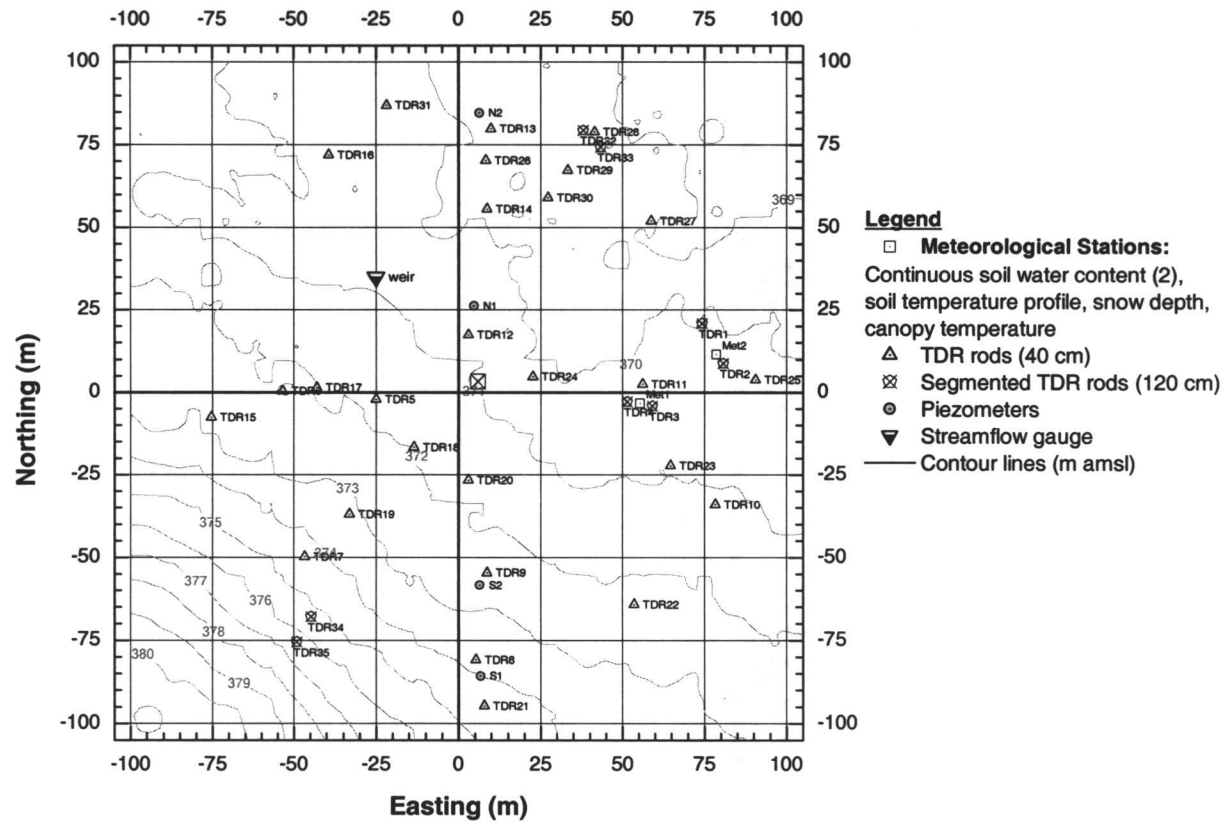


Figure 2.2. Location of climate and soil monitoring equipment at the WRCCRF.

2.3.2 Data Collection

Three datasets exist for microclimate analyses. The first consists of long-term historical climate data collected at locations near the crane site to indicate general climate characteristics of the area and provide a basis for comparison to the time periods of interest. The second class of datasets is core meteorological data collected at the WRCCRF and adjacent clearing to quantify the dominant variables driving hydrological and ecological processes. The third class is detailed intrasite data that are collected beneath the forest canopy to determine mean conditions within the crane circle, and provide a measure of intrasite variability. Climate variables, sensors, periods of record, and sampling frequency are summarized in Table 2.1.

2.3.2.1 Historical Data

Two long-term, basic meteorological datasets exist for the area. Climate conditions for the period from 1931 through 1977 were collected at the Wind River Ranger Station (WRRS) located approximately 3 km south of the crane site, at approximately 351.1 m amsl. Air temperature maxima, minima, precipitation and snow depth were collected daily at the site [NCDC, 2001]. Significant variations in air temperature means and minima can occur over relatively short distances due to localized drainage flows, therefore temperature conditions at the WRRS may not be representative of conditions present at the crane site. There were no concurrent periods of data collection at WRRS and the WRCCRF, therefore consistent air temperature differences between the two sites could not be evaluated, and were therefore not used for this analysis. Precipitation and snow depth are not expected to

Table 2.1. WRCCRF instrumentation summary

Dataset/Variable	Location	Time Period	Resolution	Instrument
Historical Climate Data				
Air Temperature	BDOR	1960 - 1990	daily	nd
Precipitation	WRRS	1931 - 1977	daily	nd
Snow Depth	WRRS	1931 - 1977	daily	nd
Core Meteorological Data				
Net Radiation	STA80	6/18/98 - 12/29/00	30 minute	Kipp & Zonen, CNR-1
Incoming Solar Radiation	STA80	6/18/98 - 12/29/00	30 minute	Kipp & Zonen, CNR-1
	OPENSTA	2/2/98 - 12/29/00	30 minute	Li-Cor, LI200
Air Temperature	STA70	2/2/98 - 12/29/00	30 minute	Vaisala, HMP35C
	STA02	2/2/98 - 12/29/00	30 minute	Vaisala, HMP35C
	OPENSTA	2/2/98 - 12/29/00	30 minute	Vaisala, HMP35C
Relative Humidity	STA70	2/2/98 - 12/29/00	30 minute	Vaisala, HMP35C
	OPENSTA	2/2/98 - 12/29/00	30 minute	Vaisala, HMP35C
	STA02	2/2/98 - 12/29/00	30 minute	Vaisala, HMP35C
Wind Speed	STA70	2/2/98 - 12/29/00	30 minute	Gill Solent HS sonic anemometer
	OPENSTA	2/2/98 - 12/29/00	30 minute	RM-Young, 03001
	STA02	2/2/98 - 12/29/00	30 minute	Handar sonic anemometer
Precipitation	STA80	12/4/98 - 12/29/00	30 minute	Belfort, Model 6071
	OPENSTA	10/23/98 - 12/29/00	30 minute	Belfort, Model 5-780
	OPENSTA	2/2/98 - 12/29/00	30 minute	Campbell, TE525/CS705
Snow Depth	OPENSTA	2/2/98 - 12/29/00	30 minute	Judd, Sonic Sensor

Table 2.1 (continued). WRCCRF instrumentation summary

Within Canopy Data	Location	Time Period	Resolution	Instrument
Solar Radiation	10 element roving array	8/10/98 - 8/13/98	1 minute	Matrix, MK-1G
		8/17/99 - 8/20/99	1 minute	Matrix, MK-1G
		9/23/00 - 9/25/00	1 minute	Matrix, MK-1G
		9/23/00 - 9/25/00	1 minute	Eppley, PSP
Thermal Radiation	3 element roving array	9/23/00 - 9/25/00	1 minute	Eppley, PIR
Throughfall	44 roving collectors	8/14/98 - 6/28/00	periodic	bottle collector
	24 roving gauges	3/30/00 - 12/27/00	10 minute	Texas Electronics, TES25I
Snow Depth	closed, gap	8/14/98 - 1/1/01	15 minute	Judd, Sonic Sensor
Soil Water Content	0-30 cm, 2 closed, 2 gap	8/14/98 - 1/1/01	15 minute	Campbell, CS615
	0-120 cm, 8 profiles throughout site	8/14/98 - 1/1/01	periodic	Moisture Point, Type A
	0-40 cm, 28 random locations	8/14/98 - 1/1/01	periodic	Trase, 6050XI
Soil Temperature	15 cm, closed, gap	8/14/98 - 1/1/01	15 minute	Campbell, CS107
	10, 20, 30, 50, 100cm, closed, gap	10/15/99 - 1/1/01	5 minute	HOBO, Pro Temp
Stream Discharge	TABR Creek	8/14/98 - 1/1/01	30 minute	EI, 0-2.5 psi transducer

Location codes:

BDOR: Cascade Locks, Oregon

WRRS: Wind River Ranger Station

STA80: 85.0m station on crane tower

STA70: 68.4m station on crane tower

STA02: 2.0 m sub-canopy station

OPENSTA: 2.5m station in open field

Note: Identical sensor suites for T_a , RH and u are installed at 11.7 m (STA10), 22.8 m (STA20), 39.9 m (STA40), and 57.0 m (STA60)

vary greatly between the two locations, therefore the record from the WRRS station was used to compare precipitation conditions from the 1999 and 2000 hydrologic years to the long-term averages.

A second long-term dataset of daily air temperature means, maxima and minima were collected at the Bonneville Dam (BDOR) in Cascade Locks, Oregon, approximately 20 km south of the crane site [WRCC, 2001]. Although absolute air temperatures were expected to be different at BDOR relative to WRCCRF, the air temperature record spanned the period from 1961 through 2000, and was therefore used to assess the regional climate differences for the period of interest relative to the long term average.

2.3.2.2 Core Meteorological Data

Core meteorological data for the study period were collected at the open field site (OPENSTA), above the canopy at 68.4 m (STA70) , and beneath a closed canopy area ~25 m east of the crane tower (STA02). A meteorological profile was also installed on the crane tower at 11.7 m (STA10), 22.8 m (STA20), 39.9 m (STA40), and 57.0 m (STA60).

Downwelling and upwelling solar (R_S) and thermal (R_L) radiation was measured with a 4 component net radiometer mounted at the highest point on the crane, 87 m above the ground (Model CNR-1, Kipp and Zonen Inc, Bohemia, NY). The incoming radiation is unobstructed by the crane structure, however the upwelling radiation sensed by the CNR-1 includes some reflection and emission from the crane tower. Downwelling solar radiation was also measured at the open site location with a silicon based pyranometer (Model Li-200, LI-COR Inc., Lincoln, NE).

Air temperature (T_a) and relative humidity (RH) were measured at STA70, STA02, and OPENSTA (Model HMP35C, Vaisala Inc., Sunnyvale, CA). The sensor at STA70 was installed in a modified Gill multi-plate radiation shield which was mechanically aspirated using a small fan to draw air through the top of the radiation shield. STA02 and OPENSTA sensors were installed in naturally aspirated Gill multi-plate radiation shields.

Wind velocity (u) at STA70 was measured with a 3-dimensional sonic anemometer (Solent Gill HS, Lymington, UK). Wind velocity at STA02 was measured using a 2-dimensional sonic anemometer (Model WAS425, Handar/Vaisala Inc., Sunnyvale, CA). The sonic anemometers were very effective for measuring low wind speeds and generally provided reliable readings under wet conditions, although the data quality degraded during high precipitation rates [Paw U *et al.*, in review]. Wind velocity at OPENSTA was recorded using a cup anemometer (Model 03001, R.M. Young Co., Traverse City, MI).

Precipitation (rain and snow) was measured at OPENSTA using a weighing precipitation gauge, equipped with a standard alter shield (Model 5-780, Belfort Instrument Co., Baltimore, MD). Precipitation (rain and snow) was also measured at OPENSTA using a tipping bucket raingauge (Model TE-525, Texas Electronics Inc., Dallas, TX), equipped with a snowfall adapter (Model CS705, Campbell Scientific, Logan, UT). Precipitation (rain and snow) was measured above the canopy using an alter-shielded large-volume weighing precipitation gauge mounted at 75 m on the counter jib of the crane (Model 6071, Belfort Instrument Co., Baltimore, MD). The gauges in use at the WRCCRF have different advantages depending on the type of

precipitation event; the TE-525 tends to undersample relatively intense events and functions poorly for snowfall, whereas the inertia in the spring of the Belfort gauges renders these devices relatively insensitive to small events. The site precipitation record was prepared by using the open site Belfort gauge during the winter and spring months, and by using the TE-525 gauge during the smaller late spring through early autumn events. The above-canopy precipitation record contained spikes apparently resulting from movement of the crane jib during windy events, and requiring tedious manual data filtering. The above canopy record was therefore used only when both precipitation gauges at OPENSTA were not functioning.

Streamflow on TABR Creek, the small ephemeral channel flowing through the site was measured using a 0.406 m deep v-notch weir equipped with a 0-2.5 psi pressure transducer (Electronic Engineering Innovations, Inc., Las Cruces, NM) and recorded on a datalogger (CR-500, Campbell Scientific, Inc., Logan, UT) at 30 minute intervals. Depth of flow through the v-notch was converted to flow volume using an empirical rating curve developed by measuring the mean flow velocity through the v-notch with an electromagnetic flow meter (Model 2000, Marsh-McBirney Inc., Frederick, MD). The lowest flow volume ($1.3 \times 10^{-3} \text{ m}^3 \text{ s}^{-1}$) was measured using the volumetric sampling method to provide an accurate rating curve over the full range of flow depths.

Gaps in the data used in these analyses were filled using a hierarchical interpolation routine. Data gaps lasting 3 hours or less in duration were interpolated by fitting a 3 point spline to the data [Akima, 1978]. Data gaps exceeding 3 hours were filled by substituting values estimated using a simple linear regression on data

from one of the other stations for the ten days preceding and the ten days succeeding the data gap. STA70 data were estimated using either OPENSTA or STA60 data, and vice versa. Gaps in the STA02 records were estimated from the data collected at STA20.

2.3.2.3 *Within Canopy Measurements*

Two supplemental sub-canopy instrument stations were installed within a recent (<5 years) canopy gap and beneath a dense canopy cover to measure the extremes of within site climate variation resulting from the overlying vegetation cover. Snow depth was recorded at each station using a sonic snow depth sensor (Judd Communications, Inc., Logan, UT). Volumetric soil water content in the upper 30 cm of the soil profile was measured using two water content reflectometers (CS615, Campbell Scientific, Inc., Logan, UT) installed vertically at each site. Soil temperature was monitored at 15 cm using thermistors (Model 107, Campbell Scientific, Inc., Logan, UT). All data were recorded at 15 minute intervals on attached dataloggers (CR-10X, Campbell Scientific, Inc., Logan, UT). At the beginning of hy2000, additional soil temperature sensors (HOBO Pro Temp, Onset Computer Corp., Bourne, MA) were installed at each site at depths of 10, 20, 30, 50, and 100 cm to provide continuous soil temperature profile data.

Radiation and throughfall below the canopy are strongly affected by variations in canopy structure. Soil moisture is influenced by canopy and root structure and by soil properties. Arrays of sensors to measure these variables were installed to determine the mean site conditions and provide a measure of intra-site variability.

Solar radiation (0.28–3.5 μm) at the forest floor was measured using a 10-element pyranometer array (Model MK1-G, Matrix Inc., Mesa, AZ). Radiation measurements were taken over three 2–4 day cloudless periods in mid to late summer. The three measurement locations were selected to be representative of typical canopy conditions for the site. Radiometers were randomly located over a 700 m^2 area and moved to new random locations once per day, to increase the number of sampling points. At one location, the Matrix array was paired with a 10-element array of reference pyranometers (Model PSP-1, Eppley Laboratory Inc., Newport, RI) [Hardy *et al.*, 1997] to assess the performance of the Matrix sensors under shortwave-depleted spectral conditions below a vegetation canopy. Thermal radiation (3.5–100 μm) below the canopy was recorded concurrently using three randomly located pyrgeometers (Model PIR-1, Eppley Laboratory Inc., Newport, RI). Sensor arrays were sampled using multiplexers (AM416, Campbell Scientific, Inc., Logan, UT) and stored to dataloggers (CR-10X, Campbell Scientific, Inc., Logan, UT) at 1 minute intervals.

Throughfall below the WRCCRF canopy was measured using 44 steep-sided funnels (94 cm^2 area) connected to storage containers having a total capacity of 400 mm. Throughfall was monitored during the snow-free periods, approximately from March 1 through December 1, for the 1999 and 2000 calendar years. Throughfall gauges were arranged according to a stratified random sampling scheme, where each collector was randomly located within each 25m x 25m quadrat within the crane circle. The accumulated throughfall was measured every 3 to 6 weeks depending on the amount of rainfall, and each gauge was randomly relocated within the quadrats

after sampling. Use of this method resulted in a total of 440 unique sampling points, which is expected to result in a sampling error of less than 5% of the mean throughfall [Lloyd and Marques, 1988]. In March 2000, an additional array of 24 tipping bucket rain gauges (TE-525I, Texas Electronics Inc., Dallas, TX) equipped with individual data loggers (HOBO Event, Onset Computer Corp., Bourne, MA) was installed within the crane circle. The automated gauges were also randomly relocated approximately every month. The automated gauges provided a high-temporal resolution throughfall record for the derivation of canopy throughfall parameters described by Rutter [1971]. A detailed description of the interception study is provided in Link *et al.*, [in review-b].

Two arrays of soil moisture sensors were installed throughout the crane circle and sampled every 2 to 6 weeks . Twenty-eight pairs of 40 cm long, 6.4 mm diameter stainless steel round rod, spaced 5 cm apart were randomly located along 4 transects traversing the crane circle. TDR pairs were carefully installed following the procedure described by Gray and Spies [1995] to avoid air pockets and roots. Sensors were interrogated using a time domain reflectometer (TDR, Model Trase 6050XI, Soil Moisture Equipment Inc., Santa Barbara, CA), and the resulting traces were stored to identify anomalous data. Analyses of soils from the crane circle also indicated relatively low organic matter content in the top 0–40 cm of the soil [Harmon *et al.*, in review], therefore volumetric soil water contents were determined using the standard calibration and trace analysis routines supplied by the manufacturer [Topp *et al.*, 1980].

Eight profiling TDR probes (Type A, Environmental Sensors Inc., San Diego, CA) were installed at areas in the site expected to encompass the full range of soil water contents in the crane circle. The segmented probes used remote diode shorting techniques [Hook *et al.*, 1992] to isolate probe segments spanning the range from 0-15, 15-30, 30-60, 60-90, and 90-120 cm, below the ground surface. Pairs of segmented probes were installed on the topographic rise south of the crane tower (relatively dry conditions), at the mid-elevation closed canopy and gap sites (mesic conditions), and in the seasonally inundated northeast quadrant (wet conditions) (Figure 2.2). Segmented rods were calibrated *in situ* by collecting bulk soil samples for gravimetric θ determination at 4 locations within 1 meter of each probe. Soil cores 5 cm in diameter by 6 cm long were collected for bulk density determination at the midpoint of each probe segment using a brass ring sampler.

2.4 Results and Discussion

2.4.1 Climate

2.4.1.1 *General Climate Conditions, hy1999 & 2000*

The climate at the WRCCRF during this study was characterized by cool, wet winters and warm, dry summers (Figure 2.3). Incoming solar radiation was typically low in the late fall and winter months (November - February), due to heavy cloud cover, and varied between years, as shown by the range of conditions that occurred during the 1998 to 2000 period (Figure 2.3a). Mean monthly net all-wave radiation ranged from 26% of mean solar radiation in December to approximately 70% of mean solar radiation near the summer solstice.

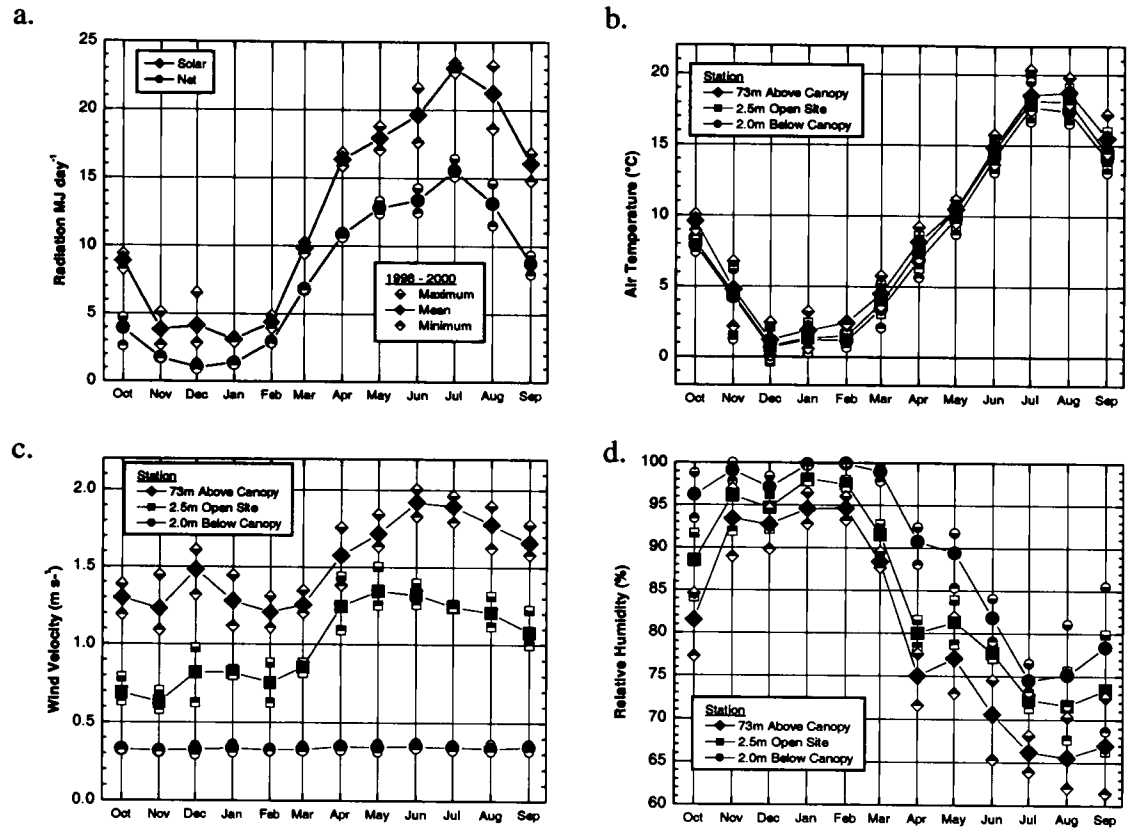


Figure 2.3. Mean climate conditions at OPENSTA, STA70 and STA02, 1998 - 2000.

The mean air temperature at the open station for the 1999 and 2000 water years was 8.1 °C. The maximum monthly mean of 17.3 °C occurred in August, and minimum monthly mean of 0.1 °C occurred in December. The largest inter-annual variations occurred during the fall and spring, due to variations in the timing of the transition from clear, dry conditions to wet conditions. Measured relative humidity showed expected seasonal variations ranging from values close to 100% during the November–February period to minimum monthly means of less than 75% during the July–September period. Between year RH variations were largest during the summer and fall months as a result of variation in precipitation events which were characterized by cooler temperatures and high humidity during and after the events.

Mean wind velocity was relatively low during the October–March period, and increased during the April–September period. The increase during the spring and summer was a result of high afternoon winds that occurred from approximately 1200h to 1800h during clear summer days. Winds during the fall and winter periods exhibited a weak diurnal pattern as local wind systems were suppressed by reduced radiative forcing. In general, wind velocities were low at the site, relative to other mountainous locations due to the valley bottom location which sheltered the site relative to more exposed mountainous locations.

The total annual precipitation for hy 1999 and 2000 was 2596 mm and 2482 mm, respectively. Precipitation was strongly seasonally distributed, as noted by *Shaw et al.* [in review], with 98% and 93% of the annual precipitation for the 1999 and 2000 water years occurring during the months of October through May.

2.4.1.2 Historical Context

The difference between the mean monthly, mean monthly maximum, and mean monthly minimum air temperatures for the study period relative to the 1961-1990 long term means at Cascade Locks are shown in Figure 2.4a. Since temperatures at Cascade Locks during the autumn, winter and spring were typically within 1 °C of temperatures at WRCCRF after adjustment for the dry adiabatic lapse rate (DALR), it is assumed that this record represents a good proxy for regional conditions during these time periods. Months where the mean monthly maxima exceeded mean monthly values indicate larger diurnal variations than the long-term conditions, whereas months where differences in minima exceed maxima indicate reduced diurnal temperature variations. For example, if the amplitude of the mean diurnal air temperature cycle for a given period is equal to the amplitude of the historical period, but the mean is warmer, the maxima, minima, and mean will all plot at the same point above the x-axis (e.g. January 1999). However, if the mean air temperature of a given period is similar to the historical mean, but the amplitude of the diurnal cycle is larger, the mean monthly maxima and minima differences will diverge from the mean (e.g. September 1999).

Both the 1999 and 2000 winters were characterized by warmer than average conditions with maximum monthly differences approaching +0.5 to +3.0 °C. Mean monthly maxima and minima differences for both winters were close to the mean differences, suggesting that the higher mean air temperatures were not a result of clearer conditions. The drier than average transition between hy1999 and hy2000, is

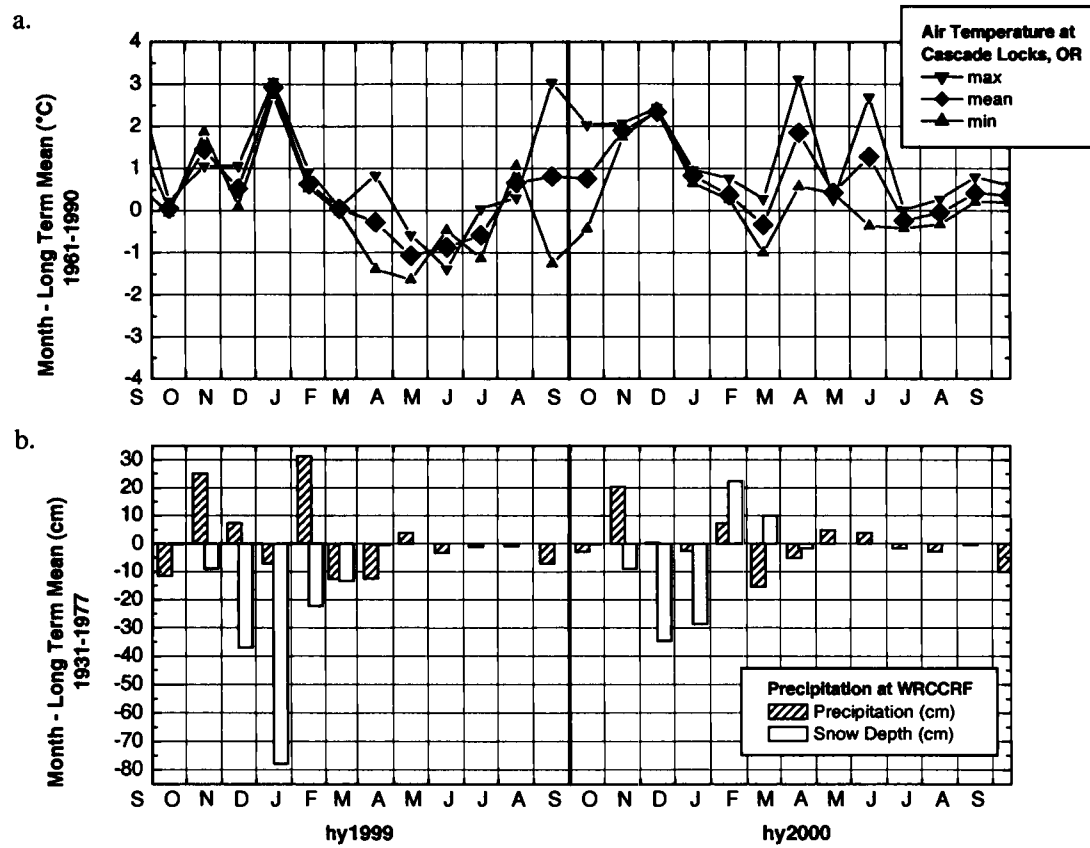


Figure 2.4. Comparison of hy 1999 and hy 2000 temperature and precipitation to long-term means.

reflected in the air temperature record by higher means and larger diurnal variations, indicating clearer than average conditions.

Precipitation for the 1999 and 2000 water years was respectively 5% and 0% greater than the long-term (1931-1977) average annual precipitation of 2467 mm measured at WRRS. The timing and climate characteristics during the seasonal transition from dry to wet conditions are important because interannual climate variability controls whether the ecosystem is a source, sink, or remains in equilibrium with regards to CO₂ fluxes [Goulden *et al.*, 1996]. The 1999 hydrologic year was characterized by relatively dry fall conditions; the first large rainfall event (exceeding 20 mm) occurred on September 18. The 1999 winter months were characterized by typical wet conditions, with an extremely wet February (Figure 2.4b). The spring and summer of 1999 was relatively dry, with below average precipitation in March and April, and June through September. The 1999-2000 hydrologic year was characterized by a late transition to wet conditions, with low September precipitation and the first major rainfall event on October 25. Precipitation in 2000 was more evenly distributed during the spring months, with above-average precipitation in May and June, and below average conditions throughout the summer. The first large event of the seasonal transition occurred on September 30, however the start of the 2001 hydrologic year characterized by unusually dry conditions.

As discussed above, snowcover conditions are particularly important for the ecosystem carbon cycle, because the timing of snowcover ablation controls soil warming, which has a strong influence on the onset of the growing season. The 1999 and 2000 hydrologic years were generally characterized by much less snowfall relative

to long-term conditions (Figure 2.4b). This is consistent with observations of elevated temperatures that caused the lower limit of the snowcover transition zone to increase in altitude. The 1999 hydrologic year was characterized by below average snowfall for all months, whereas 2000 was characterized by slightly greater than average snowpack depth during February and March. The slightly above average snowfall in February and March is consistent with temperature observations indicating conditions near the long-term average.

Warmer winter conditions and shorter periods of snowcover duration are expected to result in earlier and potentially larger amounts of CO₂ assimilation by the forest canopy relative to historical periods. Warmer conditions could also result in increased respiration from soil and coarse woody debris, possibly reducing or negating CO₂ uptake increases. Climate differences between the study period and long term conditions are a likely factor causing differences between ecosystem carbon budgets estimated from long term forest carbon inventories and the short-term estimates of net carbon fluxes using eddy-covariance (EC) techniques [*Harmon et al.*, in review; *Paw U et al.*, in review]. The results of this study suggest that the most important climatic differences potentially affecting CO₂ dynamics are warmer winter temperatures, reduced transient snowcovers, and the timing of the late summer/autumn transition from dry to wet conditions. These hypotheses should be explored using process level measurements during seasonal transitions, coupled with integrated models of water and CO₂ dynamics.

The data also indicate that researchers must be careful when extrapolating data collected in the snowcover transition zone to other areas, interpolating from regional

conditions to individual sites, or when comparing sites that span a range of elevations in the snowcover transition zone. The year 1999 was characterized by record snowpack conditions in the Pacific Northwest, with a peak snowpack at 212% of the long-term (1961-1990) average in the Lewis River basin to the north of the site. During the same year, the snowpack at the open site never exceeded 30 cm, was discontinuous below the canopy, and only persisted for about 3 weeks during February. During that same year, other forested sites in the Wind River Experimental Forest at approximately 550 m elevation maintained a deep, continuous snowcover from approximately Feb 7 through Apr. 7. Similarly, hy2000 was characterized by below average snowcover conditions in the region (62% of average in the Lewis Basin to the north of the site), yet the site maintained a deeper snowpack relative to the previous years. These observations strongly suggest that researchers must consider intersite climate differences when attempting to extend the process knowledge gained at WRCCRF to the landscape scale, or to other sites.

Transient snowcovers may affect soil temperature in a variety of ways depending on climate conditions. A deep persistent snowcover will delay soil warming in spring months until snow is completely ablated. Closed canopy areas typically melt out before canopy gaps due to higher snowcover interception, but air and soil warming below the canopy will be delayed due to the large heat sink associated with the residual snowpack. During low snowcover years, higher closed canopy interception efficiencies produce a discontinuous snowcover. Bare soils may cool or freeze relative to insulated snow covered gap areas, but may also warm more rapidly in the spring months, depending on local climate conditions. In the transition

zone, snowcover dynamics and the soil thermal regime are closely linked and are very sensitive to slight perturbations in local climate. In this region, investigations of ecological processes that are controlled or strongly affected by the soil thermal regime should therefore be conducted over multiple years due to the wide range of conditions that can result due to inter-annual climate variability. Further study of snowcover processes and the effects of climate variability on the transient snowcover and soil temperature regime is needed to improve our understanding of process interactions in the transient snow zone.

2.4.1.3 Open Site vs. Above Canopy

Differences in air temperature between OPENSTA and STA70 are presented in Figure 2.5a. On average, the open site was 0.6 °C cooler than the above canopy station, and ranged from a mean monthly minimum of 0.1 °C cooler in May to a maximum of 1.4 °C cooler in October. Elevation differences between the two sensor installations would increase these difference by a maximum of 0.07 °C, based on the dry adiabatic lapse rate. The differences in mean monthly maximum and minimum air temperatures were small the winter months, but gradually increased in magnitude through the summer and autumn months. The increase in these differences through the year indicates that the diurnal air temperature cycle above the forest canopy became increasingly damped, reaching a maximum diurnal difference of 5.2 °C less than in the open area.

Wind velocities at STA70 were on average 1.5 times greater than wind velocities at OPENSTA (Figure 2.3d). The greater windspeeds observed at STA70 are probably a result of a greater uninterrupted fetch above the forest canopy, despite the

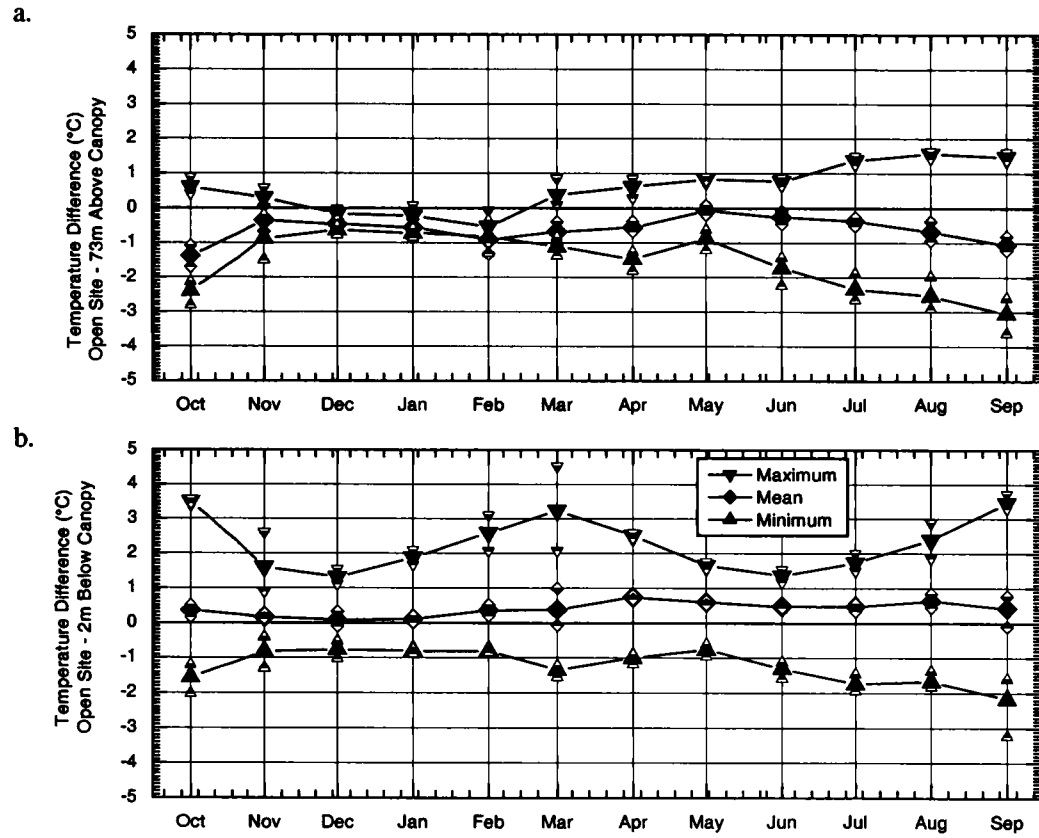


Figure 2.5. Air temperature differences between the WRCCRF climate stations.

fact that OPENSTA is located in the center of a large field, approximately 200 m from the nearest forest edge. Stronger heating of the air over the open field in summer would also be expected to produce unstable conditions, thereby reducing the vertical gradients of wind velocity relative to the more stable profile over the forest.

The warmer nighttime temperatures observed above the forest canopy may probably resulted from higher thermal radiation fluxes from the forest canopy since more solar radiation was absorbed by the forest (albedo (α) = 0.08, measured) than by the grassy area (α = 0.30, estimated). As soil moisture conditions progressively decreased throughout the year, transpiration at the open site also decreased, eventually approaching zero as the herbaceous vegetation senesced in mid summer. During this period, the albedo of the grass cover was also expected to increase, decreasing the net radiation. The resulting decrease in latent energy fluxes probably caused a greater portion of the net radiation to be partitioned into sensible heat and the amplitude of the diurnal temperature cycle to increase. Transpiration by the forest canopy also decreased, but to a lesser degree than the grass in mid to late summer, resulting in lower maximum temperatures at STA70 versus OPENSTA. Similar differences were observed over irrigated and non-irrigated regions resulting from latent flux differences [Allen, 1996]. Higher minimum air temperatures were also observed in irrigated regions as a result of higher dew point temperatures, relative to more arid non-irrigated areas. Dewpoint temperature differences between OPENSTA and STA70 were typically less than 0.5 °C, as would be expected for the small-scale landcover variations at WRCCRF. It is unlikely that the mean minimum air temperature differences would result from differences in dew point temperatures alone, and

therefore probably result from greater longwave radiation emission from the forest canopy.

The variations in air temperature, humidity and wind speed between the open site and above canopy station illustrate one source of error that may be introduced into numerical simulations of forest processes when using data collected at sites having different characteristics relative to the land cover of interest. The mean daily potential evaporation for the forest canopy was computed using both the Priestley-Taylor and Penman-Monteith methods to assess the potential magnitudes of these errors. Estimates were computed using R_n and u from STA70, and T_a and vapor pressure deficits (δe) from both STA70 and OPENSTA to assess the affect of the temperature and humidity differences on computed potential evaporation (PET). Errors associated with the windspeed differences were also expected to occur, however the computed evaporation was found to be insensitive to the windspeed differences within the range of observed magnitudes (~1% difference between the annual computed PET). For the Penman-Monteith estimate, a mean Douglas-Fir canopy conductance of 175 s m^{-1} was assumed [Monteith and Unsworth, 1990].

Estimated daily equilibrium evaporation rates and annual totals are presented in Table 2.2. The Priestley-Taylor method which is primarily radiation-driven, produced very similar results using data from both OPENSTA and STA70. The differences are caused by the influence of temperature on the terms controlling energy partitioning. Monthly computed differences ranged from -0.4 to -3.9% due to slightly cooler mean temperatures at OPENSTA. Differences in evaporation computed using the Penman-Monteith method were larger due to the combination of lower mean T_a and δe at the

Table 2.2. Potential evapotranspiration computation results

Method	Priestley-Taylor			Penman-Monteith		
	E (mm day ⁻¹)	E_{open} (mm day ⁻¹)	open – above canopy difference	E (mm day ⁻¹)	E_{open} (mm day ⁻¹)	open – above canopy difference
Oct	0.98	0.94	-3.9%	1.01	0.72	-29%
Nov	0.45	0.45	-0.6%	0.19	0.12	-38%
Dec	0.20	0.20	-1.8%	0.18	0.12	-29%
Jan	0.30	0.29	-2.0%	0.16	0.07	-54%
Feb	0.65	0.63	-3.3%	0.20	0.11	-46%
Mar	1.60	1.56	-2.5%	0.54	0.39	-29%
Apr	2.89	2.83	-1.9%	1.48	1.25	-16%
May	3.64	3.63	-0.4%	1.66	1.41	-15%
Jun	4.24	4.21	-0.6%	2.61	2.28	-13%
Jul	5.10	5.06	-0.8%	3.30	3.06	-7%
Aug	4.24	4.18	-1.3%	3.06	2.89	-6%
Sep	2.67	2.61	-2.3%	2.46	2.21	-10%
Total	822.8	811.8	-1.3%	515.5	447.6	-13%

open station. Percentage differences are greatest during the winter months (October – March) when PET is low, and range from -16% to -6% during the summer months (April – September) when PET is highest. On an annual basis, estimated PET was 13% lower when using OPENSTA data versus STA70 data. These results indicate that significant errors may result when using meteorological data collected at open sites to drive process models over vegetated land covers. Investigations using high temporal resolution meteorological data and physically-based process models are warranted to further assess the magnitudes of errors resulting from differences in open versus above canopy climate conditions.

2.4.1.4 Open Site vs. Below Canopy

The deep, high LAI canopy present at WRCCRF strongly influences the climate at the forest floor relative to open areas. Microclimatological studies of differences

between interior old growth forests and clearcuts near the WRCCRF found mean air temperatures to be 0.6 °C warmer in open areas relative to sub-canopy conditions, with a 4.7 °C reduction in diurnal variations in summer [Chen *et al.*, 1993]. The mean monthly differences between OPENSTA and STA02 are shown in Figure 2.5b. Mean monthly air temperature differences are consistent with the previous results, with the open site ranging from 0 °C to 1.0 °C warmer than the closed canopy site. The decreased diurnal range in below canopy air temperatures is also consistent with previous studies, and ranged from a minimum of 1.3 °C in November to a maximum of 6.5 °C in October. The greatest damping of diurnal air temperatures occurred in the spring and autumn when conditions were relatively clear, but when relatively little solar radiation penetrated the canopy due to low solar elevation.

RH at STA02 was higher than the OPENSTA humidity during all months, with absolute differences ranging from +21% in April to +2% in January. The mean RH difference for the June through September period was +3.7%, slightly less than previous observations of +8.5% [Chen *et al.*, 1993]. The largest between year variations in open to below canopy RH differences were in September, resulting from differences in the timing of the shift from summer to winter weather patterns.

Monthly mean below canopy windspeeds measured with the sonic anemometer were nearly constant at approximately 0.3 m s⁻¹ during the entire study period (Figure 2.3d). The mean below canopy windspeeds ranged from a maximum of 0.5 times the mean open site value in the winter to 0.25 times the mean open site value in the summer months.

Solar radiation at the forest floor is greatly reduced relative to open site conditions as expected for a deep canopy with a relatively high LAI (Figure 2.6). The

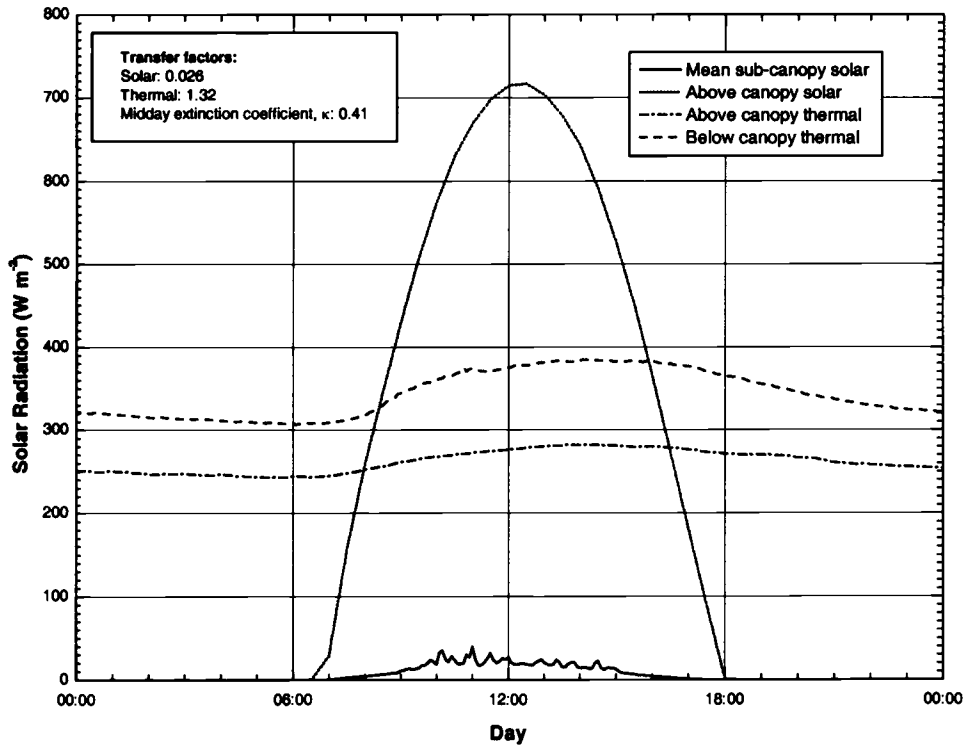


Figure 2.6. Above- and below-canopy solar and thermal radiation.

ratio of mean measured above to below canopy solar radiation for the three midsummer periods ranged from 0.026 to 0.058. The extinction coefficient κ , defined as:

$$\kappa = \ln \left(\frac{S_o}{S_f} \right) / LAI \quad (2.1)$$

where S_o is the solar radiation above the canopy, and S_f is the solar radiation at the forest floor ranged from 0.41 to 0.32 at midday. For comparison, κ was 0.46 for a *Pinus sylvestris* canopy with an LAI of 4.3, and 0.28 for a *Picea sitchensis* canopy with an LAI of 8.4 [Stewart and Baumgartner, respectively, in *Jarvis et al.*, 1976].

The ratio of below-canopy to above-canopy thermal radiation was 1.19 in early August, and 1.32 in late September. The seasonal variation in the thermal enhancement factor is consistent with higher upper canopy temperatures observed during the transitional periods.

Precipitation interception losses in summer were estimated to be 46% and 68% of gross precipitation for hy1999 and hy2000, respectively. The observed differences between years resulted from variations in precipitation regime, which strongly affected interception losses. These values are similar to other studies of similar canopies which found summer interception losses of 57% beneath old growth Douglas fir, 51% beneath old growth Douglas fir- western hemlock, and 40% below western red cedar [Rothacher, 1963]. The average direct throughfall proportion of 0.36 was derived from high temporal resolution throughfall measurements during 2000 [Link *et al.*, in review-b]. The canopy saturation storage capacity was estimated to range seasonally from 3.0 mm to 4.1 mm. These values compare with other measured saturation storage values of 2.1 mm for a Douglas fir plantation [Robins, 1974], and 1.5 mm for a single old-growth Douglas fir [Massman, 1983]. The relatively large storage capacity of the WRCCRF stand relative to other canopies probably results from a combination of high LAI and diverse epiphytic community that intercepted a large proportion of the gross rainfall.

2.4.2 Hydrology and Soil Conditions

Figure 2.7 presents the temporal trends of precipitation, snow depth in a canopy gap, shallow soil water content (θ), water table elevation, and stream discharge to show the timing and range of hydrologic variables at the WRCCRF. Precipitation is presented as the hourly intensity, recorded every 30 minutes. Individual data points and the site mean from the soil moisture array are plotted to show the average and range of variability of θ within the site. A continuous θ trend from one sensor which closely matched the site average is also included to provide a proxy for the site conditions (see below). Water table elevations were measured weekly at piezometer N1 located near the lowest elevation at the site (Figure 2.2).

The warmer and wetter conditions that occurred during the 1999 hydrologic year are evident in the shallower snowpack and higher streamflows, relative to hy2000. The wetter spring conditions in hy2000 resulted in the delayed drying of TABR Creek and groundwater decline relative to hy1999. The early stages of the record drought that occurred during hy2001 are shown by the lower precipitation frequency and magnitude, and delayed groundwater recovery in late 2000.

2.4.2.1 Soil Moisture

Mean 0–40 cm soil water content was characterized by wet conditions during most of the winter, with brief drainage periods between events and a progressive decrease caused by root water extraction through the dry seasons. During the growing season, shallow soil water content exhibited diurnal volumetric variations of 0.4 to

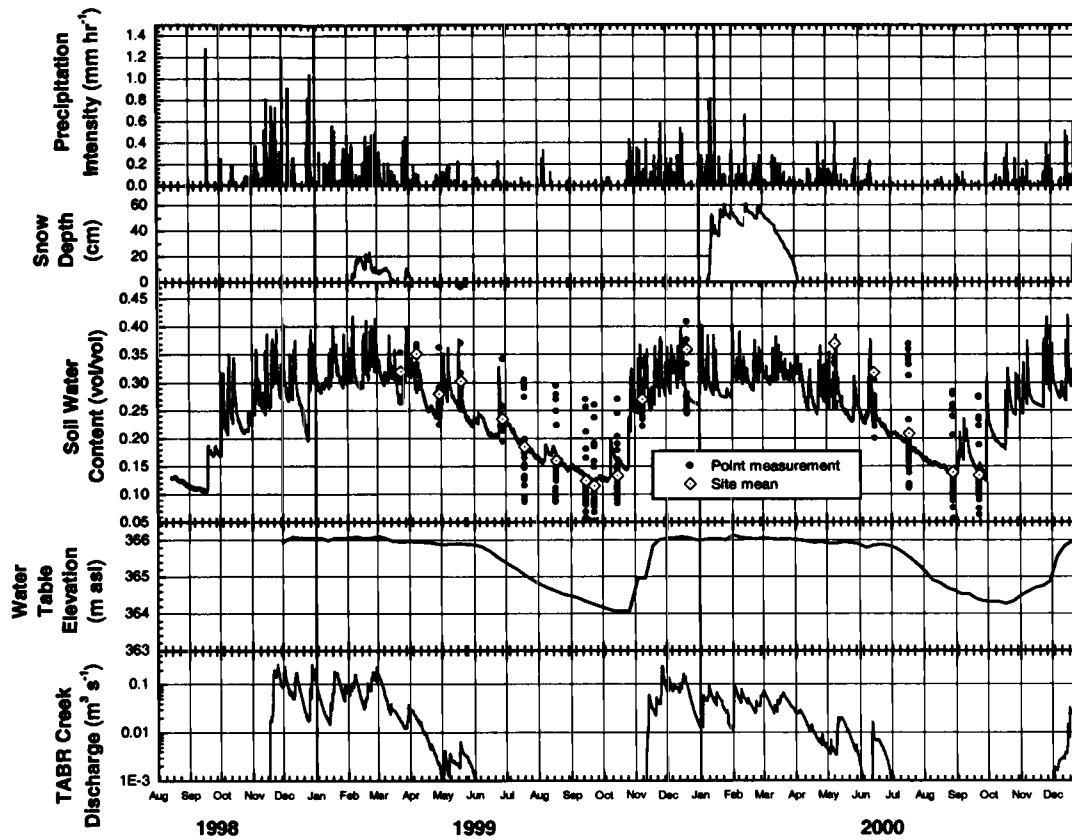
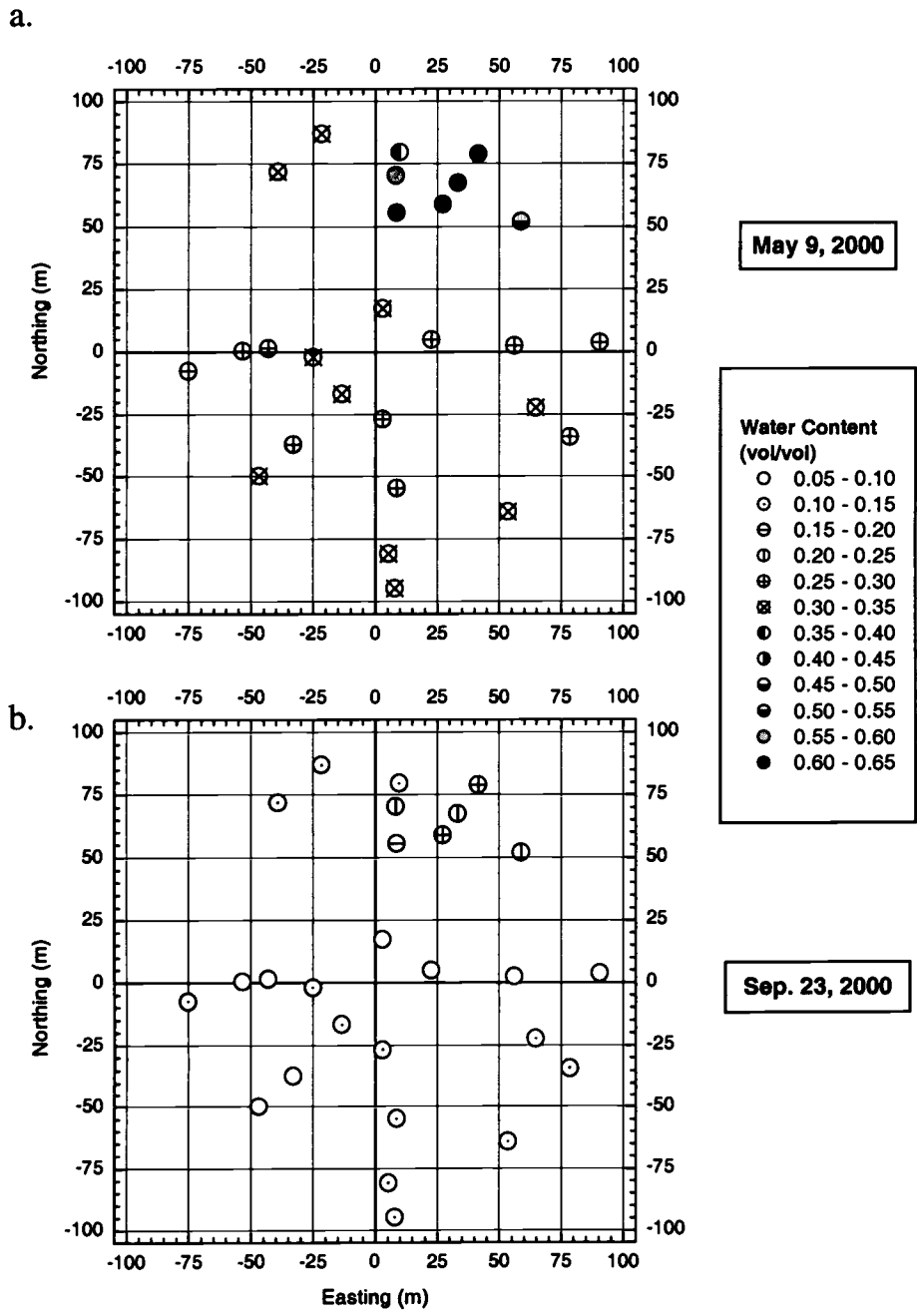


Figure 2.7. Precipitation intensity, snow depth, soil moisture, water table elevation and streamflow at WRCCRF, hy1999 - 2000.

0.7% during precipitation free periods. These periodic fluctuations probably resulted from hydraulic redistribution, where soil water that was earlier extracted by roots in deep soil was released from shallow roots at night [Dawson, 1993; Emerman and Dawson, 1996]. The redistributed water may be used by shallow-rooted understory plants the next day, or evaporated from the soil [Unsworth *et al.*, in review, Meinzer, pers. comm., Brooks, pers. comm..].

There was considerable range and variation of θ within the site ranging from 12% to 40% vol vol⁻¹ depending on the time of year. Much of the range in soil moisture resulted from persistent wet conditions in the northeast quadrant of the site (Figure 2.8). Variation between values in the three other quadrants of the site was within 10% volumetric θ over the course of the seasonal drydown. At the end of the winter wet season, θ in the northeast quadrant approached saturation values (~60%). Throughout the winter, water table depths ranged from 0.3 to 0.5 m in this quadrant. At the end of the drydown season, soils in the northeast quadrant exhibited relatively high θ (25-30 %), and water table depths ranged from 2.0 to 2.4 m below the surface.

Although the θ of surface soils did not appear to exhibit a coherent spatial pattern outside of the northeast quadrant, the θ of the deeper soil layers varied systematically with topographic position across the site. Figure 2.9 shows the temporal evolution of the soil water content profiles for hy2000 along the topographic gradient running from the southwest to the northeast quadrant (see Figure 2.2). In May, the entire soil profile at the low site was near saturation, whereas the high and mid sites showed θ increasing rapidly with depth (Figure 2.9a). At the end of the dry season in September, surface soils at the high and mid sites were similar, ranging from



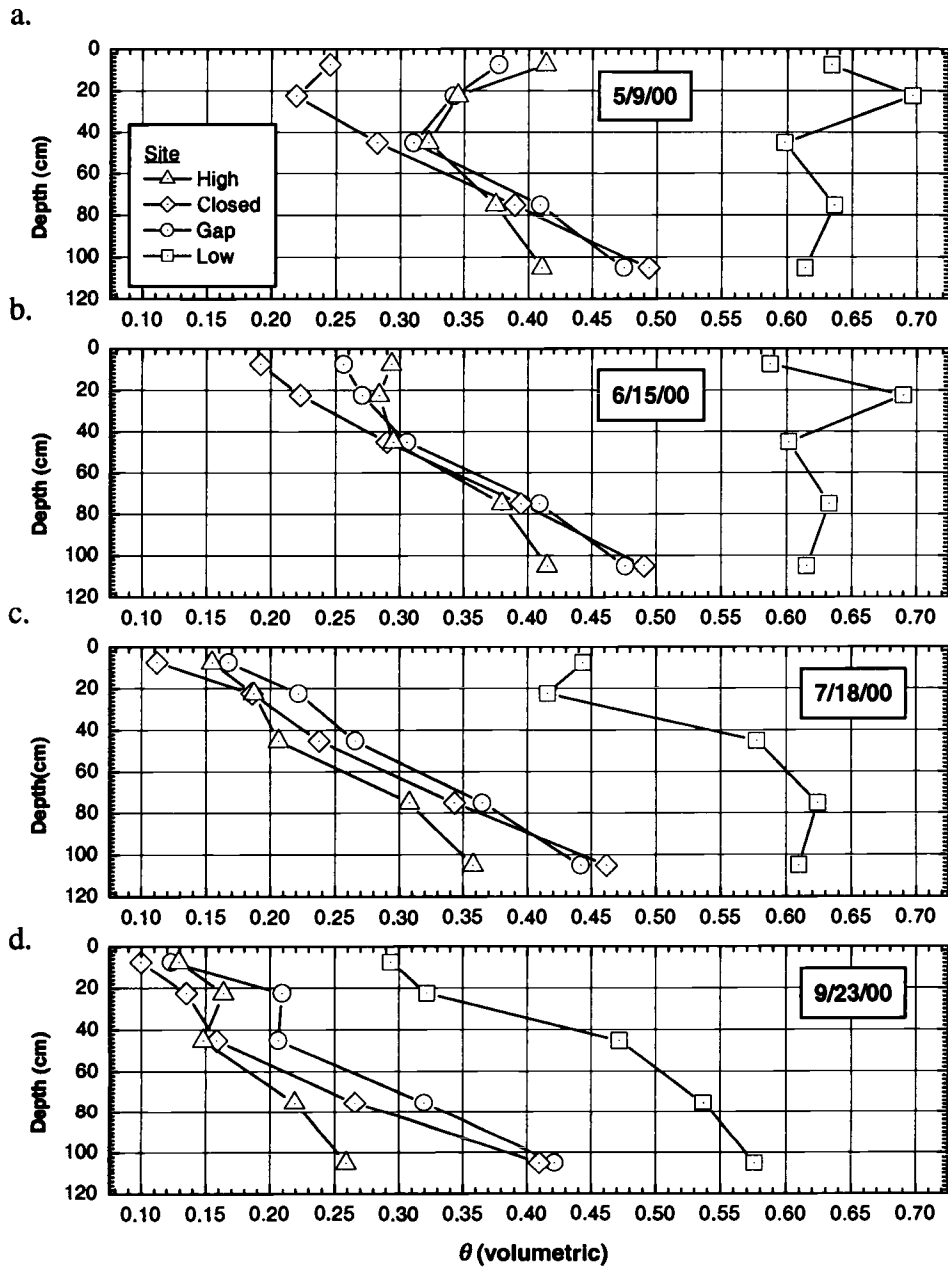


Figure 2.9. Temporal variation of soil water content profiles during the summer drydown period, hy2000.

~10% to 13%, but the deeper soils at the mid sites were ~42% compared to ~26% at the high site, as would be expected for soils where moisture is maintained by capillary rise later in the season (Figure 2.9d)..

Patterns of θ have several implications for the measurement of ecological processes and application of results at WRCCRF to other forests in the Pacific Northwest. The temporal evolution of spatial patterns of shallow θ suggest that canopy transpiration may be limited by low θ over much of the site, however trees in the northeast quadrant are not likely to be limited by available soil moisture, even late in the season. Above and below canopy eddy covariance measurements of ecosystem water fluxes may be affected by these heterogeneities in site conditions. Thus, EC measurements of ecosystem water fluxes may be relatively large when winds are from the north and east, rather than the optimal direction of fetch, to the west. Similarly, biological processes that are controlled by soil moisture status (e.g. respiration) are expected to vary strongly across the site, and may exhibit large variations over relatively short distances as a result of canopy interception processes and soil properties that influence water content.

2.4.2.2 Soil Temperature

The mean annual soil temperature (T_g) at 15 cm was 7.5 °C, at the closed canopy location, and ranged from a mean monthly minimum of 0.8 °C in March to a mean monthly maximum of 15.3 °C in August. Soil temperatures at 15 cm never reached freezing during the 1999 and 2000 hydrologic years, but shallower soil layers (0-5 cm) froze for about three days during an anomalous cold spell in December 1998. A slight

variation in the timing of soil warming was observed between the two years, where 15 cm soils exceeded 5 °C on April 17 (jd 107) in 1999 and on April 11 (jd 102) in 2000.

The largest within-site variation in soil temperature was expected to occur between dense closed canopy areas and canopy gaps, due to variations in snowcover depths and radiative transfer. Differences in soil temperatures between the gap and closed sites were greatest during periods of discontinuous snowcover below the canopy. The maximum 15 cm soil temperature difference between the closed and open sites was 3.0 °C due to greater snowcover deposition within the gap that effectively insulated soils during the onset of seasonal warming. Soil temperatures at the two sites were very similar after complete snowcover ablation, with the maximum mean monthly value of only 0.3 °C warmer in the forest gap.

Diurnal damping depths, defined as the depth where the temperature amplitude decreases to the fraction $1/e$ of the amplitude at the surface [Hillel, 1998], were computed for both sites over θ ranging from 24% to 9%. Despite the large range in θ , approximate diurnal damping depths ranged from 5.1 cm to 6.1 cm, characteristic of low bulk density soils with relatively low thermal conductivities [Hillel, 1998]. The relatively shallow diurnal damping depths indicate that diurnal intrasite microclimate variations arising from canopy cover variations will only influence the soil temperature regime near the surface. Annual damping depths were 132 cm and 99 cm for the gap and closed sites, respectively. The differences between the two sites are probably related to differences in θ and possibly soil properties, with the wetter gap site having a deeper damping depth. The deep soil temperature regime within the site

is therefore likely to be affected by θ , with the drier high site exhibiting shallower damping depths, relative to the wetter low sites.

2.5 Conclusions

Climate, canopy and θ conditions were presented for the 1999 and 2000 hydrologic years both above and below an old-growth Douglas fir/western hemlock forest, and in a nearby open field. Historical records indicate that precipitation amounts were close to average for both years, but that a greater than normal portion of the winter precipitation fell as rain, instead of snow. Nearby temperature records indicated that both winters were warmer than average, hence snow deposition zones increased in elevation. Comparison of T_a in the open field to T_a above the canopy showed a larger diurnal cycle in the open area, which increased throughout the summer apparently due to differences in net radiation and energy partitioning between the two sites. When mean open site T_a and RH data are used to estimate mean monthly potential evaporation using the Penman-Monteith method, differences from -6% to -54% occur relative to estimates using above canopy data.

Shallow soil water content varied considerably, both spatially and temporally. Wet conditions were maintained throughout the year in the northeast quadrant of the site, and in the deeper (>90 cm) soils at the mid to higher elevations. The distribution of soil water suggests that ecosystem processes controlled by soil moisture status may vary considerably across the site. Spatial variation in soil temperatures are limited to the shallow soil layers, and soil temperatures are expected to exhibit spatial similarity across the site during periods of either continuous, or no snowcover.

Observations completed at the WRCCRF indicate that site soils maintain fairly high soil water contents during the summer drought season. High θ is probably related to the location of the site, which is in a valley bottom, near a perennial wetland. Extrapolation of results from the WRCCRF site to larger scales should therefore be completed with caution, because the site may not be representative of nearby montane areas. Additional measurements are needed at larger scales, and beneath other canopies to assess the uncertainties associated with extrapolating results for the WRCCRF to other sites.

2.6 Acknowledgements

Support for this research was provided by the Western Regional Center (WESTGEC) of the National Institute for Global Environmental Change (NIGEC), the U. S. Forest Service, and the Agricultural Research Service, Northwest Watershed Research Center. Office and computing facilities were provided by the U. S. Environmental Protection Agency, Western Ecology Division.

**3. THE INTERCEPTION DYNAMICS OF A SEASONAL TEMPERATE
RAINFOREST**

Timothy Link
Mike Unsworth
Danny Marks

For submittal to the Journal of Hydrometeorology

3.1 Abstract

Net canopy interception (I_{net}) during the rainfall season in an old-growth Douglas fir-western hemlock ecosystem was found to be 22.8% and 25.0% of the gross precipitation (P_G) for 1999 and 2000, respectively. The average direct throughfall proportion (p) and canopy storage capacity (S) were derived from high-temporal resolution throughfall measurements in 2000, and were 0.36 and 3.32 mm, respectively. Derived values of S were very sensitive to the estimated evaporation during canopy wetting (I_w). Evaporation during wetting was typically small due to low vapor pressure deficits that usually occur at the start of an event, therefore I_w is best estimated using the Penman method during canopy wetting, rather than assuming a constant evaporation rate over an entire event. S varied seasonally, from an average of 3.0 mm in the spring and fall, to a maximum of 4.1 mm in the summer, coincident with canopy phenology changes. Interception losses during large storms that saturated the canopy accounted for 81% of I_{net} . Canopy drying after events comprised 47% of I_{net} , evaporation during rainfall comprised 33%, and evaporation during wetting accounted for 1%. Interception associated with small storms insufficient to saturate the canopy accounted for 19% of I_{net} . The Gash analytical model accurately estimated both I_{net} and the individual components of I_{net} in this system when applied on an event basis, and when the Penman method was used to compute evaporation during rainfall. The Gash model performed poorly when applied on a daily basis, due to a precipitation regime characterized by long-duration events, which violated the assumption of one rain event per day.

3.2 Introduction

The interception of precipitation by vegetation canopies is a major component of the surface water balance. Annual interception losses in temperate forests were observed to range from 11%-36% of gross precipitation (P_G) in deciduous canopies, and from 9% - 48% of P_G in coniferous canopies [Hörmann *et al.*, 1996]. The evaporation of intercepted water from forest canopies reduces the amount of water entering the soil profile, relative to other vegetation canopies [Calder, 1998]. Altered interception characteristics of vegetation are hypothesized to contribute to increased peak flows following forest harvest [Jones, 2000], and decreased streamflows during afforestation [Calder, 1998]. Interception reduces precipitation intensity but increases rainfall kinetic energy below forest canopies, potentially affecting soil erosion [Brooks and Spencer, 1995; Mosley, 1982]. Interception losses may also enhance the stability of large landslide complexes due to reduced groundwater recharge during winter [Miller and Sias, 1998].

Interception affects many biological processes that have important consequences for forest productivity and management. For example, at the leaf-scale, the duration of leaf wetness affects the spread of plant pathogens [Huber and Gillespie, 1992]. At the stand to regional scales, interception losses reduce the amount of water that would otherwise be available for root uptake, decreasing transpiration and altering biological processes. Questions regarding interconnections of forest hydrology to geomorphology, CO₂ dynamics, and forest pathogens are particularly important in the Pacific Northwest (PNW) region of the United States, where natural resource policy is being partly driven by environmental impacts associated with land management

practices. An improved understanding of how canopy structure and climate variability influence interception is therefore needed to assess the effects of climate variability on site hydrology and biological processes, to improve forest management in this region.

Net precipitation, or throughfall (P_n) below a vegetation canopy consists of the fraction of P_G that falls directly through the canopy (p), the fraction that drains from the canopy after the storage capacity of the canopy (S) is exhausted, and the proportion of P_G that is diverted to stemflow (p_t). Interception losses in closed canopies are largely controlled by S , p , the ratio of evaporation to rainfall during saturated conditions (E/R), and the temporal distribution of P_G that controls the number of canopy wetting and drying cycles. The total interception loss (I_{net}) for various canopies under a range of climate conditions can be used to estimate the approximate magnitudes of interception losses. However, the derivation of canopy interception and climate parameters S , p , and E/R is much more useful to predict interception losses under variable climate conditions, and may be used to parameterize interception models with a range of complexity.

A number of interception studies have been completed in tropical [Asdak *et al.*, 1998; Hutjes *et al.*, 1990; Jetten, 1996; Lloyd *et al.*, 1988], temperate broadleaf [Hörmann *et al.*, 1996; Neal *et al.*, 1993] and temperate conifer forests [Klaassen *et al.*, 1998; Rutter *et al.*, 1971] to assess I_{net} over a period of time, estimate the components of interception, and/or improve interception models. The majority of interception studies in temperate conifer canopies have been completed in relatively young plantation forests in Europe [Ford and Deans, 1978; Gash and Stewart, 1977; Gash *et al.*, 1980; Johnson, 1990; Kelliher *et al.*, 1992; Loustau *et al.*, 1992b; Rutter *et*

al., 1971; *Viville et al.*, 1993]. The objectives of previous investigations were mainly to assess the temporally-averaged canopy parameters, and most lack sufficiently high resolution throughfall and detailed within-canopy climate data to assess the influence of temporal changes in canopy structure and during-event climate variations that influence the evaporation of intercepted water. The determination of canopy parameters (e.g. S) at temporal resolutions associated with seasonal canopy structure variations is needed to improve our understanding of interception [*Loustau et al.*, 1992a]. Table 3.1 shows values of S for a variety of canopies in the literature to illustrate the general magnitudes of these quantities for different forests. More comprehensive summaries of interception losses and canopy parameters can be found in *Zinke* [1967], *Hörmann et al.* [1996], and *Llorens and Gallart* [2000].

Table 3.1. Literature values of conifer canopy storage capacities (S)

Canopy Type	S (mm)	Reference
<i>Pseudotsuga menziesii</i>	2.7-4.1	this study
<i>Pseudotsuga menziesii</i>	2.1	[<i>Rutter et al.</i> , 1975]
<i>Pseudotsuga menziesii</i>	1.5	[<i>Massman</i> , 1983]
<i>Pseudotsuga menziesii</i>	2.4	[<i>Klaassen et al.</i> , 1998]
<i>Pinus sylvestris</i>	1.02	[<i>Gash et al.</i> , 1980]
<i>Pinus sylvestris</i>	0.8	[<i>Gash and Morton</i> , 1978]
<i>Pinus sp.</i>	0.58-0.66	[<i>Loustau et al.</i> , 1992a]
<i>Picea stichensis</i>	3.68	[<i>Hutchings et al.</i> , 1988]
<i>Picea stichensis</i>	0.8-1.2	[<i>Gash et al.</i> , 1980]

Old growth ecosystems in the PNW are characterized by tall canopies, often exceeding 60 m in height, high leaf area index (LAI), large spatial variation in species diversity and canopy closure, abundant lichen and bryophyte communities, and large

quantity of coarse woody debris [Franklin and Waring, 1980]. Annual climate conditions are highly variable in this region and are characterized by extended periods of frequent rainfall in the winter, shorter periods of rain in the spring and autumn months, and isolated, brief showers during the summer. Canopy parameters derived for younger, predominantly plantation forests are unlikely to be applicable to the complex, highly heterogeneous ancient forests of this region. Furthermore, simplified canopy interception models developed and tested in other climates should be validated for the variable northwestern U.S. climate prior to widespread application in this region.

Previous studies in old-growth Douglas-fir ecosystems in Oregon found the net interception loss to be 14% of P_G for the months of October through April, and 24% of P_G for the period from May through September [Rothacher, 1963]. Studies of old-growth Douglas fir – western hemlock ecosystems on Vancouver Island, BC found annual interception losses to range from 20% to 40% of P_G over a 5.5 year period [McMinn, 1960]. Interception losses from the same stands during the summer ranged from 30% to 57% of P_G . Similarly, interception losses in second growth coast redwood and Douglas-fir in northern California are approximately 20% of winter P_G [Lewis et al.,]. Previous old-growth interception studies did not attempt to determine S or p for these systems. Detailed canopy interception characteristics are needed to improve our understanding of the interception process in these systems, to test generalized models, and ultimately lead to improved hydrologic models.

A variety of empirical, physically-based, and analytical models have been developed to estimate interception losses from climate data. The simplest models are

empirical; of the form $P_n = aP_G + b$, where a and b are regression coefficients [Zinke, 1967]. Empirical models are developed for a given set of conditions in specific vegetation covers, and are therefore of limited utility outside the conditions for which they were developed. Rutter developed a simple physically-based model that tracks a running canopy water balance to estimate I_n from derived or estimated canopy parameters (p and S), and computes E_s using the Penman method [Rutter *et al.*, 1971; Rutter and Morton, 1977; Rutter *et al.*, 1975]. The Rutter and similar models have been widely applied and tested in a range of environments and conditions [Gash and Morton, 1978; Jetten, 1996; Lankreijer *et al.*, 1993; Schellekens *et al.*, 1999].

Physically-based models require detailed, high-resolution meteorological data that are not widely available, therefore analytical models that combine the simplicity of the empirical models with a physical representation of the interception process have been developed to estimate P_n from P_G records and estimates of mean E/R ratios [Gash, 1979; Gash *et al.*, 1995; Gash *et al.*, 1980]. Other interception models account for the dynamic variation S as a function of drop size [Calder, 1996a; Calder, 1996b; Calder *et al.*, 1996; Hall *et al.*, 1996], or wind speed [Hörmann *et al.*, 1996] to provide more accurate estimates of I_{net} . These models require non-standard forcing data or empirical relationships that are difficult to define in the field, and are therefore of limited utility for estimating P_n from standard meteorological data.

This objective of this investigation was to evaluate the dynamics of rainfall interception processes in an old-growth Douglas fir / western hemlock seasonal temperate rainforest. This study builds on previous investigations of net throughfall in similar ecosystems [McMinn, 1960; Rothacher, 1963] to determine the key canopy

parameters for interception modeling and to evaluate how these parameters change seasonally. We also evaluated the performance of a simple analytical model [Gash, 1979] to estimate the interception losses in this system.

This investigation specifically seeks to: 1.) Empirically determine p and S for an old-growth conifer canopy at the precipitation event scale, and explore the effects of event characteristics on interception losses. 2.) Test the sensitivity of different techniques used to derive S from measured throughfall volumes. 3.) Determine the temporal variation in S . 4.) Compare the interception characteristics of old-growth forests to other forest canopies. 5.) Evaluate the magnitude of interception components in PNW old-growth forests. 6.) Test the validity of the Gash analytical model on a daily and event basis, using several methods to estimate E/R .

3.3 Methods and Materials

3.3.1 Site Description

This study was conducted at the Wind River Canopy Crane Research Facility (WRCCRF), located within the T.T. Munger Research Natural Area of the Gifford Pinchot National Forest, in southwestern Washington, USA (Figure 2.1.). The site is located on a gently sloping alluvial fan in the Wind River Valley in the Cascade Mountains at 45° 49' N latitude, 121° 57' W longitude, at an elevation of 367.5 m amsl. A tower crane is located in the center of the 4 ha² study plot, and is used for canopy access and as a sensor platform for micrometeorological measurements. The crane is 85 m high, with a jib range of 87 m that inscribes a 2.3 ha circular area within the plot where measurements were conducted. The physical setting, ecological

characteristics, and infrastructure of the WRCCRF are described in detail by *Shaw et al.* [in review].

The site is a 500-600 year old forest, dominated by Douglas fir (*Pseudotsuga menziesii*), western hemlock (*Tsuga heterophylla*), and western redcedar (*Thuja plicata*). Understory tree species include pacific yew (*Taxus brevifolia*), Pacific silver fir (*Abies amabilis*), and vine maple (*Acer circinatum*). Dominant species of the lowest layer include salal (*Gaultheria shallon*), Oregon grape (*Berberis nervosa*) and vanilla leaf (*Achlys triphylla*). The canopy height is approximately 60 m, with the tallest trees reaching 65 m [*Ishii et al.*, 2000]. The canopy exhibits many old-growth characteristics, including a high degree of spatial heterogeneity in species and canopy depth, a multi-layered canopy, and high degree of biodiversity in the plant community [*Franklin and Spies*, 1991]. A high diversity of non vascular plants exist in the canopy, dominated by lichens (~1.3 metric tons ha⁻¹) in the mid and upper canopy and a similar amount of bryophytes in the lower canopy [*McCune et al.*, 1997]. The presence of canopy epiphytes is important for interception processes, because lichens and mosses can absorb roughly 6 to 10 times their dry weight of water [*McCune*, pers. comm.]. Hence, these components of the ecosystem can absorb 2-3 mm of water [*Unsworth et al.*, in review], and intercept additional amounts on their foliage. The average (over 3 years) LAI of all species at the site was 8.6 ± 1.1 , ranging from 9.3 ± 2.1 to 8.2 ± 1.8 using the vertical line intercept method [*Thomas and Winner*, 2000].

Climate at the site is characterized by cool, wet winters and warm, dry summers, with an average annual precipitation of 2467 mm (Table 3.2). Less than 10% of the precipitation occurs between June and September [*Shaw et al.*, in review]. Average

Table 3.2. WRCCRF mean climate conditions, 1999 and 2000.

Month	T_a (°C)		precipitation (mm)		
	1999	2000	1999	2000	1931-1977
January	2.4	0.3	359	404	429
February	1.8	1.2	621	383	308
March	3.2	3.1	168	140	293
April	6.3	8.6	23	95	147
May	9.3	11.1	131	139	91
June	13.6	15.3	28	100	61
July	17.3	17.2	5	0	17
August	18.1	17.0	23	3	32
September	13.6	13.7	3	67	73
October	8.4	8.4	175	103	203
November	6.3	1.5	569	132	365
December	2.1	-0.3	451	193	447
Mean/Total	8.5	8.1	2559	1759	2467

annual snowfall is 1806 mm, most of which falls from November to March. Fog is rarely observed at the site, and input of occult precipitation is assumed to be negligible. Mean annual air temperature is 8.7 °C, with the mean monthly maximum of 17.3 °C occurring in August, and the mean monthly minimum of -0.1 °C in January. The snow-free period below the forest canopy for the 1999 and 2000 years ranged from April 5, 1999 through January 10, 2000, and from April 4 through December 21, 2000 [Link *et al.*, in review-a]. Precipitation conditions during this period were close to average, except during the fall of 2000, which was significantly drier (41%) than average. This drier period was advantageous for the determination of canopy interception parameters, because precipitation events were isolated between extended periods of dry weather, permitting the canopy to completely dry between events.

3.3.2 Throughfall Measurements

Throughfall was measured using two roving arrays of rain gauges to reduce errors in throughfall sampling by increasing the number of sampling points within the plot [Lloyd and Marques, 1988; Wilm, 1943]. One array contained 24 automatic tipping bucket rain gauges (TE-525I, Texas Electronics Inc., Dallas, TX) equipped with individual data loggers (HOBO Event, Onset Computer Corp., Bourne, MA). Gauges had a 325 cm² collection area, and were calibrated to record 0.254 mm per tip. A second array of 44 manually measured throughfall collectors with a 94 cm² collection area, and total storage capacity of 400 mm was used to measure total throughfall over extended periods. The manual array was operated from April 8 to November 8, 1999 and from March 30 to June 16, 2000. The tipping bucket array was operated from March 30 to December 4, 2000. The total throughfall volumes measured by the automatic and manual arrays were 262.6 mm and 257.1 mm (2.1 % difference) during the period when both arrays were run concurrently, confirming that the two arrays measured comparable P_n . During the 1999 and 2000 sampling periods, precipitation was 62% and 65% of the long-term average, respectively.

Gauges were located using a nested random sampling design along 4 radial transects (Figure 3.1). Transects were established along boardwalks, placed to minimize site impacts. Each gauge was randomly located within each 25 m section of the transects to provide even coverage of the entire plot while capturing the full range of scales of variation. Gauges were randomly relocated every 4 to 8 weeks depending on the number of precipitation events occurring in the preceding sampling period. Gauges were mounted approximately 1 m above the ground to minimize collection of

splashed water and debris. Gauge funnels and tipping buckets were cleaned and leveled after each relocation.

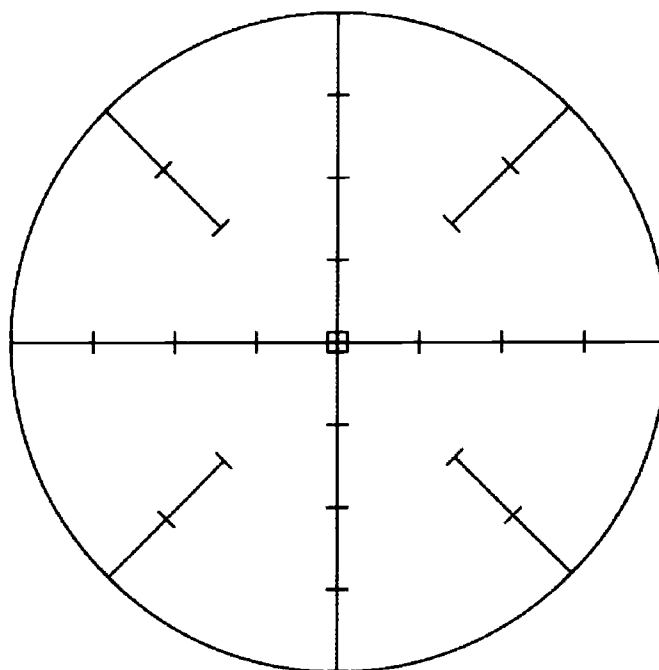


Figure 3.1. Schematic throughfall sampling scheme. 1 tipping bucket precipitation gauge was randomly located within each 25 m quadrat. The diameter of the 2.3 ha crane circle is 200 m.

3.3.3 Meteorological Data Collection

Gross precipitation was measured with a tipping bucket gauge at a meteorological station located in an open area approximately 500 m to the south of the crane plot. Additional precipitation instrumentation at the open site included an alter-shielded weighing precipitation gauge (Model 5-780, Belfort Instrument Co., Baltimore, MD) and sonic snow depth sensor (Judd Communications, Inc., Logan, UT), recorded at half-hour intervals on a datalogger (CR-10X, Campbell Scientific,

Inc., Logan, UT). The supplemental records were used to validate the tipping-bucket record, and to identify snow events, respectively.

Downwelling and upwelling solar (R_S) and thermal (R_L) radiation was measured with a 4-component net radiometer mounted at the highest point on the crane, 85 m above the ground (Model CNR-1, Kipp and Zonen Inc, Bohemia, NY). A series of meteorological stations were installed on the crane tower at 73 m, 57 m, 40 m, 23 m and 12 m above the ground. A sub-canopy station was located approximately 25 east of the crane tower, with sensors installed at 2 m. Air temperature (T_a) and relative humidity (RH) sensors (Model HMP35C, Vaisala Inc., Sunnyvale, CA) were installed in modified Gill multi-plate radiation shields that were mechanically aspirated using a small computer fan to draw air through the top of the shield. Wind velocities (u) were measured with a 3-dimensional sonic anemometer (Gill Solent HS, Lymington, UK) at 73 m and with 2-dimensional sonic anemometers (Gill Solent R2) at a 57, 40, 23, 12 and 2 m stations. The sonic anemometers operated acceptably during low rainfall rates, but data quality was observed to degrade at higher rainfall rates [Paw U *et al.*, in review].

3.3.4 Methods for Calculation of Interception Parameters

3.3.4.1 Theory

When a rainfall event begins, throughfall is composed entirely of the direct component (i.e. rainfall that has not contacted the foliage), and P_n will increase relative to P_G at a constant rate < 1 , until the canopy becomes saturated (Figure 3.2).

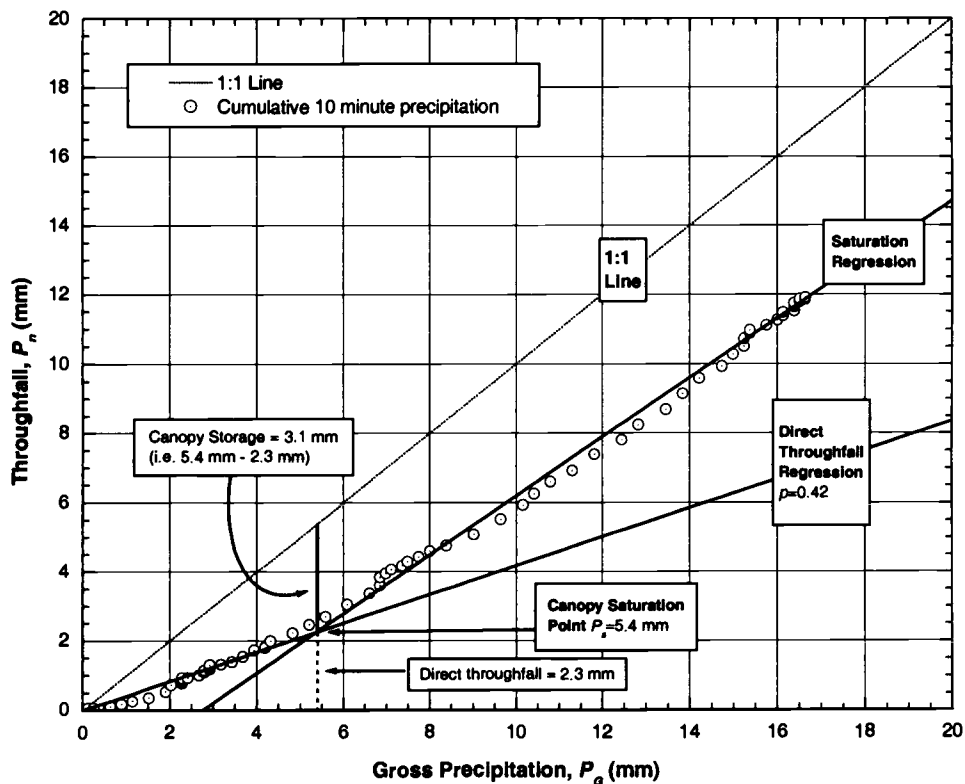


Figure 3.2. Example event plot of data used to determine canopy direct throughfall proportion and saturation storage capacity.. Linear regressions are fit to a scatterplot of throughfall versus gross precipitation, by optimizing the fit of equations (3.1) and (3.2).

Once the canopy becomes saturated at $P_G = P_s$, an inflection point is reached, and the P_n rate increases. After the canopy is saturated, the slope of the P_n - P_G curve will be unity if there is no evaporation, will be <1 if evaporation during rainfall is occurring, or could be greater than 1 if occult precipitation interception exceeds evaporative losses. Throughfall components are described based on the conceptual model developed by Gash [1979], where the throughfall during canopy wetting is given:

$$P_n = pP_G, \quad P_G < P_s \quad (3.1)$$

The throughfall after saturation is reached is given:

$$P_n = pP_s + \left(1 - \frac{E}{R}\right)(P_G - P_s), \quad P_G \geq P_s \quad (3.2)$$

where E/R is the ratio of evaporation to rainfall during saturated canopy conditions. S is computed:

$$S = (1 - p)P_s - I_w \quad (3.3)$$

where I_w is intercepted precipitation that is evaporated during canopy wetting. I_w can either be assumed negligible, estimated using the Penman method (described in Section 4.5.2), or estimated as $(E/R)P_s$ assuming that E/R is constant throughout the entire event. Constant E/R during precipitation was typically assumed in many historical interception studies.

Canopy interception parameters are commonly derived from the relationship between cumulative P_G and P_n volumes collected on a weekly or event basis [Gash and Morton, 1978; Klaassen et al., 1998; Leyton et al., 1967; Rowe, 1983]. Using the simplest method (minimum method), the canopy saturation point is estimated by identifying the inflection point in the $P_n:P_G$ relation subjectively, and a line with slope = 1 fit to events with minimal evaporation (Figure 3.3). S is then determined from the intercept with the x-axis, and p as the slope of the regression line for all points less than P_s . S can also be computed using an iterative least squares fitting procedure on (3.1) and (3.2) to optimize the values for p , P_s , and E/R (mean method). Modifications to this method have been made to account for lower evaporation during

partial canopy saturation [Gash *et al.*, 1995], however it has been shown that this refinement has minimal impact on the derived value of S [Klaassen *et al.*, 1998].

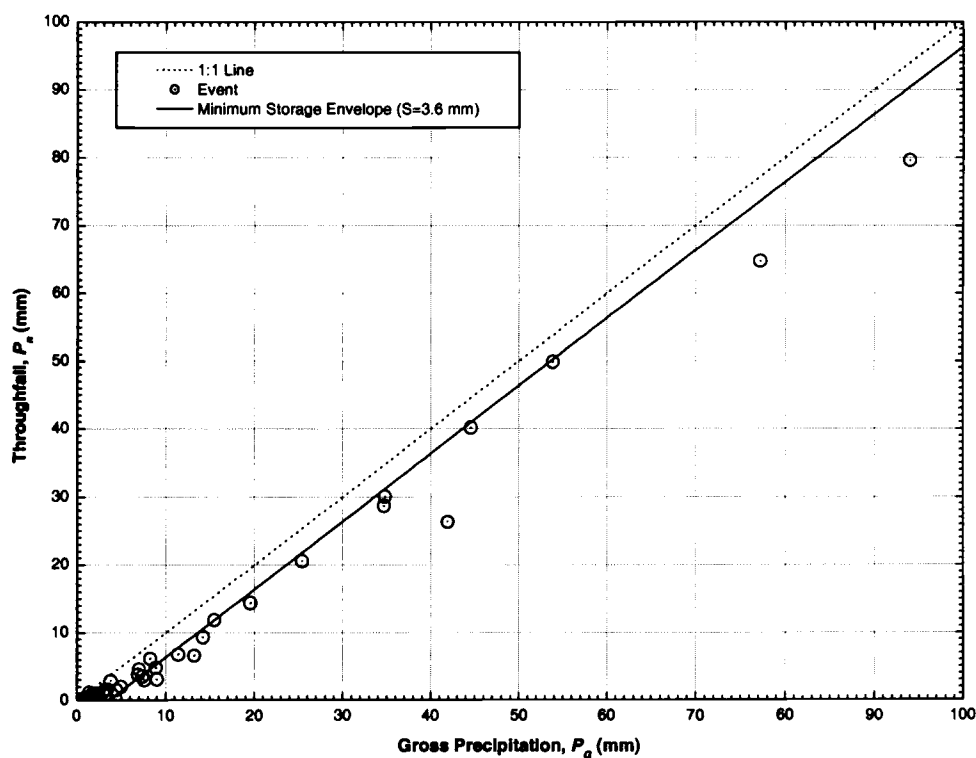


Figure 3.3. Canopy saturation storage capacity estimated using the minimum method.

3.3.4.2 Derivation of Canopy Parameters

For this analysis, precipitation events were defined as cumulative gross precipitation exceeding 0.5 mm, with a minimum of 6 hours without precipitation between events. Cumulative precipitation records for each gauge and event were manually evaluated to identify gauges that had clogged or failed during an individual event. The average P_n was computed for each event from all functioning throughfall gauges. Clogging of gauge funnels by ice was observed in the field and in the gauge

records during late autumn when nighttime temperatures dropped below 0 °C. Several late-season events were therefore eliminated from the analysis during this time period.

Canopy interception parameters were derived using the minimum method from P_G to P_n ratios for all events measured with the automatic array in 2000. Interception parameters were also derived from 10 min resolution P_G and P_n records for each event, using the iterative least squares method described above. Canopy storage capacity was determined for each event exceeding 10 mm P_G , and preceded by a minimum dry period of 24 hours, to assure that the forest canopy was completely dry prior to wetting. Although the canopy is likely to saturate at $P_G < 10$ mm, the higher threshold was used to assure a distinct inflection point for the determination of P_s using the optimization technique. To test the sensitivity of S to I_w , S was computed from (3.3) by three methods. I_w was assumed negligible, estimated from E/R , and computed using the Penman method. The parameter p and ratio E/R ratio were determined from the slopes of the regression lines in (3.1) and (3.2), respectively.

Previous studies in old-growth ecosystems indicated that stemflow (p_t) was about 0.3% of P_G [Rothacher, 1963]. Other studies of coniferous forests also found stemflow to be a minor component of the water balance of mature canopies, where stemflow was roughly 2% of P_G in a 63 year old stand [Johnson, 1990]. The presence of a large epiphyte community was also noted to decrease stemflow [Scatena, 1990], therefore we assumed stemflow to be negligible in this ecosystem.

3.3.5 The Gash Analytical Model

The Gash analytical model is a useful tool to estimate I_n , and explore how it is influenced by climate, because it can be applied with a reasonable degree of confidence given estimates of S , p and E/R , and measured event or daily precipitation data [Gash, 1979; Gash et al., 1995; Gash et al., 1980]. The model typically assumes that: 1.) Only one event occurs per day; 2.) Rainfall may be represented by a succession of discrete storms, separated by periods to allow the canopy to completely dry; and 3.) Rainfall and evaporation rates are constant for all periods of rainfall. The model also includes a formulation for stemflow and evaporation of water stored on wetted trunks. In this evaluation, we make the assumption that stemflow is negligible, and implicitly include the storage associated with branches and trunks into the derivation of S .

3.3.5.1 Interception Components

For this investigation, we computed the interception components by applying a simplified version of the Gash analytical model [Gash, 1979], containing the assumptions noted above. The amount of interception for m small storms insufficient to saturate the canopy (I_c) is computed:

$$I_c = (1 - p) \sum_{j=1}^m P_{G,j} \quad (3.4)$$

The amount of interception for n large storms $\geq P_s$ is estimated by computing the interception occurring during wetting up of the canopy (I_w), the evaporation during canopy saturation (I_s), and the evaporation after rainfall ceases (I_a), given by:

$$I_w = n(1-p)P_s - nS \quad (3.5)$$

$$I_s = (E/R) \sum_{j=1}^n (P_{G,j} - P_s) \quad (3.6)$$

$$I_a = nS \quad (3.7)$$

The net interception loss (I_{net}) is computed:

$$I_{net} = I_c + I_w + I_s + I_a \quad (3.8)$$

The mean amount of precipitation necessary to saturate the canopy (P_s) is derived from interception theory presented by *Gash* [1979], and is computed:

$$P_s = -\frac{RS}{E} \ln[1 - (E/R(1-p))] \quad (3.9)$$

3.3.5.2 Evaporation

The mean evaporation rate can be estimated either using the slope of linear regression relating P_G to P_n when the canopy is saturated, or the Penman equation [*Loustau et al.*, 1992a; *Pearce and Rowe*, 1981]. Evaporation (E) during rainfall is computed using the Penman equation, assuming negligible soil and storage fluxes:

$$E = \frac{\Delta R_n + \rho_a c_a \delta e g_{a,H}}{\lambda(\Delta + \gamma)} \quad (3.10)$$

where Δ is the slope of the saturation vapor pressure/temperature curve ($\text{Pa } ^\circ\text{C}^{-1}$), R_n is the net radiation (W m^{-2}), ρ_a is the density of air (kg m^{-3}), c_a is the specific heat of air ($\text{J kg}^{-1} ^\circ\text{C}^{-1}$), δe is the vapor pressure deficit of the air (Pa), $g_{a,H}$ is the aerodynamic conductance for heat (s m^{-1}), λ is the latent heat of vaporization (J kg^{-1}), and γ is the psychrometric constant ($\text{Pa } ^\circ\text{C}^{-1}$). The aerodynamic conductance for heat is computed:

$$g_{a,H} = k^2 u / \left[\ln \left\{ \frac{(z_s - d)}{z_{0,M}} \right\} \ln \left\{ \frac{(z_s - d)}{z_{0,H}} \right\} \right] \quad (3.11)$$

where k is the von Kármán constant (0.4, dimensionless), u is the wind speed (m s^{-1}), z_s is the measurement height (m), d is the zero plane displacement (m), $z_{0,M}$ is the roughness length for momentum (m), and $z_{0,H}$ is the roughness length for heat (m).

The roughness lengths are computed from canopy height (h) using the relationships described by *Lankreijer et al.* [1993], after *Gash* [1979] and *Garratt and Francey* [1978], where:

$$z_{0,M} = 0.1h, \text{ and} \quad (3.12)$$

$$z_{0,H} = z_{0,M} e^{-2} = 0.14z_{0,M} \quad (3.13)$$

Application of separate roughness lengths for heat and momentum is recommended for interception studies to prevent the overestimation of evaporation during rainfall [*Lankreijer et al.*, 1993].

Seasonal variations in evaporation rate and canopy structure parameters can be incorporated by parsing the larger time period of interest into periods of homogeneous conditions and using separate parameterizations for each period. Evaporation rates may be closely related to precipitation and climate variations occurring during individual events rather than between seasons, therefore, in many environments the application of a constant evaporation rate is appropriate. For this investigation, we estimate E/R using both the regression and Penman techniques, and assume E/R is constant for the entire study period to evaluate the sensitivity of the model to this parameter.

3.4 Results and Discussion

The results obtained in this study include high spatial and temporal resolution throughfall data and a detailed vertical profile of the meteorological variables that control interception and evaporation during rainfall. The high temporal resolution throughfall data enable the investigation of how saturation storage changes over the course of a season in a conifer canopy. S is normally considered to be static in conifer canopies [Gash *et al.*, 1980; Rutter *et al.*, 1975], however LAI varies seasonally with phenological development, and may change as a result of storm damage [Thomas and Winner, 2000], thereby affecting S . S variations at WRCCRF were also affected by the presence of deciduous understory species (mainly vine maple) that undergo a large seasonal change in leaf area.

3.4.1 During Event Climate and Precipitation Variability

Detailed precipitation and within canopy climate data for events with low evaporation (event 30) and with relatively high evaporation (event 15) are shown in Figures 3.4 and 3.5, respectively. These figures illustrate the effect of the forest canopy on throughfall intensity, and exemplify the range of conditions controlling evaporation during precipitation events.

Event 30 (Figure 3.4), began at 2100h on September 29 at and lasted 31 hours. During this period, over 53 mm of precipitation occurred. The event was characterized by relatively low precipitation intensity, low net radiation and wind speeds, and very low δe . Total interception loss was 4.0 mm, principally from canopy drying after the event. Event 15, shown in Figure 3.5, began at 0310h on May 9, and

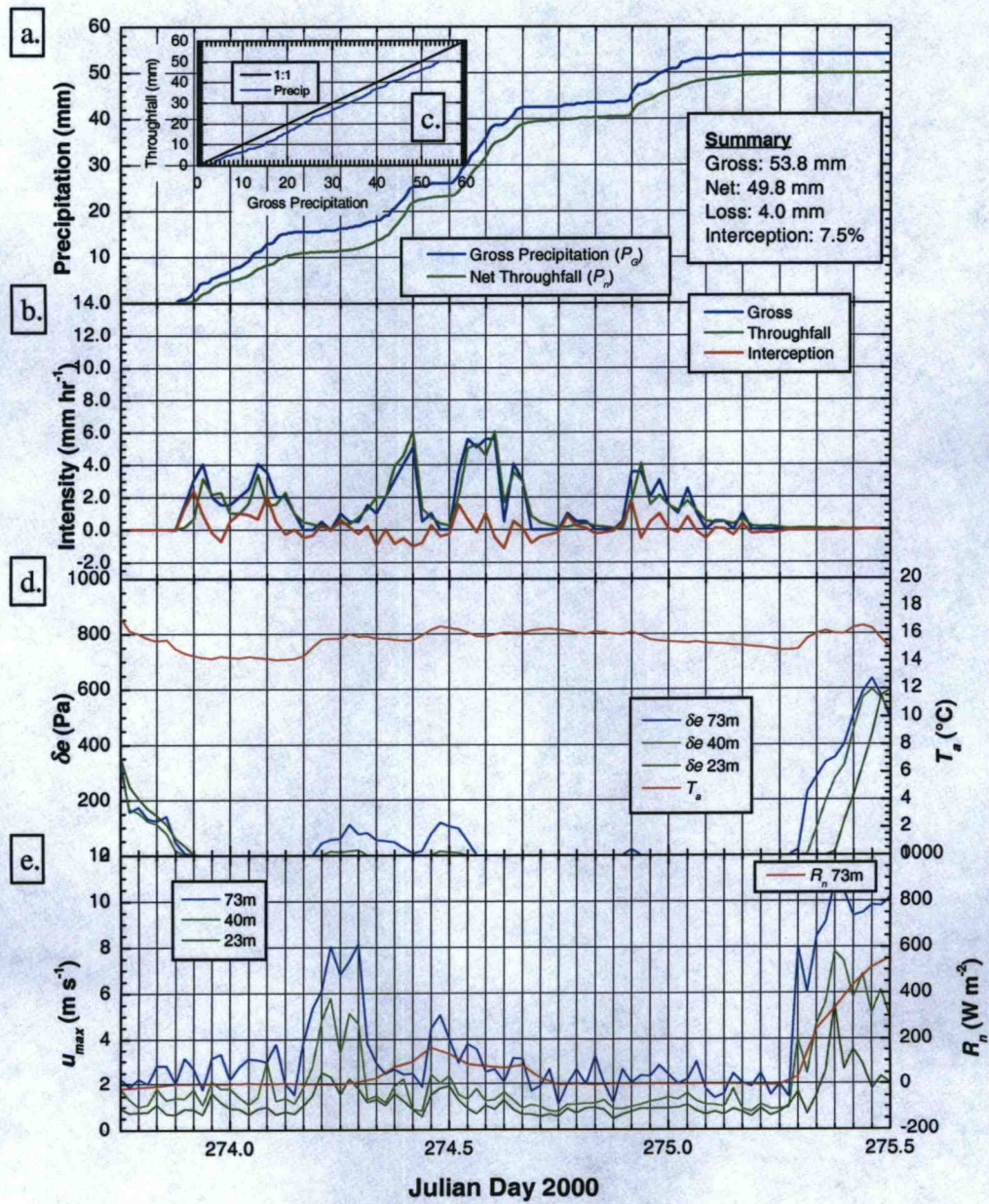


Figure 3.4. Detailed meteorological data for a precipitation event with low evaporation (Event 30).

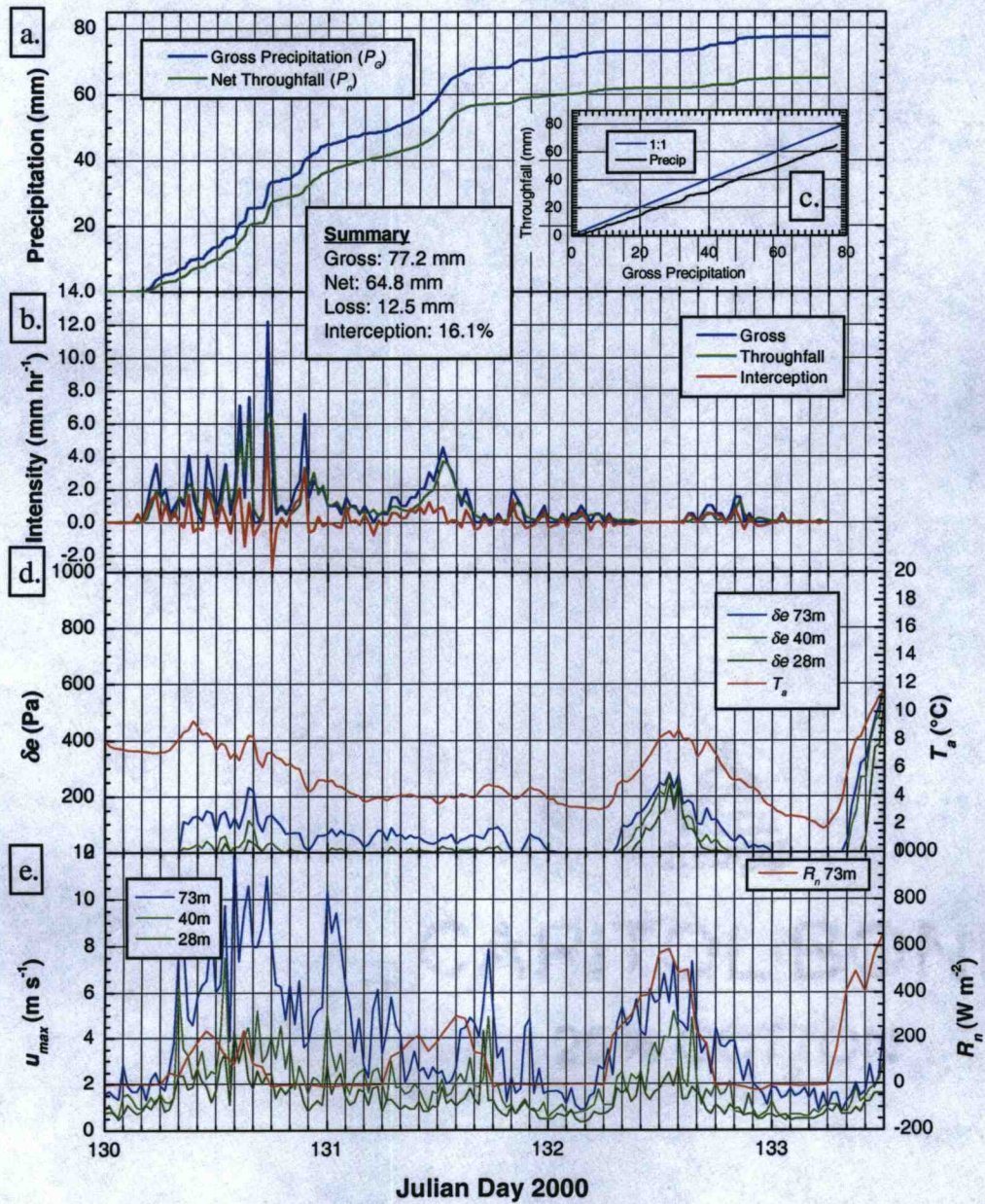


Figure 3.5. Detailed meteorological data for a precipitation event with relatively high evaporation (event 15).

lasted 70 hours. During this period, over 77 mm of precipitation occurred. This event was characterized by high winds with several brief pulses of intense precipitation, relatively high net radiation, and a consistent and fairly large δe .

In both figures, the cumulative P_G and P_n over time are shown in plot a. Both events illustrate the typical time lag of 1-2 hours between significant cumulative P_G and P_n , associated with wetting up of the canopy. Plot b. shows the mean P_G , P_n and interception intensities, computed over half hour intervals to smooth the noise associated with the 10 minute data. The interception intensity is the rate at which the canopy storage is changing, computed as the difference between P_G and P_n for each time interval. Positive values indicate that the canopy is gaining water; negative values indicate that the canopy is losing water. Canopy wetting at the beginning of each event is indicated by a period where interception intensity is positive. Once the canopy is saturated, interception intensity oscillates around zero, probably as a result of a combination of S briefly decreasing during high winds and due to the temporal lag between periods of canopy supersaturation and drainage caused by variability in precipitation intensity. This oscillation is more intense for Event 15 which had very high wind speeds and large short-term variation in precipitation intensity, while Event 30 shows a more damped oscillation. The dynamic relationship between wind speed and canopy storage has been observed in other detailed studies [Hörmann *et al.*, 1996]. While a dynamic relationship between S and precipitation intensity has been hypothesized and is included in physically-based interception models [Rutter *et al.*, 1971; Rutter *et al.*, 1975], these data are some of the few actual observations of this relationship that we are aware of.

The inset Figure c. in both Figures 3.4 and 3.5 is a graph of cumulative P_n vs. P_G to illustrate the effect of the forest canopy on the volume of throughfall received at the forest floor. The inflection point where direct throughfall shifts to saturated canopy throughfall is evident on both insets. The saturated throughfall line in Figure 3.4c has a slope (R/E) of 1.00, indicating that insignificant evaporation is occurred during this event. The higher rate of evaporation that occurred during event 15 is indicated by R/E of 0.86, shown in Figure 3.5c.

Meteorological conditions above and within the forest are shown in plots d. and e. Plot d. shows the air temperature (T_a) measured at 73 m, and δe at 73 m, 40 m and 23 m. Plot e. shows the net radiation (R_n) measured at 85 m and the maximum half-hourly wind speeds (u_{max}) at 73 m, 40 m, and 23 m. Maximum wind speeds are presented because mechanical dislodging of intercepted water is likely to be a function of the maximum, rather than the mean wind speed. Net radiation data are included to provide an indication of radiation variations during precipitation events.

The microclimate differences that account for there being virtually no evaporation during event 30, and relatively large evaporation during event 15 can be observed by comparing plots d. and e. between Figures 3.4 and 3.5. During event 30, δe at 73 m decreased prior to the event, and remained close to zero for the duration of the event. Very small δe values at the beginning of events are typical of most events, and are hypothesized to occur due to evaporating raindrops [Klaassen *et al.*, 1996]. The vapor pressure deficit within the canopy was also very small throughout the entire event, indicating that negligible evaporation could occur, as observed in the throughfall record. During event 15, δe above 40 m was greater than zero during most

of the event, wind speeds were relatively high, and R_n was positive during the day, indicating a relatively high potential for evaporation. Increases in T_a can also produce δe values that extend through the entire canopy, as occurred during day 132. The δe increases, coupled with the associated R_n and u increases, caused the canopy to partially dry and rewet during the event, thereby producing the relatively large interception losses observed in the P_n record. Events characterized by periods of rainfall punctuated by brief periods of clearing and warming, such as is common with post-frontal showers in the PNW are therefore more likely to have higher interception losses than frontal storms characterized by continuous cloud cover and precipitation.

Evaporation during rainfall may also be influenced by other processes. Brief advection events can replace the air within the canopy with air from higher levels in the boundary layer [Paw U *et al.*, 1992]. Other studies have noted that large-scale advection frequently augments the energy necessary to produce observed latent heat fluxes in saturated forest canopies [Calder, 1998; Klaassen *et al.*, 1998]. Advection events may not be captured in the half-hour resolution scalar climate variables measured on the crane tower, but may strongly affect the evaporation of intercepted water. Replacement of cool, humid air in the canopy with warmer, drier air from aloft may cause the canopy to dry rapidly during brief hiatuses in precipitation.

3.4.2 Throughfall and Interception Loss

Table 3.3 summarizes the gross precipitation and throughfall (and hence by difference, interception loss) for the entire 1999 and 2000 measurement periods. P_G , P_n , I_{net} , and percent losses for the 43 events that occurred in 2000 are presented in

Table 3.3. Precipitation and interception summary

Measurement Period	P_G (mm)	P_n (mm)	I_{net} (mm)	% I_{net}
Apr. 8 – Nov. 8, 1999	450.9	348.2	102.7	22.8
Mar. 30 – Dec. 3, 2000	618.7	398.0	155.0	25.0

Table 3.4, to show the variability in event characteristics. Estimated ratios of E/R from the throughfall record for events exceeding 10 mm are also shown in Table 3.4. I_n was 22.8% and 25.0% of P_G for the measurement periods in 1999 and 2000, respectively, despite differences in P_G and measurement periods. In 2000, I_{net} was 28.0%, 69.4%, and 18.0% of P_G for the spring, summer, and autumn periods respectively; and are similar to values obtained in previous studies [McMinn, 1960; Rothacher, 1963]. Table 3.4 shows that interception losses are highly variable, and are closely correlated with event size, decreasing as event magnitude increases. The sampling periods were selected to cover periods unaffected by snowfall and mixed phase events when precipitation is highest (see Table 3.2), therefore annual percent I_{net} is expected to be less than observed during our study periods.

The average evaporation rate during saturated canopy conditions (E_s) was 0.14 mm hr⁻¹, and rates were highly variable, ranging from 0.01 mm hr⁻¹ to 0.26 mm hr⁻¹ (not shown). E_s magnitudes are similar to evaporation rates observed in plantation forests, which ranged from 0.03 mm hr⁻¹ to 0.24 mm hr⁻¹ [Rutter *et al.*, 1971]. The relatively high maximum values for evaporation from a saturated canopy results from the large roughness lengths associated with forests, which enhances evaporation [Calder, 1979; Mahfouf and Jacquemin, 1989]. There did not appear to be a

Table 3.4. Detailed interception summary, 2000

Event	Start (Julian Day)	Duration (hrs)	P_G (mm)	P_n (mm)	I_{net} (mm)	%loss	E/R	S (mm)	p (dimensionless)
1	95.51	2.67	0.51	0.09	0.42	82.6			0.17
2	97.17	14.16	6.86	3.80	3.06	44.6			0.17
3	104.48	50.16	41.91	26.38	15.53	37.0	0.34	2.71	0.38
4	107.14	3.83	1.02	0.40	0.62	60.9			0.35
5	112.94	6.33	4.95	2.00	2.95	59.6			0.25
6	113.67	16.17	3.81	2.85	0.96	25.2			0.19
7	114.51	6.50	6.99	4.58	2.40	34.4			0.30
8	116.15	15.33	19.56	14.39	5.17	26.4	0.18	2.93	0.33
9	118.65	30.67	13.21	6.57	6.64	50.3	0.38	2.92	0.23
10	122.93	7.00	1.78	0.63	1.15	64.6			0.37
11	123.99	12.67	15.49	11.90	3.59	23.2	0.14	2.76	0.42
12	125.11	20.83	1.65	0.57	1.09	65.7			0.34
13	126.06	21.17	8.89	4.77	4.12	46.4			0.39
14	129.42	12.83	4.45	1.52	2.92	65.7			0.32
15	130.13	69.50	77.22	64.76	12.46	16.1	0.14	3.38	0.41
16	136.29	0.66	1.40	0.52	0.88	62.7			0.35
17	139.85	7.83	2.41	1.08	1.33	55.1			0.29
18	147.06	9.33	7.37	3.48	3.89	52.8			0.32
19	148.22	6.00	8.26	6.16	2.09	25.3			0.36
20	149.19	13.67	9.02	3.09	5.93	65.8			0.28
21	158.97	15.33	3.18	1.50	1.67	52.6			0.26
22	160.00	4.33	1.78	1.04	0.74	41.8			0.55
23	161.57	91.67	93.98	79.56	14.42	15.3	0.12	3.89	0.58
24	231.61	14.00	2.29	0.07	2.22	97.1			0.03
25	246.31	7.50	3.18	0.68	2.49	78.4			0.18
26	246.94	12.17	1.40	0.46	0.93	66.8			0.32
27	248.62	9.00	2.03	0.53	1.50	73.9			0.26
28	252.08	31.33	7.62	2.98	4.64	60.9			0.16
29	254.10	19.00	2.92	1.21	1.71	58.4			0.30
30	273.88	31.00	53.85	49.82	4.03	7.5	0.02	4.14	0.64
31	283.41	15.33	3.43	1.63	1.79	52.3			0.29
32	287.78	8.17	1.65	0.67	0.98	59.2			0.40
33	290.15	4.17	1.65	0.53	1.12	67.9			0.29
34	291.90	8.67	14.22	9.30	4.93	34.6	0.16	4.06	0.32
35	293.87	35.83	44.58	40.14	4.43	9.9	0.04	4.13	0.48
36	300.26	3.67	1.91	0.73	1.18	61.9			0.35
37	301.86	36.83	25.40	20.55	4.85	19.1	0.16	2.73	0.55
38	309.10	20.00	11.43	6.75	4.68	41.0	0.31	2.75	0.33
39	310.72	9.83	1.40	1.20	0.20	14.3			0.85
40	312.92	43.83	26.80	19.07	7.73	28.8		na	na

Table 3.4 (continued). Detailed interception summary, 2000

41	331.68	16.17	34.67	28.70	5.97	17.2	0.13	3.24	0.50
42	334.94	19.33	34.80	30.04	4.76	13.7	0.13	3.55	0.37
43	337.13	6.00	7.87	7.08	0.79	10.0			0.73
Total			618.74	463.79	154.95	25.0			
Mean		18.38	14.39	10.79		45.28	0.17	3.32	0.36
Min		0.66	0.51	0.07		7.49	0.02	2.71	0.03
Max		91.67	93.98	79.56		97.10	0.38	4.14	0.85

Note: Approximately 25% of the throughfall array gauges clogged due to heavy litterfall prior to event 40 and were excluded from the analysis, therefore S and p were not computed for this event.

relationship between estimated evaporation rate and time of year. Evaporation was closely related to both meteorological conditions and precipitation regime (i.e. continuity and intensity), particularly where canopy partially dries and rewets during an event, as shown in Figure 3.5.

The frequency distribution of individual gauge catch volumes for all events exceeding 10 mm is presented in Figure 3.6. Inclusion of small events <10 mm would produce a second peak (not shown) near the y-axis, associated with sampling locations that receive little to no throughfall during events that fail to saturate the entire canopy. Of the 237 sampling points, 23% of the gauges recorded throughfall equaling or exceeding P_G , due to gaps and drip points in the canopy. This compares with a 3% P_G exceedance found in a young plantation forest [Gash and Stewart, 1977]; the difference is probably due to greater structural complexity of the old growth canopy.

Although the throughfall measurements were made close to the ground below the majority of the leaf area, the volume of water entering the soil profile will be less than that measured due to interception by woody debris and fine litter on the forest

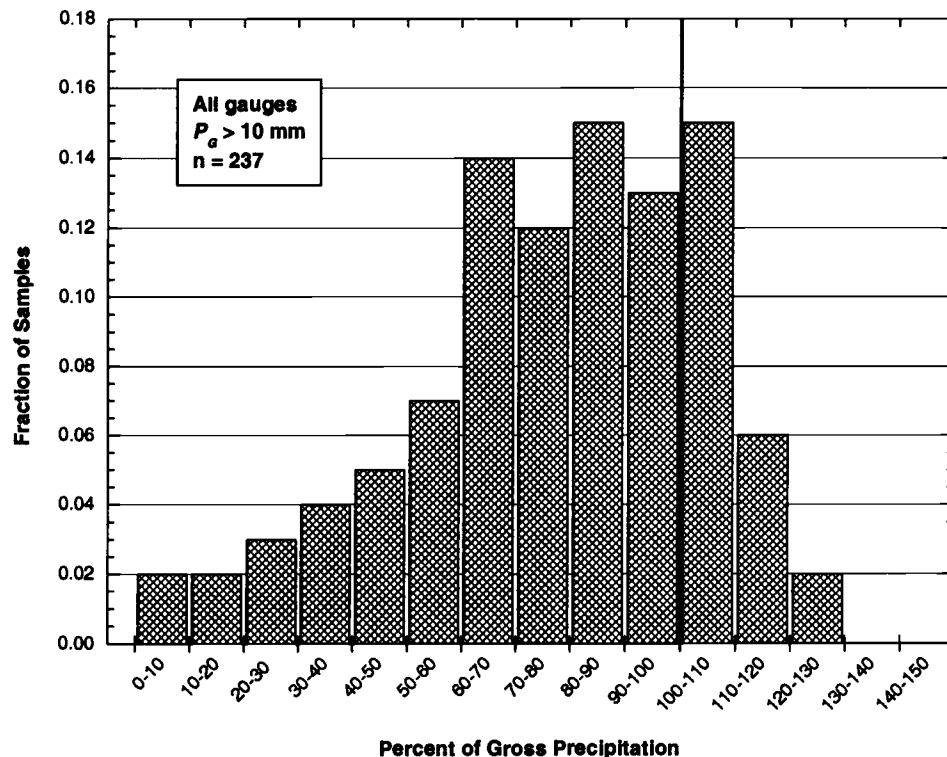


Figure 3.6. Frequency distribution of the gauge catch expressed as a percentage of the gross rainfall, for all events exceeding 10 mm.

floor. The masses of coarse woody debris in the form of logs and fine woody debris within the crane circle are $41.9 \text{ Mg C ha}^{-1}$, and 4.5 Mg C ha^{-1} , respectively [Harmon *et al.*, in review]. Interception losses from detritus in similar stands was estimated to approach 2% of P_G [Harmon and Sexton, 1995]. Evaporation from debris can be significant in forests, as was observed in young, recently pruned stands, where interception losses from slash covering roughly 60% of the forest floor was estimated to be 10% of P_G [Kelliher *et al.*, 1992]. Furthermore, the interception capacity of fine

litter in catchments with conifer covers was observed to be highly variable, with a mean of 2.8 mm [Putuhena and Cordery, 1996]. Storage capacities of both coarse and fine detritus should be considered for modeling investigations of the soil-plant-atmosphere system, and for basin-scale investigations, particularly in stands which are more productive, and contain more debris relative to WRCCRF.

3.4.3 Canopy Interception Parameters

3.4.3.1 Direct Throughfall

The advantage of using an array of tipping bucket gauges to measure the time variation of throughfall, is that p and S can be determined for each event to investigate the change in canopy interception parameters over time. The average value for p was found to be 0.36, but this value ranged from 0.03 to 0.85 between events (Table 3.4). The value for p was slightly higher than values for plantation forests that have smaller LAI, but may have more continuous canopy cover.

The frequency distribution for p is shown in Figure 3.7. Almost 70% of the values range between 0.20 and 0.50. The canopy gap fraction is frequently used as a proxy for p [e.g. Flerchinger and Saxton, 1989; Jetten, 1996], and is usually assumed to be a static quantity. The canopy gap fraction was determined to be approximately 0.3 from spatially distributed radiation measurements [Parker *et al.*, in review], similar to the value estimated from the P_n record. The range of variation in p probably results from variations in precipitation drop sizes [Calder, 1996a] and dislodging of intercepted drops by wind gusts [Hörmann *et al.*, 1996] during periods of partial canopy saturation. No relationship was found between p and time since last rainfall,

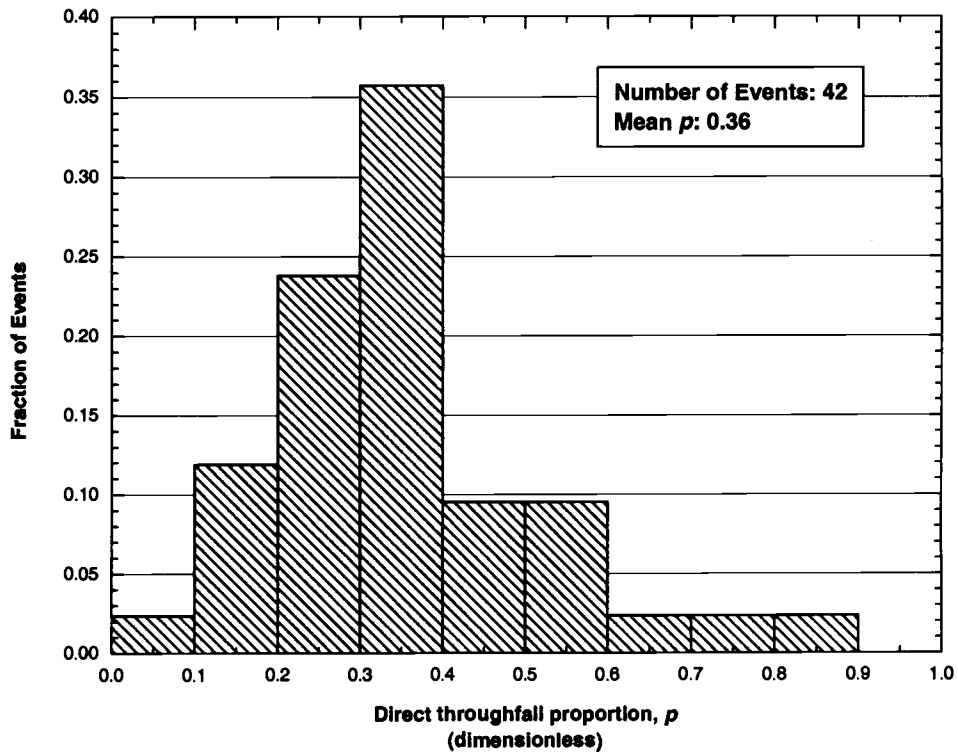


Figure 3.7. Frequency distribution of the direct throughfall proportion computed for all events.

u_{max} , intensity during wetting, or season. This variability indicates that the assumption of a constant p is frequently incorrect, as precipitation may contact the canopy and dislodge prior to canopy saturation. The components of interception affected by p (I_c and I_w) are relatively small, as discussed in Section 3.5.2, therefore errors in p resulting from the observed variations are expected to be of minor importance when estimating I_{net} over extended periods.

3.4.3.2 Saturation Storage

S values computed from (3.3) when I_w was assumed negligible, estimated from E/R , and estimated using the Penman equation are shown in Table 3.5. Comparison between the S values computed for $I_w = 0$, and I_w using the Penman method indicate

Table 3.5. Saturation storage derivation.

All Events, Technique		Saturation Storage (mm)	
Minimum (Leyton)		3.60	
Mean (NLSF on all points)		3.49	
Individual Events			
Event	I_w assumed negligible S (mm)	I_w estimated as E/R for $P_G > P_s$ S (mm)	I_w estimated using Eqs. 3.10–3.13 S (mm)
3	3.3	1.7	2.7
8	2.9	2.7	2.9
9	3.7	1.4	2.9
11	3.1	2.3	2.8
15	3.4	2.7	3.4
23	5.7	4.2	3.9
30	4.1	4.1	4.1
34	4.2	3.6	4.1
35	4.1	4.2	4.1
37	2.7	1.9	2.7
38	2.7	2.1	2.8
41	3.2	2.3	3.2
42	3.5	3.5	3.6
Mean	3.6	2.8	3.3

that the assumption of negligible I_w is valid for most events due to negligible δe during canopy wetting. Several events with sporadic precipitation and high evaporative demand during wetting (e.g. 9 and 23) exhibited larger differences between S computed using the different methods. The assumption of constant E/R during events

is not appropriate during the wetting phase, and may contribute to the observed underestimation of S when using the mean method [Klaassen *et al.*, 1998].

The mean S for the 13 storms large enough to completely saturate the canopy was 3.3 mm, and ranged from 2.7 to 4.1 mm (Table 3.4). The values for S appeared to be related to season, increasing 37% from an average of 3.0 in the spring and autumn to a maximum of 4.1 in the summer (Figure 3.8). Phenological measurements [Shaw, unpublished data] indicate that the rise in S was coincident with the timing of bud

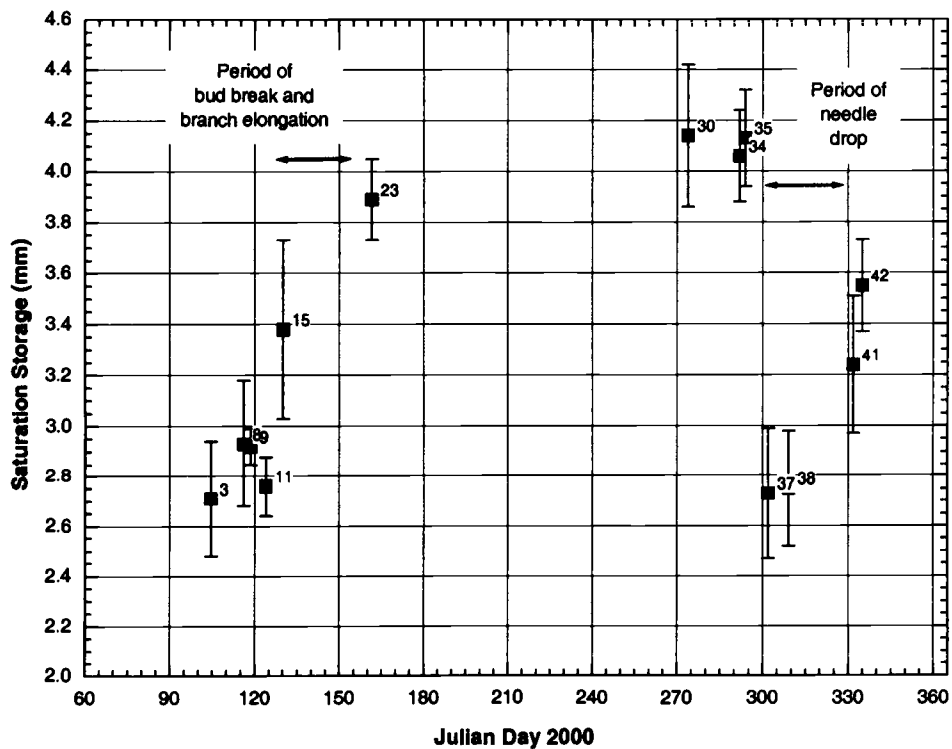


Figure 3.8. Temporal variation in the canopy saturation storage capacity. Error bars are determined by propagation errors associated with the parameters p , P_s , and E/R , determined by the optimization technique.

break and branch elongation. The timing of the S decrease in autumn was consistent with the timing of seasonal needle drop [Klopatek, pers. comm.]. S may also be affected by the moisture status of other canopy elements such as bark and canopy epiphytes, which may dry at a slower rate than the foliage and therefore absorb less water in the spring and autumn periods characterized by low δe and shorter intervals between events.

The values for S are high relative to values determined for other conifer canopies (Table 3.1). The large S probably results from the unique characteristics of old-growth forests. In particular, S is expected to be strongly affected by the larger leaf areas, abundant bryophyte and epiphyte communities, and high storage capacity of the deep, rough bark characteristic of old trees.

Using the mean values for LAI and S , the storage volume per unit leaf area (S_c) was estimated to be 0.39 mm m^{-2} . Although we do not explicitly consider the volume of water stored on branch and stem elements, these volumes were implicitly accounted for in the derivation of S . S_c is a common parameter in many hydrological models but varies greatly between models (e.g. 0.1 mm m^{-2} [Wigmosta et al., 1994], 0.2 mm m^{-2} [Dickinson, 1984], 1.0 mm m^{-2} [Flerchinger et al., 1996b]). These results will therefore improve the simulation of interception processes in hydrologic models of old-growth forests.

Values for S above 65 unique random sample locations were computed to assess the within canopy variation of this parameter (Figure 3.9). The relationship between the fraction of mean canopy storage and fraction of locations is approximated by an

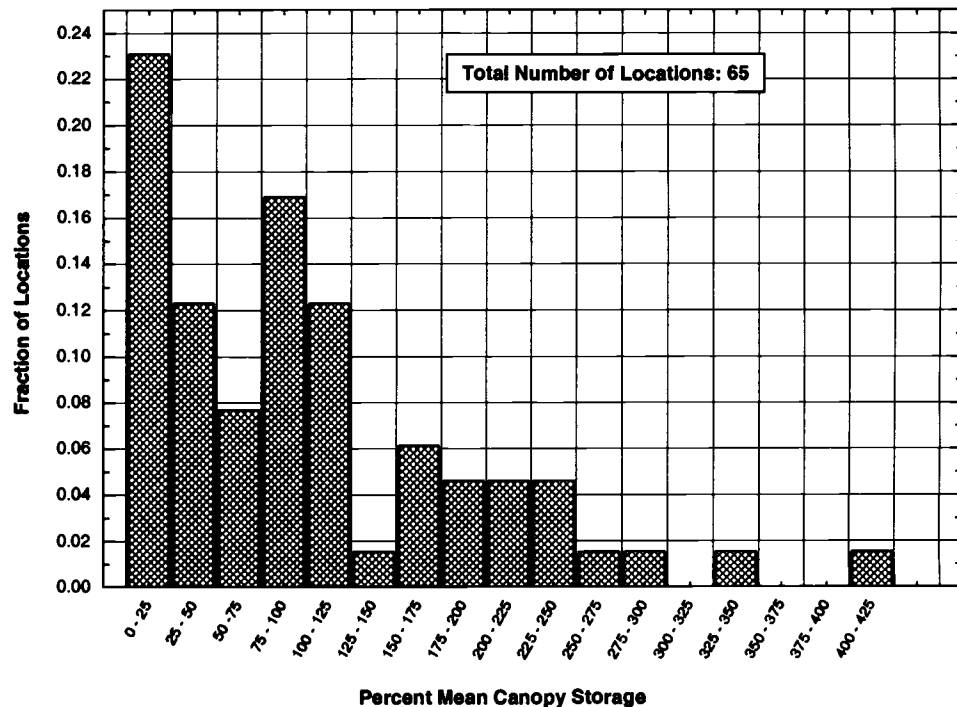


Figure 3.9. Variability of canopy saturation storage capacity within the WRCCRF crane circle.

exponential function, with values $\ll S$ corresponding to canopy gaps, and values $\gg S$ corresponding to dense areas of branch overlap. Assuming that S equals 3.3 mm, the range of variability in S suggests that over 13 mm of rainfall is necessary to completely saturate all portions of the canopy. The observed curvature at the inflection point in the P_G vs. P_n curves probably results from sequential saturation of different portions of the canopy during the wetting phase. Likewise, the high variability of S produced a high spatial variability of throughfall volumes for small storms as noted in Section 3.4.2, whereas the variability decreased for larger events.

In deciduous forests, wind speed was demonstrated to reduce S by the mechanical shaking of the canopy elements [Hörmann *et al.*, 1996]. When computed on an event basis, no relationship was found between S and either mean u or u_{max} . Wind does not appear to be a major factor controlling the interception capacity of this canopy, perhaps because of: 1. lower u relative to other sites, 2. stronger retention of water by conifers relative to deciduous canopies, and 3. attenuation of wind in the upper portion of the canopy which has a relatively low LAI and corresponding storage capacity. Also, the upper layers of the canopy will dry the most rapidly during events, therefore wind may only influence S if high windspeeds occur during rainfall when the upper canopy layers are at or above saturation.

In conifer forests, S has also been observed to vary dynamically with precipitation intensity, which acts as a proxy for raindrop size / kinetic energy [Calder, 1996a]. S exhibited no relationship to precipitation intensity during the wetting phase (defined as $P_G < 10$ mm), therefore we conclude that S was not strongly related to precipitation intensity in this canopy. Raindrop sizes are modified by contact with foliage, therefore the particularly deep canopy at this site may reduce the dependence of S on intensity, by homogenizing the size distribution of raindrops in the upper layers of the canopy prior to contact with the lower layers.

Results from this study can be applied to other old-growth ecosystems, particularly if S_c is used. S may vary by species, but may also vary within similar species assemblages if other factors such as epiphyte communities are significantly different. In addition, stem densities and crown closure may also vary between stands, and may therefore affect both p and S . The stand at WRCCRF exhibits moderate to

low productivity relative to other stands in the Pacific Northwest [*Shaw et al.*, in review], therefore we anticipate that S may be low, and p high, relative to other old-growth stands. For similar precipitation regimes, other old growth stands may therefore exhibit greater interception losses and lower throughfall intensities to those observed in this study.

3.5 Testing a Simple Analytical Model

3.5.1 Model Application

The simplified Gash analytical model neglecting stemflow was applied for the 1999 and 2000 measurement periods to capture all events unaffected by snowfall. The model was applied on an event basis using both the throughfall-estimated E/R from 2000, and the E/R estimated using the Penman equation to assess the differences between the interception components estimated using each technique. The model was also applied on a daily basis, to assess the errors associated with using this technique. A strong seasonal variation in both rainfall and evaporation rates were not evident, therefore mean E/R rates, of 0.122 and 0.106, estimated using the throughfall record and Penman equation, respectively, were assumed for the entire 2000 period. In 1999, the mean E/R of 0.122 from the 2000 regressions, and E/R of 0.059 estimated using the Penman method were used. Mean canopy parameters $S = 3.32$ mm and $p = 0.36$ were used for the entire time periods. The components of interception loss associated with events $< P_s$ (I_c), and with the canopy wetting (I_w), saturated canopy (I_s) and drying phases (I_a) of events $\geq P_s$ are compared to evaluate the importance of each component of the canopy water balance.

In 2000, the actual amounts of the interception components were computed for each event from the high-resolution throughfall records, and summed to determine the seasonal totals. I_c was determined by computing the difference between P_G and P_n for all events $< P_s$. I_s was determined by computing the difference between P_G and P_n for the time period between canopy saturation and cessation of P_G for all events $> P_s$. The optimized P_s and S values computed from (1)–(3) were used for events > 10 mm, and estimated from the mean P_s and S values for all events $> P_s$ and < 10 mm (i.e. events for which the inflection point on the P_G vs. P_n plot is poorly defined). I_a was computed from the S values either derived for each event, or estimated as discussed above. I_w was computed from the difference between I_{net} and $I_a + I_s$.

3.5.2 Model Results and Discussion

Results of the Gash analytical model for 1999 and 2000 are presented in Table 3.6. Interception components I_c , I_w , I_s , and I_a could only be measured in 2000 when the tipping bucket array was operational. In 2000, I_a was the largest component of I_{net} , comprising approximately half of the total volume, followed by I_s and I_c . Evaporation from small storms comprised a larger proportion of interception loss relative to sparse canopies [Loustau *et al.*, 1992a], due to the high S associated with this stand. I_s was a large component (33%), due to the interaction of relatively high E/R , in a precipitation regime characterized by long-duration storms (Table 3.4). The relative contributions of the four interception components were very close to the values of 19%, 5%, 34%, and 42%, for I_c , I_w , I_s , and I_a , respectively observed by Gash [1979] in a temperate conifer forest.

Table 3.6. Gash analytical model performance

Interception Component	Measured		Event, P_n estimated E/R			Event, Penman estimated E/R			Daily, Penman estimated E/R		
	I (mm)	%total	I (mm)	% total	%error	I (mm)	% total	%error	I (mm)	% total	%error
1999											
I_c			37.0	29.2%		37.0	34.5%		54.8	40.0%	
I_w			5.1	4.0%		5.1	4.8%		6.5	4.7%	
I_s			38.1	30.1%		18.6	17.4%		15.9	11.6%	
I_a			46.5	36.7%		46.5	43.4%		59.8	43.6%	
Total, I_{net}	102.7		126.7	100.0%	23.4%	107.1	100.0%	4.3%	137.0	100.0%	33.4%
% Loss	22.8%		28.1%			23.8%			30.4%		
2000											
I_c	28.8	19%	31.3	19%	9%	31.3	20%	9%	48.4	24%	68%
I_w	1.5	1%	8.0	5%	417%	8.0	5%	417%	11.6	6%	652%
I_s	51.5	33%	54.0	32%	5%	47.1	30%	-9%	38.2	19%	-26%
I_a	73.1	47%	73.1	44%	0%	73.1	46%	0%	106.3	52%	45%
Total, I_{net}	155.0	100%	166.4	100%	7%	159.4	100%	3%	204.4	100.0%	32%
% Loss	25.0%		27%			26%			33%		

Note: 59 events, and 65 days with precipitation occurred during the 1999 period
 43 events, and 73 days with precipitation occurred during the 2000 period

The I_{net} estimated with the event-based Gash analytical model, using the Penman-estimated E/R closely matched the measured I_{net} values for both years. The individual components of the interception loss varied from the actual components of interception loss, due to errors introduced by assuming static values for p , S , and E/R . Relatively good agreement also occurred when using the E/R estimated from the throughfall record for 2000, however the errors are much greater when applying the 2000-derived E/R to 1999 (0.122), due to a much lower Penman estimated E/R value (0.059) for this period. These results also show that mean E/R values can vary greatly between years, and may introduce error when using the Gash model to compute interception loss. These results indicate that the Penman method should be used to estimate evaporation during rainfall if sufficient data exist, due to the between-year variability of E/R .

The daily application of the Gash analytical model overestimated I_{net} by an average of 33% for the two years. The inherent assumptions of the daily application, that only 1 event occurs per rain day, and that the canopy dries completely between events caused multi-day continuous storms to be parsed into a series of smaller events. As a result, I_c was overestimated due to a greater estimated number of small storms. Estimated I_a also increased due to a larger number of canopy wetting and drying cycles. I_s was underestimated due to a smaller amount of precipitation that was assumed to occur under saturated canopy conditions. Similar errors of 34.6% in I_{net} were observed for daily application of the model [Hutjes *et al.*, 1990], although the error was due to the model simulating multiple wetting cycles within the course of a single day as discrete events. The year 2000 was relatively dry, therefore it is

expected that errors would be even greater when applying the daily version of the Gash model to wetter periods. Application of the Gash model to estimate interception from daily data may be used with success in this environment if a stochastic technique such as a scale-variant random cascade precipitation model [Rupp *et al.*, in review] is used to parse long-term volumes into smaller events, to more accurately estimate the precipitation regime.

The results of the modeling investigation indicate the importance of the precipitation regime in controlling I_{net} and influencing model performance. If a precipitation season is characterized by a large number of events that are close to P_s , I_{net} will be relatively large, as suggested by the daily application of the model. Events characterized by intermittent precipitation where the canopy partially dries during an event, will result in larger E/R relative to continuous events, greater I_s and larger I_n . However, if the precipitation regime is characterized by large continuous events, the fractional loss will be smaller due to a reduced number of canopy wetting cycles. In addition, conditions of prolonged precipitation with shorter dry intervals, may result in lower I_{net} relative to Gash estimates in cases where the assumption of complete canopy drying between events is violated, and water is retained on canopy elements between events. Although the performance of the analytical model was very good for both 1999 and 2000, the assumption of complete canopy drying between events is likely to be violated during periods with more frequent precipitation and low evaporative demand, such as winter months. The application of an analytical model that explicitly accounts for the temporal variability in rainfall [e.g. Zeng *et al.*, 2000], may therefore be more appropriate during these periods.

3.6 Conclusions

The mean direct throughfall coefficient for an old-growth conifer forest was 0.36, and the mean saturation storage capacity of the canopy was estimated to be 3.32 mm during 2000. S varied seasonally from an average of 4.1 mm for the months of June through October, to an average of 3.0 mm for the remaining months. The seasonal change in S appears to result primarily from seasonal LAI changes, but may also be affected by antecedent conditions that affect the moisture status of the canopy elements (i.e. leaves, bark, branches, and epiphytes). Detailed analysis of the components of interception indicated that I_a dominated I_{net} , but that I_s comprised 33% of the interception budget. The Gash analytical model was effective in estimating both the magnitude and relative proportions of the I_{net} components when applied on an event basis, and when using the Penman method to estimate I_s . High resolution throughfall and micrometeorological data suggest that the evaporation rate of intercepted water is highly dynamic, and dependent on precipitation regime, especially when the canopy may partially dry and rewet during an event. The assumption that E/R is relatively constant, and can be used to estimate I_s , may not be appropriate under highly variable precipitation regimes, as was observed for the 1999 and 2000 seasons. In the PNW, which is characterized by highly variable and extended periods of continuous rainfall, interception should either be estimated using analytical models with event-level data, or with physically-based models driven by high-resolution data.

Additional study of interception processes in this environment using physically-based, layered canopy models should be implemented to improve our understanding of the rate at which water evaporates from individual canopy layers.

Micrometeorological scalars suggest that evaporation from deep canopy layers should be limited by low T_a , δe and u . However, evaporation may be strongly influenced by advection events, causing relatively rapid drying of deep canopy layers. Future modeling efforts should be undertaken in conjunction with detailed micrometeorological measurements to evaluate the effects of turbulent events and determine how rapidly the canopy dries between events. Measurements of vertical profiles of leaf, bark and epiphyte moisture status should be completed to provide validation data, and to improve our understanding of how individual canopy elements contribute to I_n . Determination of drying rates of the individual canopy elements will further improve interception models of complex canopies.

3.7 Acknowledgements

Support for this research was provided by the Western Regional Center (WESTGEC) of the National Institute for Global Environmental Change (NIGEC), the U. S. Forest Service (USFS), and the Agricultural Research Service (ARS), Northwest Watershed Research Center. Office and computing facilities were provided by the U. S. Environmental Protection Agency (USEPA), Western Ecology Division.

**4. SIMULATION OF WATER AND ENERGY FLUXES IN AN OLD
GROWTH SEASONAL TEMPERATE RAINFOREST USING THE
SIMULTANEOUS HEAT AND WATER (SHAW) MODEL**

Timothy E. Link
Gerald N. Flerchinger
Mike Unsworth
Danny Marks

For submittal to the Journal of Hydrometeorology

4.1 Abstract

In the Pacific Northwest (PNW), concern about the impacts of climate and land cover change on water resources and flood-generating processes emphasize the need for a mechanistic understanding of the interactions between forest canopies and hydrological processes. Detailed measurements during the 1999 and 2000 hydrologic years were used to modify the Simultaneous Heat and Water (SHAW) Model for application in forested systems. Changes to the model include improved representation of interception dynamics, stomatal conductance, and within-canopy energy transfer processes. The model was calibrated for the 1999 hydrologic year, and validated for the 2000 season. The model effectively simulated canopy air and vapor density profiles, snowcover processes, throughfall, soil water content profiles, shallow soil temperatures, and transpiration fluxes for both years. The largest discrepancies between soil moisture and temperature were observed during periods of discontinuous snowcover. Soil warming at bare locations was delayed until most of the snowcover ablated due to the large heat sink associated with the residual snow patches. During the summer, simulated evapotranspiration decreased from a maximum monthly mean of 2.17 mm day^{-1} in July to 1.34 mm day^{-1} in September, as a result of decreasing soil moisture and declining net radiation. Our results indicate that a relatively simple parameterization of the SHAW model for the vegetation canopy can accurately simulate seasonal hydrologic fluxes in this environment. The model could be used to assess the potential effects of climate or landcover changes on hydrological processes in PNW old-growth ecosystems. Application and validation of the model in other

forest systems will establish similarities and differences in the interactions of vegetation and hydrology, and assess the sensitivity of other systems to natural and anthropogenic perturbations.

4.2 Introduction

The transport of mass and energy in forested environments is of great interest in many regions of the world due to concerns regarding the effects of climate on vegetation, and influences of forest management on floods, seasonal low flows, and geomorphic processes. Intensive, interdisciplinary field studies and complementary modeling programs have increased our understanding of the processes controlling mass and energy fluxes in forested environments. Physically-based process models have greatly increased our understanding of the complex interactions between hydrological processes and vegetation by providing tools for simulation, prediction and hypothesis testing. The continued development of robust modeling tools is particularly important in regions such as the Pacific Northwest (PNW) of the U. S., where competing demands on water and forest resources have raised many questions regarding the effects and landcover and climate variability on hydrologic systems.

In the PNW, alteration of the native forest cover may increase peak stream flows [Jones, 2000; Jones and Grant, 1996], although the magnitude of the increase, return interval of the affected peaks, and size of affected basins have been debated [Beschta et al., 2000; Thomas and Megahan, 1998]. The PNW is characterized by an extended seasonal drought during the summer months, and questions of how land management influences the low flow regime have recently increased due to concerns about water

resource availability and endangered species [Keppeler and Ziemer, 1990]. The statistically-based studies referenced above suggest a variety of physical mechanisms associated with canopy alteration that may affect streamflows, including precipitation interception, transpiration, and alteration of the snowcover and soil moisture regimes. An improved mechanistic understanding of the interactions of vegetation and hydrology is therefore necessary to distinguish the relative importance of these mechanisms.

Physically-based numerical models are a powerful tool to help understand interactions of vegetation and hydrology, and to test hypotheses regarding the effects of landcover and climatic variability on hydrological processes. The accurate simulation of processes over large scales requires the testing and validation of models at the plot scale. Existing soil-plant-atmosphere models simulate a number of interrelated mass and energy transfer processes through layered soil-vegetation-atmosphere systems [e.g. *Flerchinger et al.*, 1996b; *Kaduk et al.*, in review; *Sellers et al.*, 1996; *Wigmosta et al.*, 1994; *Williams et al.*, 2001]. Physically based models are commonly developed and validated in a particular environment and within a range of driving variables. If limited validation data exist, reasonable results may occur if counteracting and conflicting assumptions or errors are made when developing and/or parameterizing the model. The utility of process models may be extended by fully testing and validating the processes simulated by model across a range of distinctly different environments.

This paper describes further development of the Simultaneous Heat and Water (SHAW) model, a one-dimensional hydrological model that integrates the coupled

transport of mass and energy through a soil-vegetation-atmosphere system into a simultaneous solution [Flerchinger *et al.*, 1996b; Flerchinger and Saxton, 1989]. The model was developed and extensively validated over a variety of vegetation types present in semiarid and arid croplands and rangelands. Many aspects of the model have been tested, including the effect of vegetation on soil temperature and moisture [Flerchinger and Pierson, 1997], snowmelt [Flerchinger *et al.*, 1996a; Flerchinger *et al.*, 1994], soil freezing [Flerchinger and Saxton, 1989], evapotranspiration and surface energy budgets [Flerchinger *et al.*, 1996b], and radiometric surface temperature [Flerchinger *et al.*, 1998]. To date, the SHAW model has not been tested in humid forested environments, however the detailed representation of the physics and vegetation structure in the model indicate that it could be an effective tool to simulate hydrological processes in such environments.

The primary objective of this research is therefore to develop the SHAW model for application in an old-growth seasonal temperate rainforest. Specifically, we seek to: 1.) Test the model for a complete annual cycle in the PNW, to encompass the full range of seasonal climate variability in the region; 2.) Validate the individual hydrological processes and state variables simulated by the model, including within-canopy temperature and vapor concentrations, snowcover deposition and ablation, soil water content, soil temperatures, canopy interception losses and transpiration fluxes; 3.) Validate the simulations for a year of independent data (i.e. data not used for parameterizing the model); and 4.) Quantify the annual and monthly components of the site energy and water balances.

4.3 Methods

4.3.1 Site Description

This study was conducted at the Wind River Canopy Crane Research Facility (WRCCRF), located within the T.T. Munger Research Natural Area of the Gifford Pinchot National Forest, in southwestern Washington, USA (Figure 2.1). The site is located on a gently sloping alluvial fan in the Wind River Valley in the Cascade Mountains at 45° 49' N latitude, 121° 57' W longitude, at an elevation of 367.5 m amsl. A Liebherr 550HC tower crane is located in the center of the 4 ha² study plot, and is used for canopy access and as a sensor platform for micrometeorological measurements. The crane is 85 m high, with a jib range of 87 m that inscribes a 2.3 ha circular area within the plot where measurements are conducted. The physical setting, ecological characteristics, and infrastructure of the WRCCRF are described in detail by *Shaw et al.* [in review].

Dominant vegetation species at the site are Douglas fir (*Pseudotsuga menziesii*), western hemlock (*Tsuga heterophylla*), and western red cedar (*Thuja plicata*) with many individuals exceeding 450 years in age. The canopy height is approximately 60 m, with the tallest trees reaching 65 m [*Ishii et al.*, 2000]. The canopy exhibits many old-growth characteristics, including a high degree of spatial heterogeneity in species and canopy depth, a multi-layered canopy, and high degree of biodiversity in the plant community [*Franklin and Spies*, 1991]. Understory tree species include pacific yew (*Taxus brevifolia*), Pacific silver fir (*Abies amabilis*), and vine maple (*Acer circinatum*). Dominant species of the lowest layer include salal (*Gaultheria shallon*),

Oregon grape (*Berberis nervosa*) and vanilla leaf (*Achlys triphylla*). The 3 year average leaf area index (LAI) of the site was 8.6 ± 1.1 , ranging from 9.3 ± 2.1 to 8.2 ± 1.8 measured by the vertical line intercept method [Thomas and Winner, 2000].

A thick litter layer composed of coarse and fine woody debris, needles and leaves, and mosses ranges from roughly 2 to 10 cm across the site. Soils at the site originated as a volcanic ash deposit, and are described as shotty loamy sands and sandy loams [Harmon *et al.*, 1995, High, 2000, unpublished data]. Soils are classified as frigid andisols, and are characterized by low bulk densities (ρ_b), and high porosities (n).

Climate at the site is characterized by cool, wet winters and warm, dry summers, with an average annual precipitation of 2467 mm. Less than 10% of the precipitation occurs between June and September [Shaw *et al.*, in review]. Average annual snowfall is 1806 mm, most of which falls from November to March. Mean annual air temperature is 8.7 °C, with the mean monthly maximum of 17.3 °C occurring in August and the mean monthly minimum of -0.1 °C occurring in January. Precipitation conditions during this period were slightly more (3%) than average [Link *et al.*, in review-a]. The 1999 winter was warmer than average, and a greater proportion of the precipitation occurred as rain rather than snow, therefore a spatially continuous snowcover never developed at the site. A detailed discussion of the climate conditions and canopy characteristics during the 1999 and 2000 hydrologic years are provided by Link *et al.*, [in review-a].

4.3.2 Data Collection and Instrumentation

Meteorological data for driving the model were collected above the canopy at 85 m (STA80) and 68.4 m (STA70) on the crane tower, and at an open field site (OPENSTA) approximately 1.5 km south of the crane tower. Meteorological data were collected on the crane tower at 57.0 m (STA60), 39.9 m (STA40), 22.8 m (STA20), 11.7 m (STA10), and at 2 m beneath a closed canopy area ~25 m east of the crane tower (STA02) (Figure 2.2). Validation data for soil water content (θ), soil temperature (T_g), throughfall (P_n) and snow depth (z_{snow}) were collected throughout the 2.3 ha crane circle and at sites beneath a closed canopy and canopy gap area. Details of the instrument installations are provided by *Link et al.*, [in review-a].

4.3.2.1 Meteorological Data

Solar radiation (R_S) was collected at STA80 using a 4-component net radiometer (Model CNR-1, Kipp and Zonen Inc, Bohemia, NY). Air temperature (T_a) and relative humidity (RH) sensors (Model HMP35C, Vaisala Inc., Sunnyvale, CA) were installed at STA70, STA60, STA40, STA20, STA10, and STA02 in mechanically aspirated Gill multi-plate radiation shields. Wind velocity (u) and direction (u_{dir}) at STA70 were measured with a 3-dimensional sonic anemometer (Solent Gill HS, Lymington, UK), and with 2-dimensional sonic anemometers (Model WAS425, Handar/Vaisala Inc., Sunnyvale, CA) at all other profile locations.

Precipitation (P_G) was collected above the canopy at STA80 with an alter-shielded weighing gauge (Model 6071, Belfort Instrument Co., Baltimore, MD), and at OPENSTA using a both a weighing (Model 5-780, Belfort Instrument Co.,

Baltimore, MD) and a tipping bucket raingauge (Model TE-525, Texas Electronics Inc., Dallas, TX), equipped with a snowfall adapter (Model CS705, Campbell Scientific, Logan, UT).

4.3.2.2 Validation Data

Volumetric 0-40 cm soil water content(θ) was measured with 28 pairs of stainless steel rods that were manually interrogated every 3 to 4 weeks using a time domain reflectometer (TDR, Model Trase 6050XI, Soil Moisture Equipment Inc., Santa Barbara, CA). Continuous 0-30 cm θ was also monitored at the closed canopy and gap sites using two frequency reflectometers (CS615, Campbell Scientific, Inc., Logan, UT) and recorded on a datalogger (CR-10X, Campbell Scientific, Inc., Logan, UT) every 15 minutes. A continuous sensor that served as a proxy for the mean site θ was identified by comparison to the mean site θ , estimated from the manual array. Water content over depth intervals spanning 0-15 cm, 15-30 cm, 30-60 cm, 60-90 cm, and 90-120 cm were measured with segmented TDR probes (Type A, Environmental Sensors Inc., San Diego, CA), interrogated manually with a portable TDR unit (Model MP-917, Environmental Sensors Inc., San Diego, CA).

Soil temperature (T_g) was measured with thermistors (Model 107, Campbell Scientific, Inc., Logan, UT), installed at 15 cm at the gap and closed canopy sites to estimate the maximum range of T_g resulting from variations in the overlying canopy cover. Soil temperature at both sites was very similar during most of the year, and is therefore assumed to represent the overall site conditions.

Throughfall (P_n) during snow-free periods was measured during the 1999 water year using a 44-element array of collectors, composed of a steep sided funnel attached to a 400 mm capacity reservoir. Throughfall during the 2000 water year was also collected with a 24-element array of tipping bucket rain gauges (TE-525I, Texas Electronics Inc., Dallas, TX) equipped with individual data loggers (HOBO Event, Onset Computer Corp., Bourne, MA), validated against the collection array. Snow depths at the gap and closed sites were measured with sonic depth sensors (Judd Communications, Inc., Logan, UT). A detailed analysis of the precipitation interception dynamics and the derivation of canopy interception parameters is presented by *Link et al.*, [in review-b].

Ecosystem water flux (ET) was measured by an eddy covariance (EC) system mounted at 70 m on the crane tower. Estimates of vertical water fluxes were made using a 3-D sonic anemometer and a fast-response infra-red gas analyzer (Model 6262, LiCor Inc., Lincoln, NE) which measured the velocity vector, sonic temperature, and water vapor concentration at 10 Hz. Sample lines were 4.5 m long to limit adsorption and signal time lags, and externally heated to minimize condensation. *Paw U et al.*, [in review] gave full details of the system, methods and data corrections. The footprint of the sensors at 70 m may extend less than 100 m upwind during unstable daytime conditions, but may exceed 1 km during stable conditions at night. Measurements are affected by the crane tower when the wind originated from the 45° to 135° quadrant, and were therefore screened to reduce spurious water flux data. EC data were available for the period from May 20, 1998 through July 31, 1999 at the time this analysis was completed.

4.3.2.3 Modeling Dataset Preparation

Complete and continuous datasets were prepared for modeling investigations using a hierarchical interpolation routine to fill data gaps. The data hierarchy for model driving variables is presented in Table 4.1. Data gaps ≤ 3 hours for S , T_a , RH , and u were interpolated by fitting a 3 point spline to the data [Akima, 1978]. Data gaps > 3 hours were filled by substituting values estimated using a simple linear regression on data from either OPENSTA or STA60 for the ten days preceding and the ten days succeeding the data gap.

A continuous P_G record was developed as a composite of site gauge records. Problematic data periods for each gauge were identified manually by plotting all gauge records with the corresponding soil moisture trend for the canopy gap. During periods of mixed snow and rain conditions (November through April), the record from the OPENSTA Belfort was preferentially used. During periods of light rain, inertia in the spring of the Belfort gauge can produce spurious measurements, therefore the record from the OPENSTA tipping bucket gauge was preferentially used during the dry season (May through October). When OPENSTA data were unavailable, data from the STA80 precipitation gauge were used. During brief periods when no precipitation data from any instruments at the site were available, precipitation was estimated from the Surprise Lakes SNOTEL station located approximately 25 km to the northeast of the site, using an empirical regression.

Table 4.1 Model driving data hierarchy

Variable	Preference	Source	Method	Instrument
Solar radiation	1	STA80	Interpolation	Kipp & Zonen, CNR-1
	2	OPENSTA	regression	Li-Cor, Li-200
	3	STA70	interpolation	Li-Cor, Li-190
	4	Modeled clear sky	corrected based on sky conditions at Portland, OR	
Air temperature,	1	STA70	interpolation	Vaisala, HMP35C
Relative humidity	2	STA60	regression	Vaisala, HMP35C
	3	OPENSTA	regression	Vaisala, HMP35C
Wind speed	1	STA70	interpolation	Handar WAS425
	2	OPENSTA	regression	R.M. Young 03001
	3	STA60	regression	Handar WAS425
Precipitation	1,2*	OPENSTA	direct	Texas Electronics TE-525
	2,1*	OPENSTA	direct	Belfort 5-780
	3	STA80	direct	Belfort 6071
	4	Surprise Lakes SNOTEL	regression	NRCS SNOTEL Gauge

* the tipping bucket gauge was preferred during the dry season (May-Oct), whereas the Belfort gauge was preferred during the wet season (Nov. - Apr.)

4.3.3 SHAW Model Developments

4.3.3.1 Model Description

The SHAW model simulates a vertical, 1-dimensional system extending from above a vegetation canopy through a snow cover (if present), litter, and soil, to a specified depth within the soil profile. A conceptual diagram of the model structure is shown in Figure 4.1. The model integrates the detailed physics of interrelated mass and energy transfer through a multi-layer canopy, snow, litter and soil system into one simultaneous solution. Hourly predictions include evaporation, transpiration, air temperature and vapor density in the canopy air space, snow depth, runoff and profiles of soil water content, soil temperature, and soil ice content.

Boundary conditions are defined by meteorological variables (S , T_a , RH, u and P_G) above the canopy, and soil variables (θ and T_g) at the lower boundary. A layered system is established through the model domain, with each layer represented by a node. After computing fluxes at the upper boundary, the heat, liquid water and vapor fluxes between layers are simulated. Heat and water fluxes through the system are computed simultaneously using implicit finite difference equations that are solved iteratively using a Newton-Raphson procedure [Campbell, 1985]. The model can simulate transfer in canopies comprised of several different plant species, including standing dead material. Vegetation height, biomass, leaf area index (LAI), rooting depth, and leaf dimension throughout the year are specified by the user. Details of the numerical implementation of the SHAW model are presented in *Flerchinger et al.* [1996b; 1998; 1989].

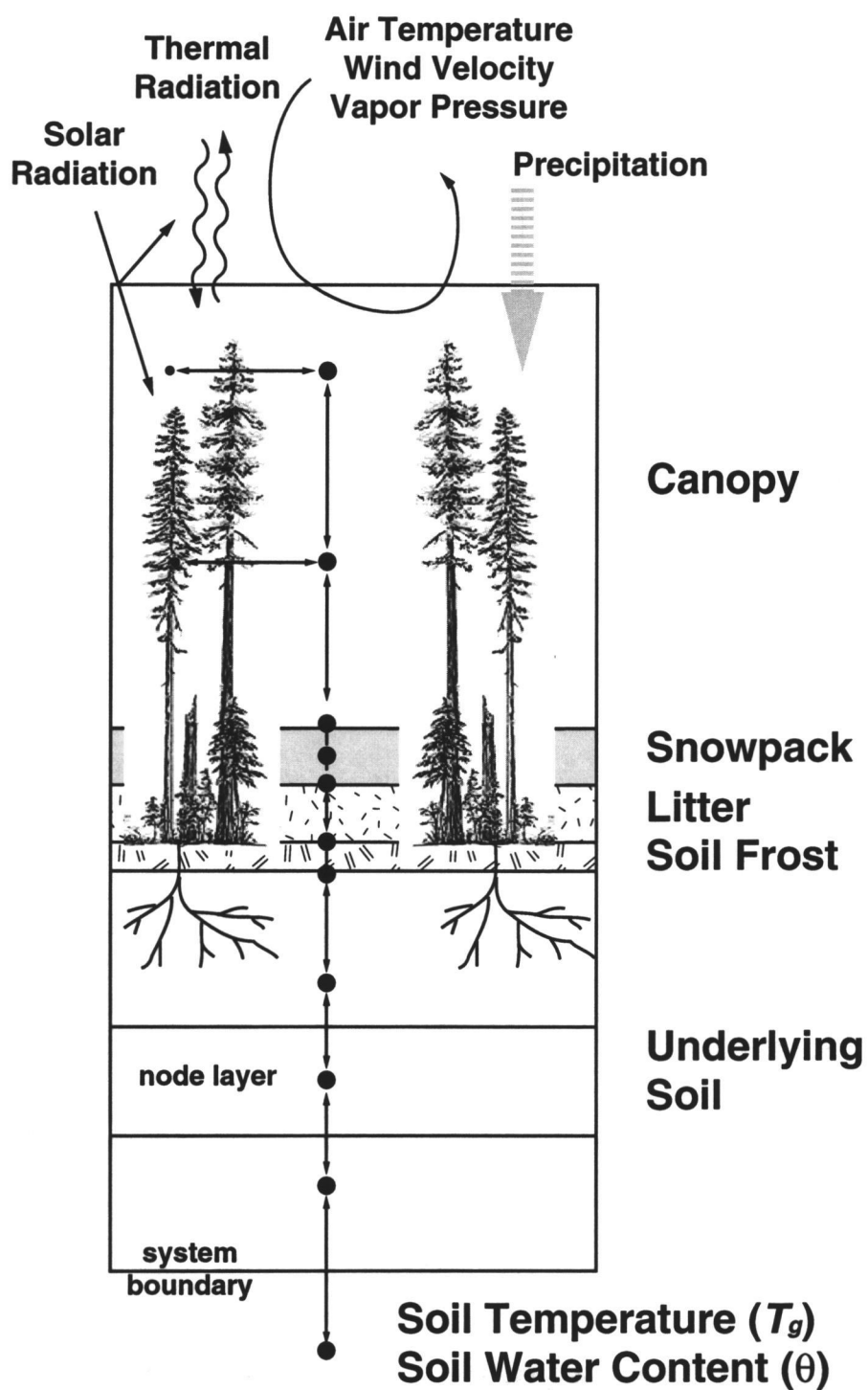


Figure 4.1. Conceptual diagram of the Simultaneous Heat and Water (SHAW) model.

As discussed above, the SHAW model has been extensively tested over a range of vegetation types in semi-arid and arid environments. In the following section we present recent modifications of the model to more accurately simulate forested environments under a wide range of meteorological conditions. The most significant changes were in the canopy interception, canopy conductance to vapor transport (g_c) and within-canopy energy transfer processes.

4.3.3.2 Canopy Interception

The two most important canopy parameters that control the interception process are the direct throughfall proportion (p) and canopy storage capacity per unit leaf area (S_c). Values for p and S_c of the WRCCRF canopy were derived from detailed analysis of canopy throughfall [Link *et al.*, in review-b]. Previous versions of SHAW defined p as the canopy transmissivity to direct radiation (τ_b), computed as an exponential function of LAI. The mean measured p for 43 storms in 2000 was 0.36 [Link *et al.*, in review-b], much larger than the estimated value of 0.013, based on LAI. S_c in the previous version of SHAW was specified as 1.0 mm m⁻² of leaf area. Detailed throughfall measurements indicated that the mean value for S_c at the WRCCRF is 3.32 mm, which corresponds to a value of 0.386 mm m⁻² of leaf area. Consequently, the SHAW model was modified to include the derived interception parameters p and S_c rather than the previous estimates. The modifications increase the simulated throughfall (P_n), and transpiration (E_t) fluxes, particularly during the dry months, by simulating less interception (I_{net}), higher P_n , and by decreasing the amount of time that the canopy remains wetted.

4.3.3.3 Canopy Conductance Model

The physicochemical and physiological processes that interact to control stomatal mechanics are complex and poorly understood [Nobel, 1991]. Stomatal conductance (g_s) is related to vapor pressure deficit (δe), leaf temperature (T_l), solar radiation, soil water status and CO₂ concentration within the stomates [Jarvis, 1976; Ogink-Hendriks, 1995; Stewart, 1988]. Two common models of g_s are the Jarvis-Stewart model, which estimates g_s as a function of the environmental variables δe , T_a (as a proxy for T_l), S , and θ , and A - g_s parameterizations that balance CO₂ assimilation (A) with water use [Calvet, 2000].

The SHAW model does not include a carbon cycle, therefore g_s is estimated from environmental conditions. In previous versions of the model, g_s was computed as a function of leaf water potential (ψ_l):

$$1/g_s = r_{s0} \left[1 + (\psi_l/\psi_c)^n \right] \quad (4.1)$$

where r_{s0} is stomatal resistance with no water stress, ψ_c is a critical leaf water potential at which stomatal resistance is twice its minimum value, and n is an empirical coefficient [Campbell, 1985]. The estimate of g_s in Eq. (4.1) is strongly dependent on soil water status, and weakly dependent on δe , T_a , and S , through the influence on T_l and ψ_l , and has been noted to function effectively for semi-arid vegetation [Flerchinger et al., 1996b; Flerchinger et al., 1998; Flerchinger and Pierson, 1997].

The formulation in (4.1) may not be applicable to forests particularly during the transition from spring to summer conditions, when θ is high, and large diurnal swings in T_a and δe occur. During this period, vegetation must reduce g_s to balance

transpiration against the ability to take up water from the soil. The Jarvis-Stewart parameterization is an effective technique to estimate the effect of all environmental variables on g_s , however its full implementation requires the estimation of six parameters [e.g. *Ogink-Hendriks, 1995*]. These parameters are most effectively derived from controlled environment experiments, but can be estimated from a large quantity of *in situ* transpiration measurements using a non-linear least squares fitting procedure. The derivation of the Jarvis-Stewart parameters from natural sites can be confounded by correlations between the environmental variables, and by data that do not adequately fill the variable space. This may result in mutual parameter dependency during the fitting procedure, indicating that the model is overparameterized with respect to the available data. These data issues are significant in many environments such as the PNW, due to the strong correlation between T_a and δe , and a weaker correlation between θ and δe [see *Link et al.*, in review-a].

A simplified version of the Jarvis-Stewart model was added to the SHAW model to more effectively simulate water dynamics in forested systems, while maintaining the relative simplicity of the model and parameter parsimony. The computed conductance from Eq. (4.1) is multiplied by a reduction factor (f) computed as a function of δe , defined as:

$$f(\delta e) = K_{\delta e} + (1 - K_{\delta e})r^{\delta e / 1000} \quad (4.2)$$

where $K_{\delta e}$ is the maximum g_s reduction at high δe , and r is an empirical fitting parameter (Figure 4.2) [*Ogink-Hendriks, 1995*]. T_a and δe are strongly correlated,

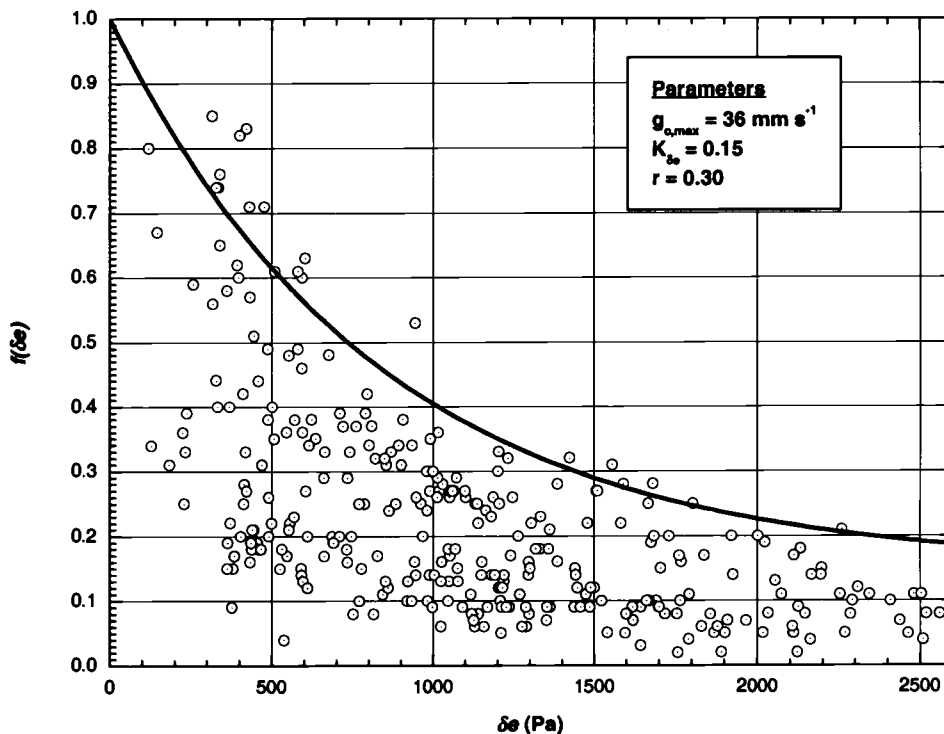


Figure 4.2. Scatterplot of relative canopy conductance vs. vapor pressure deficit. Individual data points were derived from EC measurements of total ecosystem water flux. The solid line is a plot of (4.2).

therefore the effect of temperature is implicitly included in the model. Adding (4.2) reduces g_s early in the growing season, when θ is high. Later in the season when δe reaches maximum values and the system becomes increasingly limited by θ , computed g_s is further limited by (4.1). The effect of R_S on g_s is not included in the current model, because we assume that when R_S is low, transpiration (E_t) will be limited by small driving gradients, and the net impact on the computed flux will be negligible.

4.3.3.4 Within Canopy Processes

Simulation of energy transfer in deep multi-layered canopies presents additional modeling challenges that did not occur in the shorter semi-arid canopies where the SHAW model was developed. Foliage in conifer canopies is not uniformly distributed, resulting in greater radiation transmission efficiency than is predicted with simple exponential models [Law *et al.*, 2001; Mencuccini and Grace, 1996]. The modified version of the SHAW model includes a foliage clumping factor (Ω), ranging from 0.0 to 1.0 in the computation of the transmissivity of the canopy to direct radiation (τ_b):

$$\tau_b = \exp\left(-\sum_j^{NP} \Omega_j K_j L_j\right) \quad (4.3)$$

where K_j , and L_j are the extinction coefficient and leaf area index for vegetation species j , and NP is the number of species in the simulation. The clumping factor can be measured for a given canopy with pyranometer arrays, or estimated from values in the literature.

During the night, when wind speeds are low and consequently forced convection is small, free convection can develop within the canopy, driven by soil heat flux and radiative cooling of the upper canopy. Free convection transports heat away from the forest floor, enhancing the cooling of the litter and soil layers at night. In the modified model, heat transfer during free convection conditions in the canopy airspace is computed by including a velocity of free convection (h) in the computation of the transfer coefficient (k_e) above the zero plane displacement, d :

$$k_e = k(u^* + h)(z_s - d + z_H) / \phi_H \quad (4.4)$$

and below d ,

$$k_e = k(u^* + h)z_H / \phi_H \quad (4.5)$$

where ρ_a is the air density, c_a is the heat capacity of air, k is the von Kármán constant, u^* is the friction velocity, z_s is the sensor height, d is the zero-plane displacement for heat, z_H is the roughness length for heat, and ϕ_H is a diabatic correction factor dependent on the Richardson number, and where h is computed:

$$h = k\Delta z_c \sqrt{\frac{-g}{T_c} \left(\frac{\Delta T_c}{\Delta z_c} - T_L \right)} \quad (4.6)$$

where g is gravitational acceleration, T_c is the air temperature within the canopy (K), z_c is the depth within the canopy, and T_L is the adiabatic lapse rate [Weaver, 1984].

4.3.4 Model Parameterization

Mass and energy dynamics were simulated for the 1999 and 2000 hydrologic years. The parameterization of the model was optimized using data collected during 1999, and applied without modification for the 2000 hydrologic year. Details of the parameterization are listed in Table 4.2. All parameters were derived from measurements at the site where possible, or estimated from literature values where no data existed.

Table 4.2. SHAW model parameterization

Variable Definition	Value	Unit
Site Properties		
Site longitude		deg,min
Site latitude	45,49	deg, min
Site slope	6	%
Site aspect	45	degrees
Site elevation	355	m
Time of solar noon	12.25	h
Number of plant species	1	
Measurement height	68	m
Number of canopy nodes	11	
Number of residue nodes	6	
Number of soil nodes	24	
Vegetation Properties		
Height of species	60	m
Characteristic dimension of leaves ^b	0.5	cm
Dry biomass of canopy ^c	30.7	kg m ²
Leaf area index ^d	8.6	m ² m ⁻²
Rooting depth ^e	1.2	m
Albedo of species ^b	0.25	dimensionless
Transpiration threshold ^b	3.0	°C
Minimum stomatal resistance ^a	240	s m ⁻¹
Resistance function exponent ^b	2	dimensionless
Critical leaf water potential ^b	-150	m
Leaf resistance ^b	3.28E+04	kg m ⁻³ s ⁻¹
Root resistance ^b	6.60E+04	kg m ⁻³ s ⁻¹
Snow Properties		
Maximum temperature for snow ^b	2.0	°C
Roughness length ^b	0.15	cm
Residue Properties		
Fraction of surface covered ^b	1.0	
Albedo of residue ^b	0.20	dimensionless
Dry mass of residue ^c	9000	kg ha ⁻¹
Thickness of residue ^b	6	cm
Residue resistance to vapor transport ^b	50,000	s m ⁻¹

Table 4.2 continued. SHAW model parameterization

Soil Properties		
Layer 1		
Depth of layer	0-50	cm
Bulk density ^a	800	kg m ⁻³
θ_{sat}^a	0.5	vol vol ⁻¹
Sand/Silt/Clay/OM ^b	20/70/10/15	
K_{sat}^b	40	cm hr ⁻¹
Ψ_e^a	-0.02	cm
Pore size distribution index ^a	6.0	dimensionless
Layer 2		
Depth of layer	50-100	cm
Bulk density ^a	800	kg m ⁻³
θ_{sat}^a	0.65	vol vol ⁻¹
Sand/Silt/Clay/OM ^b	20/70/10/15	
K_{sat}^b	40	cm hr ⁻¹
Ψ_e^a	-0.02	cm
Pore size distribution index ^a	7.0	dimensionless
Layer 3		
Depth of layer	100-200	cm
Bulk density ^a	1000	kg m ⁻³
θ_{sat}^a	0.65	vol vol ⁻¹
Sand/Silt/Clay/OM ^b	25/65/10/3	
K_{sat}^b	10	cm hr ⁻¹
Ψ_e^a	-0.03	cm
Pore size distribution index ^a	15	dimensionless

Data sources:^a measured, this study^b estimated^c [Harmon *et al.*, in review]^d [Thomas and Winner, 2000]^e [Kramer, pers. comm.]

4.3.4.1 Canopy Characteristics

The objective of this analysis was to model the dynamics of the entire site, therefore the parameterization was designed to be as simple as possible, while effectively capturing the dominant behavior of the system. The canopy was modeled as 10 layers, ranging from 4 to 10 m thick, selected to correspond to sensor locations on the crane tower. We treated the vegetation canopy as a single species, since much of the validation data (i.e. θ and ET) is at the stand scale, and does not differentiate between inter-species variation. Seasonal variations in the canopy structure are relatively small in conifer canopies, therefore canopy characteristics were assumed to remain constant over time. The total LAI of the canopy was assumed to be the mean leaf area of 8.6 for the 1997-1999 years [Thomas and Winner, 2000]. The foliage clumping factor was estimated from measurements of global radiation at the forest floor discussed by Link *et al.* [in review-a]. Canopy biomass was estimated from a detailed canopy inventory using allometric techniques [Harmon *et al.*, in review]. Rooting depth was estimated to be 1.2 m, with approximately 90% of the total biomass in the top 30 cm based on mini-rhizotron measurements [Kramer, pers. comm.] and from observation of soil cores and pits.

4.3.4.2 Canopy Conductance

Stomatal conductance parameters were derived from 30-minute resolution EC measurements of ET completed during the period from May 20 through December 30, 1998, obtained from the Ameriflux website [Falk, 2000; <http://cdiac.esd.ornl.gov/ftp/-ameriflux/data/us-sites/preliminary-data/Wind-River/>]. The data were screened to

extract periods where measured transpiration fluxes are expected to be most reliable. Periods where the wind was blowing from the quadrant upwind of the crane tower ($45 < u_{dir} < 135$) were rejected. The remaining data included fluxes measured when the wind was blowing from directions outside of the optimal direction of fetch (i.e. $225 < u_{dir} < 315$), to maximize the volume of data. Data were screened to include only data collected between 1000h and 1400h, when soil heat (G) and canopy storage (St) fluxes are presumed to be negligible. All data within 6 hours of a precipitation event were rejected to assure that ET was composed predominantly of E_t . The filtering procedure reduced the dataset to less than 6% of the original values, from 10,766 to 599 points for the g_c analysis.

The measured sensible and latent heat fluxes in the filtered dataset were corrected for energy balance closure by assuming a constant Bowen ratio (β), and multiplying by an eddy-covariance correction factor (f_{EC}), defined as:

$$f_{EC} = R_{n,rad} / (H_{EC} + \lambda E_{EC}) \quad (4.7)$$

where $R_{n,rad}$ is the measured net radiation, and H_{EC} and λE_{EC} are the ecosystem sensible and latent heat fluxes measured by the EC system [Blanken *et al.*, 1997].

The corrected E_t fluxes (E'_t) were used to derive g_c for each data value by inverting the Penman-Monteith equation:

$$g_c = \frac{\gamma g_{aw}}{[(\Delta R_n + \rho_a c_p \delta_e g_{aw} / \lambda E'_t) - \Delta - \gamma]} \quad (4.8)$$

where Δ is the slope of the saturation vapor pressure/temperature curve, γ is psychrometric constant, λ is the latent heat of vaporization, and g_{aw} is the atmospheric

conductance to water vapor, assumed to be equivalent to the conductance for momentum:

$$g_{aw} = g_{am} = u_*^2 / u \quad (4.9)$$

where u_* is the friction velocity measured by the EC system. The canopy conductance relative to the maximum was computed:

$$g_{rel} = g_c / g_{c,max} \quad (4.10)$$

where $g_{c,max}$ was estimated from the upper envelope of the computed g_c at very low values of δe .

The maximum canopy conductance was approximately 36 mm s^{-1} which corresponds to a maximum stomatal conductance of 4.2 mm s^{-1} , assuming an LAI of 8.6. The estimate of $g_{c,max}$ is near the upper limit obtained from leaf-level measurements of stomatal conductance (g_s) for tree species in general [Nobel, 1991], and for Douglas-fir [Bond and Kavanagh, 1999].

The parameters for the canopy conductance model were derived for periods when transpiration was not expected to be strongly limited by θ (i.e. $\theta \geq 20\% \text{ vol vol}^{-1}$). Parameters were derived by plotting all computed values of $f(\delta e)$ against δe (Figure 4.2.). T_a and δe were closely correlated, therefore $f(\delta e)$ values below the maximum $f(\delta e)$ for a given δe are expected to be largely controlled by variations in S . Dividing the dataset into ranges of R_s did not produce a series of unique curves, as expected according to the conceptual Jarvis model [Jarvis, 1976]. We therefore estimated the parameters for the canopy conductance model by fitting Eq. (4.2) to the approximate upper envelope of the $f(\delta e)$ vs. δe data, as shown in Figure 4.2.

4.3.4.3 Litter and Soil Properties

The WRCCRF site is characterized by a thick litter layer of needles and fine woody debris. The litter layer is an important component of the physical system because it insulates the underlying mineral soil from heat transfer and intercepts a portion of the throughfall reaching the litter surface. The litter depth and mass per unit area were measured throughout the crane circle [Harmon *et al.*, 1998], and all other parameters were estimated from values in the literature. The litter is represented in the model domain by six nodes.

Four soil cores within the crane circle and 8 soil pits in the vicinity of the site indicate that the soil profile is composed of 3 primary layers roughly corresponding to the A, B, and C horizons. The upper layer extends from the surface to 50 cm, a middle layer extends from 50 to 100 cm and a very compact lower layer extends from approximately 100 cm to the lower boundary of the model domain at 200 cm (Table 4.2). The bulk density (ρ_b), porosity (n), and water characteristic function from 0 – 15 bars was measured on eighteen soil cores, 6 cm long, collected in the upper 120 cm of the soil profile. Soil properties were similar to other analyses completed in the region that found low bulk densities ranging from ~ 0.8 to 1.1 g cm^{-2} , and high porosities ranging from 50-75% [Harmon *et al.*, 1998]. The analyses indicate that the upper portion of the profile to 100 cm drains relatively freely, whereas the lower compact layer retains relatively high water contents at high soil tensions (Table 4.2).

The soil profile is represented by 24 nodes in the model domain. The SHAW model can effectively simulate soil processes with fewer nodes, however the higher number was selected to provide a direct comparison to T_g and θ validation data

locations. During the winter, depth to groundwater was very shallow, usually within 0.5 to 1.5 m of the surface [Link *et al.*, in review-a]. The rise of groundwater into the soil profile is approximated by parameterizing the deepest layer as a low conductivity unit to simulate saturated conditions at depth during very wet periods.

4.4 Results and Discussion

The overall goal of this research was to simulate the seasonal variation in hydrological processes occurring over the entire 2.3 ha crane circle, therefore we assessed the model performance based on mean site conditions. Near surface conditions may be affected by overlying canopy properties, which influence interception of radiation and precipitation, and may produce apparent errors because of differences in the sampling and modeling scales. Intra-site variability, such as litter depth and quality, soil properties, preferential flowpaths, and topographic position that affects depth to groundwater and capillary rise may also introduce apparent errors. We did not expect perfect agreement between measured and modeled values, but sought to reproduce the general daily and seasonal trends of fluxes and scalars.

4.4.1 Within Canopy Air Temperature and Vapor Density

In tall dense canopies, large variations between T_a measured above a forest canopy and at the forest floor occur during fair weather [Link *et al.*, in review-a]. The simulation of within canopy scalars (i.e. T_a and vapor density (ρ_v)) is important to evaluate when using multi-layer models, because the computed magnitudes define the gradients that drive mass and energy fluxes within the system and influence the stomatal mechanics that limit water fluxes. Figure 4.3 illustrates an example of a

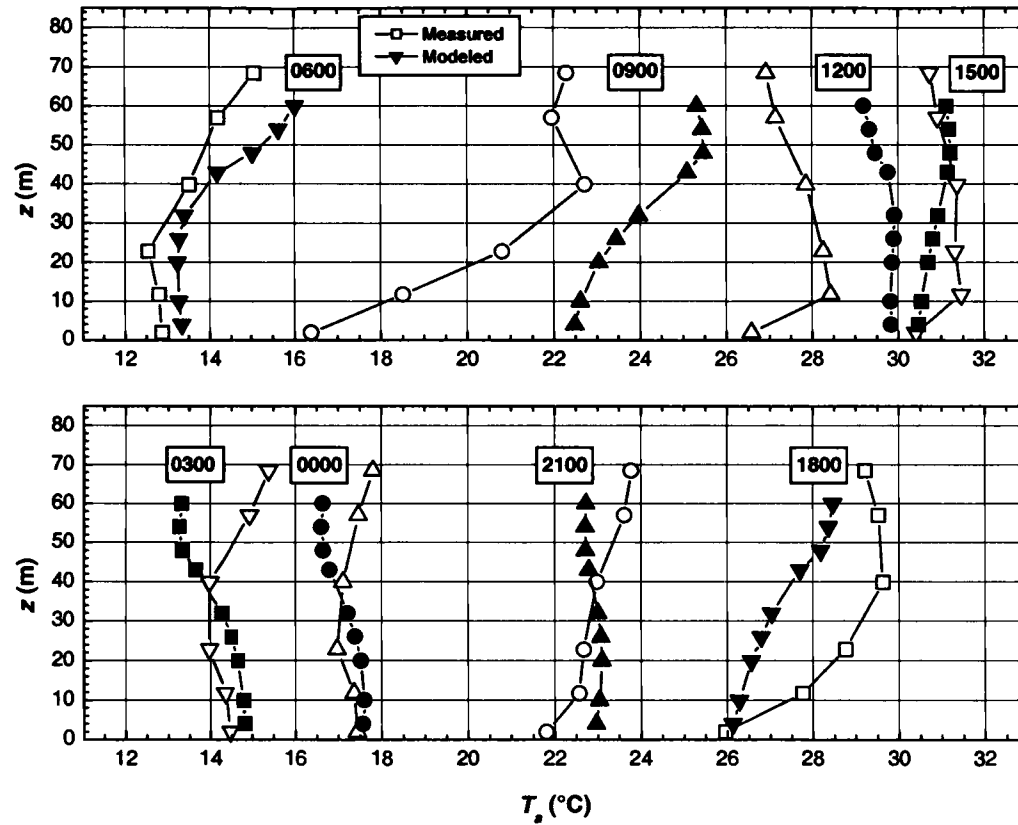


Figure 4.3. Measured and modeled within canopy air temperature profiles. Upper plot shows canopy warming from 0600h to 1500h; the lower plot shows canopy cooling from 1800h to 0300h. The differences during rapid warming and cooling represent simulated temporal lead of approximately 1 hour.

complete diurnal canopy warming and cooling cycle during a clear summer day when diurnal fluctuations are large. The upper layers of the canopy began to warm by 0600h, exhibited maximum vertical variation during rapid warming around 0900h, and became isothermal by 1200h. The canopy cooled after reaching a maximum at approximately 1500h, and reached a minimum temperature between 0300h and 0600h.

Measured and simulated canopy T_a values were generally within 1°C through the day, and exhibited the greatest difference during rapid warming at 0900h and cooling at 1800h. Although these differences appear to be large, they only correspond to a temporal difference of roughly 1 hour; that is, the simulated T_a responds more rapidly to environmental forcing than the measured values. These differences may be due to errors in the computed G or Sr terms of the energy balance arising from errors in the estimated biomass and/or thermal conductivities of the biomass or litter/soil layers. Discrepancies may also be due to the effect of comparing time-averaged validation data, to instantaneous modeled values.

Within canopy vapor densities (ρ_v) generally increase with canopy depth, and exhibit a relatively small range of variation (not shown). The SHAW model correctly simulated the increase of ρ_v with depth and the range of diurnal variation. During fair summer weather, the greatest diurnal variation was characterized by rapid vapor decreases occurring during afternoon periods from approximately 1300h to 1800h. These times correspond precisely to diurnal wind increases, and represent advection of drier air into the site. The simulated within-canopy ρ_v exhibited the largest differences relative to the measurements during these periods of rapid change. As was observed

for the T_a variation, the differences could be interpreted as a temporal lag in the simulated ρ_v of approximately 1 h.

4.4.2 Snow Processes

The 1999 winter was warmer than average, and a greater proportion of the winter precipitation than average occurred as rain rather than snow [Link *et al.*, in review-a]. Most snowfall during the 1999 winter occurred as very small events ranging from 5 to 20 mm of snow water equivalent (SWE), typically ablated soon after deposition, and never developed into a spatially continuous snowpack. Accurate simulation of snowpack dynamics under these conditions is particularly difficult because the simulation of the precipitation phase is controlled by T_a , which oscillates about the snow/rain threshold temperature. Mixed snow/rain and snow events in the PNW typically occur over a range of temperatures from -1 °C to 3 °C [U.S. Army Corps of Engineers, 1956], indicating that slight variations in T_a may shift the simulated proportion of rain to snow. Furthermore, the assumption of a continuous snowcover is invalid during these periods, which introduces error into the computation of snowmelt.

Despite the problems associated with modeling transient, discontinuous snowcover dynamics, the SHAW model correctly simulated the development and ablation of a transient snowcover at the gap site to within 4 days during the 1999 winter. In 2000, when a shallow but continuous snowcover developed at the site, SHAW reasonably simulated the snowcover dynamics (Table 4.3). However, the simulated snowcover both developed and ablated approximately 1 week before the

Table 4.3. Measured and modeled snowcover variables, 2000

Variable	Measured	Modeled
Deposition Date	January 10	January 2
Ablation Date	March 31 – April 4	March 27
SWE, Jan. 27	164-179 mm	158 mm
SWE, Mar. 8	225 mm	223 mm

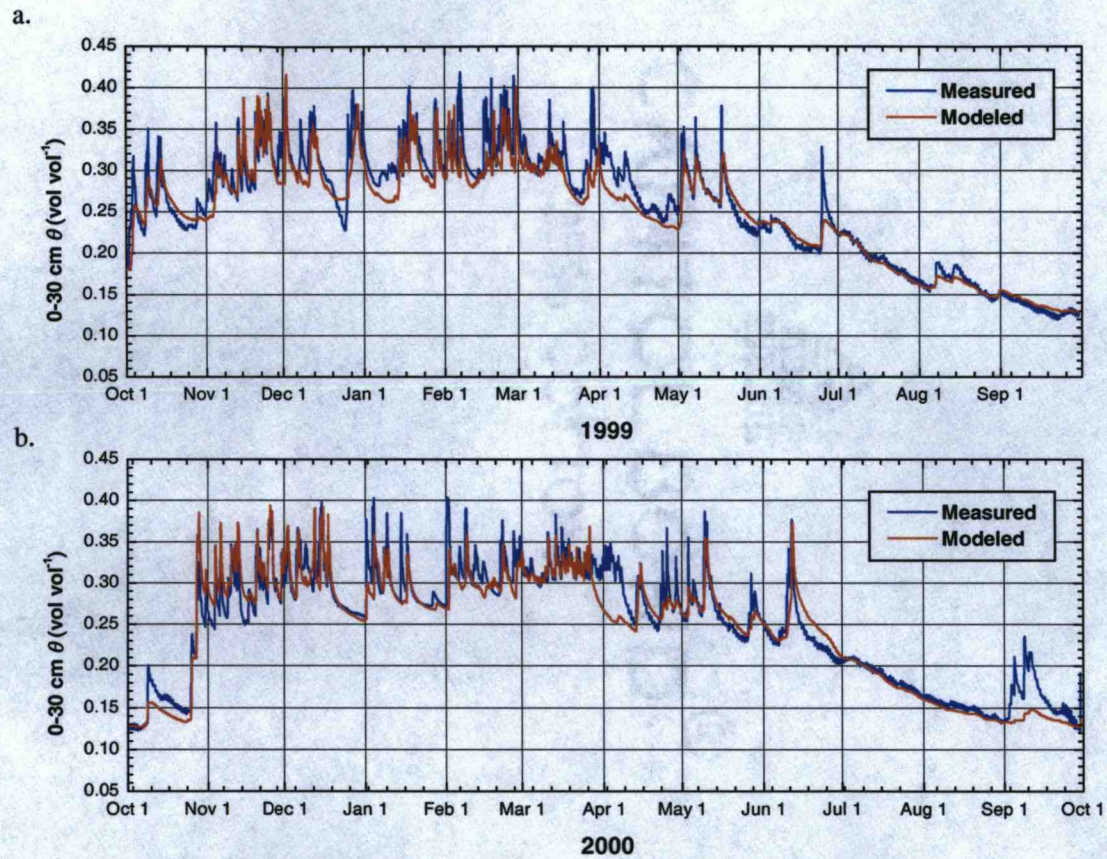
measured dates. This discrepancy may also be due to errors in the measured ablation date because the accuracy of the snow sensor declines for very shallow snowcovers, due to scattering of the signal by the non-uniform snow surface. Simulated midwinter

SWE exhibited good agreement to manual measurements made with a density cutter. Considering the wide range of snowcover variability and difficulty of measuring and simulating shallow snowcovers, we considered the model performance to be reasonable for snowcover processes in this environment.

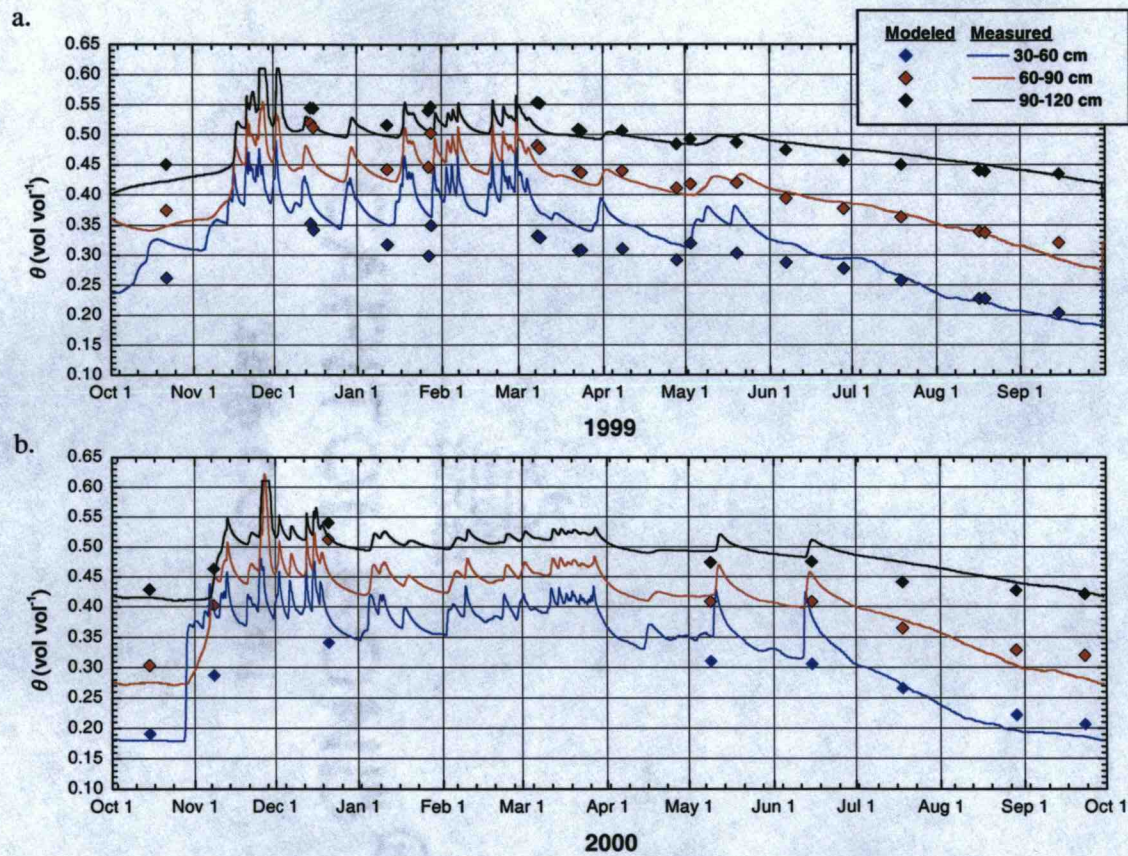
4.4.3 Soil Water Content

Results of soil water content (θ) simulations are presented in Figures 4.4a and b for the 1999 and 2000 hydrologic years, respectively. The average 0-30 cm θ is compared with measurements from automated sensor that serves as a proxy for the mean site θ [see *Link et al.*, in review-a]. Results of deeper θ simulations are shown in Figures 4.5a and b. Midwinter measurements of deep θ using the segmented probes could not be completed during the winter of 2000, because of snow cover.

Both hydrologic years exhibited typical seasonal soil water trends for the PNW, where soils were typically wet during the fall and winter, followed by a progressive drying during the summer and early fall. The model effectively simulated the



Figures 4.4a and b. Measured and modeled 0-30 cm soil water content. Relatively large differences during early April of both years are due to spatial variation or simulation errors in the snowcover.



Figures 4.5a and b. Measured and modeled deep soil water content. Midwinter measurements could not be completed due to the development of a continuous snowcover that restricted access to TDR probes.

moisture conditions at shallow depths over the annual cycle for both the calibrated and uncalibrated years, indicating that the model parameterization developed for 1999 is effective. The largest differences between the measured and modeled values occurred during the midwinter months due to errors in the simulation of the timing and rate of snowcover deposition and ablation. A large degree of spatial variation in the sub-canopy snowcover was observed during these periods owing to variations in canopy interception, so these modeling differences are not surprising when using data from a proxy sensor to validate stand-level simulations. The simulated response of θ to precipitation events is often less than the measured response, probably because the model simulates mean site canopy conditions, whereas the measurement was made in a canopy gap with greater throughfall.

Model performance statistics for shallow θ are presented in Table 4.4. The Nash-Sutcliffe coefficient or model efficiency, (ME) describes the variation in measured values accounted for by the model, calculated as:

$$ME = 1 - \frac{\sum_{i=1}^n (x_{obs} - x_{sim})^2}{\sum_{i=1}^n (x_{obs} - x_{avg})^2} \quad (4.11)$$

where n is the total number of observations, x_{obs} is the observed quantity at a given timestep, x_{sim} is the simulated quantity at the same timestep, and x_{avg} is the mean of observed values. The table also presents the root mean square difference (RMSD), calculated as

$$RMSD = \frac{1}{n} \sqrt{\sum_{i=1}^n (x_{sim} - x_{obs})^2}, \quad (4.12)$$

the absolute mean bias difference (AMBD) calculated as

$$AMBD = \frac{1}{n} \sum_{i=1}^n (x_{sim} - x_{obs}), \quad (4.13)$$

and the relative mean bias difference (RMBD) calculated as the quotient of the AMBD and the mean of the measured values.

Table 4.4. Model fitting statistics

Parameter	1999		2000	
	θ (0-30cm)	T_g (15cm)	θ (0-30cm)	T_g (15cm)
ME	0.89	0.99	0.90	0.98
RMSD	2.1 vol vol ⁻¹	0.53 °C	2.2 vol vol ⁻¹	0.65 °C
AMBD	0.8 vol vol ⁻¹	0.08 °C	0.5 vol vol ⁻¹	0.12 °C
RMBD	3.2 %	—	2.1 %	—
Mean	25.0 vol vol ⁻¹	7.15 °C	24.4 vol vol ⁻¹	7.61 °C

The ME for θ in the 0–30 cm layer was 0.89 and 0.90 for the two years, indicating that the model reasonably simulated the water content dynamics at the site. RMSDs for the two years were slightly greater than 2% vol vol⁻¹, with AMBDs less than 1% vol vol⁻¹. The modeled differences were well within the measurement error, and were much less than the spatial variability observed within the site [Link *et al.*, in review-a]. Performance statistics were slightly better for the uncalibrated year, probably due to greater errors in the simulated snowcover deposition and ablation that occurred during the warmer 1999 winter, which was characterized by a highly transient and discontinuous snowcover.

Simulations of θ at greater depths are validated against periodic measurements of θ with the segmented moisture probes and are shown in Figures 4.5a and b. The

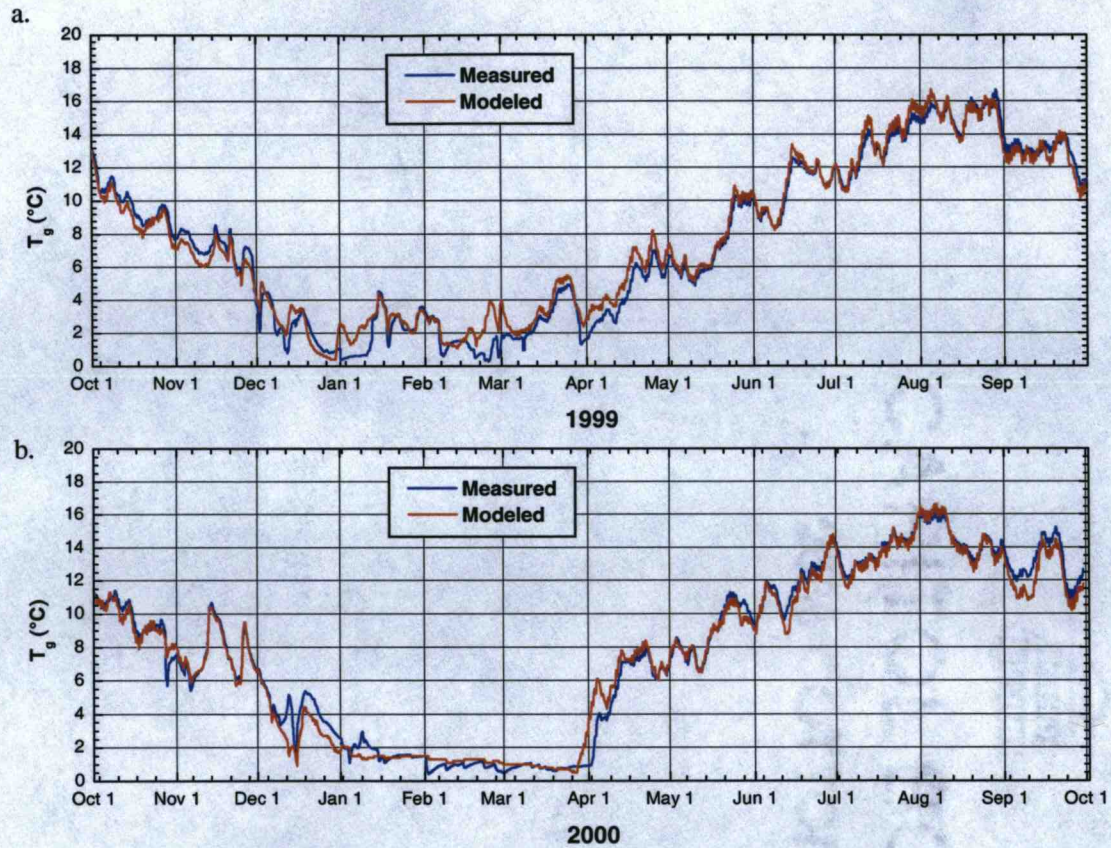
measured and modeled θ for the 60 – 90 cm and 90 – 120 cm soil layers exhibited reasonable agreement for both years. The simulated θ of the 30 – 60 cm layer was consistently about 5% vol vol⁻¹ higher than the measured values during the winter months, but showed good agreement during the summer drydown period.

4.4.4 Soil Temperature

Figures 4.6a and b show simulations of soil temperature (T_g) at 15 cm; model fitting statistics are included in Table 4.4. The model accurately simulated T_g during both years, as indicated by high MEs of 0.98 to 0.99, RMSDs less than 1 °C, and a negligible (< 0.1 °C) bias throughout the year. Model performance for the uncalibrated year was very similar to the calibrated year, indicating that the parameterization was also effective for soil heat dynamics.

During the 1999 winter, when the snowcover was highly transient and discontinuous, T_g showed considerable variation. In 2000, when there was a deeper, continuous snowcover, soils maintained a low and relatively constant temperature through the winter, followed by a rapid rise after the snowcover ablated. Comparison between the two years showed the pronounced effect of the seasonal snow cover on the soil temperature regime and timing of soil warming. An understanding of snowcover dynamics is therefore critical to understand the timing of soil warming and the onset of transpiration.

The largest differences between the measured and modeled T_g also occurred during the winter months due to slight errors in either the timing and/or the spatial distribution of the below-canopy snowcover. When the simulated snowcover was



Figures 4.6a and b. Measured and modeled 15 cm soil temperature trends. As noted in Figures 4 and b, the largest differences between the measured and modeled values are related to spatial variation or simulation errors in the snowcover.

depleted, simulated T_g increased rapidly in response to environmental conditions (Figure 4.6b). However, when the actual snowcover over a T_g sensor is depleted, but large quantities of snow remain in other areas of the site, soil warming will be suppressed because the existing snow will act as a heat sink, preventing within canopy air temperature increase. The discrepancy that occurred during late February - early March in 1999 is a result of this phenomenon. After most of the snow beneath the canopy was depleted, simulated T_g trends closely matched the measured trends. In both simulations, the timing of the seasonal T_g increase was well represented, with simulated values at 15 cm exceeding 3 °C only 5 days prior to the measured date. Further improvement of the canopy mass and energy transfer formulations will improve the simulated timing of snowcover ablation and soil warming.

4.4.5 Evaporation and Transpiration

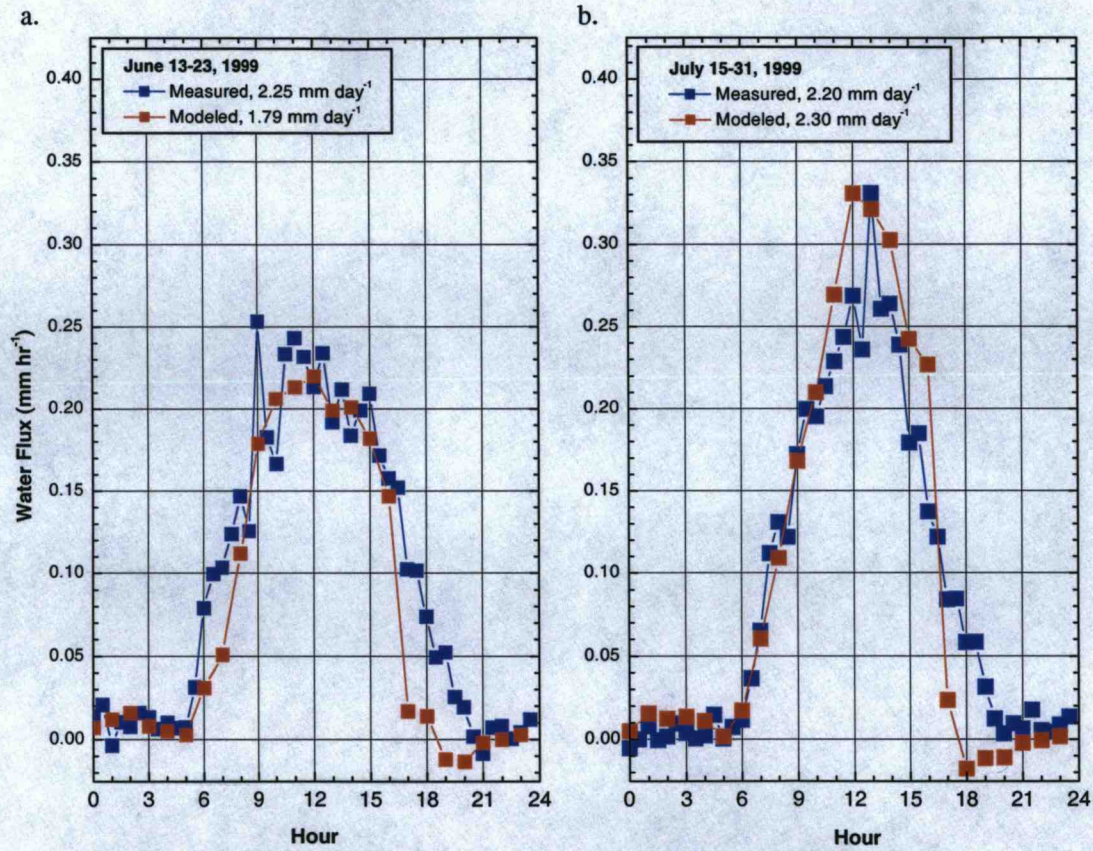
Table 4.5 presents the total precipitation (P_G), throughfall (P_n) and interception losses (I_{net}) for the 1999 and 2000 measurement periods. Simulated throughfall results spanned the snow-free measurement periods during the 1999 - 2000 and 2000 - 2001 water years for direct comparison to the measured data [Link *et al.*, in review-b]. Simulated throughfall closely matched the measured results as indicated by small (< 4%) differences between measured and simulated P_n and interception loss (I_{net}). The throughfall validation indicates that the application of the mean canopy throughfall parameters (see Section 3.3.2) are effective for computing long-term interception dynamics with the SHAW model.

Table 4.5. Throughfall and interception summary

Precipitation Component	Throughfall Measurement Period	
	Apr 8 - Nov 8 1999	Mar 30 - Dec 3 2000
P_G (mm)	450.9	618.7
Measured P_n (mm)	348.2	463.8
Modeled P_n (mm)	350.8	468.9
Difference (%)	0.7	1.1
Measured E_i (mm)	102.7	155.0
Modeled E_i (mm)	100.1	149.8
Difference (%)	-2.5	-3.4

A comparison between simulated and measured (by EC) diurnal ET trends is presented in Figures 4.7a and b. The diurnal trends represent ensemble-averaged fluxes for an 11 and a 17-day period in June and July respectively, to correspond to the periods analyzed by *Unsworth et al.* [in review]. The measured ET fluxes were filtered to exclude periods when u_{dir} was blowing through the tower, from 45° to 135°. Ensemble averages were used to produce representative diurnal trends, despite data gaps resulting from the filtering procedure. The selected periods were characterized by dry conditions, therefore the fluxes were predominantly of transpiration, to validate the simulation of E_i by the SHAW model.

Modeled fluxes during the June and July periods generally matched the pattern of the measured fluxes, with a simulated hourly maximum of 0.22 mm hr⁻¹, compared to the EC-measured maximum of 0.24 mm hr⁻¹. During the July period, simulated maximum hourly ET fluxes were 0.33 mm hr⁻¹, which closely matched the measured maximum of 0.30 mm hr⁻¹. The largest differences occurred in the morning and afternoon periods, when measured fluxes were larger. The rapid increase in the



Figures 4.7a and b. Measured and simulated ensemble-averaged total ecosystem water fluxes.

measured flux in the morning can probably be attributed to transpiration of stored water within the stems of vegetation, which is not explicitly represented in the model. The more rapid simulated decline in ET flux rates in the afternoon may be due to errors in the g_s parameterization, or due to a differing response of stomata to environmental conditions during the 1998 parameter derivation period.

Modeled and estimated ET for the 3 ensemble periods in June, July and September discussed by *Unsworth, et al.* [in review] are presented in Table 4.6. Values of ET were estimated with the EC system (E_{EC}), from changes in soil water content (E_{θ}), and by the sum of overstory transpiration (E_t) estimated from sap flux measurements, the EC understory water flux (E_u), and the flux from woody debris (E_d), estimated from measured changes in water content. In June, the simulated mean daily ET flux was 20% less than the EC mean daily flux, but was similar to the fluxes estimated using other techniques. In July, the modeled ET flux exceeded all other estimates, but was only 5% greater than the E_{EC} estimate. No EC data were available after August 1, 1999 at the time this manuscript was written. Simulated ET in September was very similar to the E_{θ} estimate. The late summer declines in the estimates of ET agreed qualitatively with sapflux declines, which were estimated to be 1.01 mm day^{-1} during the September period. These observations are consistent with other studies that noted apparent underestimation of ET using the sap flux technique, despite a good qualitative comparison to other techniques [*Wilson et al.*, 2001].

Table 4.6. Mean daily evapotranspiration results.

Ensemble Period	Modeled ET	E_{EC}	$E_t + E_u + E_d$	E_θ
June 13-23	1.79	1.97	1.83	1.71
July 15-31	2.30	2.20	1.84	1.97
September 7-17	1.88	nd	1.01 (E_t only)	1.98

note: All values are in mm day^{-1}

E_{EC} : EC estimated water flux

$E_t + E_u + E_d$: Ecosystem water flux estimated from sap flux, sub canopy EC, and water content changes of coarse woody debris.

E_θ : Water flux estimated from soil water content changes

Several possible sources of error may contribute to the observed discrepancy between the EC and simulated ET fluxes. The parameterization of the SHAW model was optimized from local measurements to represent the 2.3 ha plot, and other estimates of ET based on $E_t + E_u + E_d$ and E_θ were made from measurements at the local scale. In contrast, the areal footprint sampled by the EC system is larger, and varies in size, shape, and location depending on the wind velocity and direction [Baldocchi, 1997; Lee, 1998]. Source wind directions outside of the optimal direction of fetch are also included in the ensemble averages, therefore the measured data may not be exactly representative of site conditions. The flux measurements used in this evaluation only included the vertical component, and did not include the horizontal, advected, mass-flow component which can be large on gently sloping sites like WRCCRF due to drainage flows [Lee, 1998]. Finally, meteorological data were collected on the crane tower which was located in a canopy gap, which may not perfectly represent the microclimate above the forest canopy, and thereby introduce errors. Considering the good agreement between the measured and simulated ET and

potential sources of error due to measurement methods and scales we conclude that the SHAW model effectively simulated transpiration in this environment.

4.4.6 Simulated Energy and Water Fluxes

Results of the model performance and validation presented above indicate that the SHAW model accurately simulated within-canopy conditions, snowcover processes, soil moisture and temperature, rainfall interception and transpiration at daily to seasonal scales. We therefore assume that modeled seasonal variations in energy and water fluxes are accurate for the 1999 and 2000 hydrologic years.

Table 4.7 contains a summary of simulated mean monthly R_n , H , λE , and $S + G$ fluxes, and the Bowen ratio (β) for the 1999 and 2000 hydrologic years. Monthly sums of precipitation, and modeled evaporation, transpiration, runoff and Δ storage are presented in Table 4.8. Positive values indicate fluxes toward the surface, and negative values indicate fluxes away from the surface. The shift from positive to negative H occurred between February and March in 1999, and between March and April in 2000. Latent fluxes were negative for all months, except for December 1998, which was characterized by anomalously cold conditions. In 1999, β was variable in the spring, but decreased from June through September. The spring months with higher Bowen ratios occurred during periods of relatively low precipitation, which resulted in smaller interception losses, and hence lower λE . In 2000, β increased steadily from April to July and decreased from July through September. It is anticipated that β might increase through the summer drought period as T_a increases and the vegetation becomes increasingly water-limited. However, as dry season

Table 4.7. Simulated mean monthly energy flux summary.

hy	Month	R_n (W m^{-2})	H (W m^{-2})	λE (W m^{-2})	$St+G$ (W m^{-2})	β
1999	Oct	35.1	4.5	-40.1	0.5	-0.11
	Nov	13.2	11.3	-20.9	-3.6	-0.54
	Dec	2.2	34.7	8	-44.9	4.34
	Jan	9.8	53.5	-22	-41.3	-2.43
	Feb	27.3	62.2	-31.7	-57.8	-1.96
	Mar	70.6	-7.4	-45.4	-17.9	0.16
	Apr	135.8	-86.1	-52.2	2.5	1.65
	May	165	-94	-82.9	11.9	1.13
	Jun	167.9	-107.6	-64.3	4	1.67
	Jul	205.6	-117.4	-84.6	-3.6	1.39
	Aug	155.5	-77	-75.7	-2.8	1.02
	Sep	114.9	-50.9	-61.2	-2.7	0.83
	Total	92.2	-31.6	-47.9	-12.7	0.66
2000	Oct	38.8	12.4	-40.1	-11.2	-0.31
	Nov	12.2	22.9	-21	-14.2	-1.09
	Dec	2.6	24.7	-5.8	-21.5	-4.26
	Jan	13.4	47.2	-30.3	-30.2	-1.56
	Feb	30	45.6	-37	-38.6	-1.23
	Mar	79.7	22.8	-58.4	-44.1	-0.39
	Apr	128.5	-37.3	-81.3	-9.9	0.46
	May	162.8	-58.5	-91.7	-12.6	0.64
	Jun	196.1	-85.8	-96.4	-13.9	0.89
	Jul	203.2	-115.7	-84	-3.4	1.38
	Aug	182.6	-94.9	-85.3	-2.4	1.11
	Sep	107.4	-34.4	-60.3	-12.7	0.57
	Total	96.8	-21.3	-57.7	-17.8	0.37

Note: The sign convention for fluxes is that negative values correspond to transfer from the surface to the atmosphere.

Table 4.8. SHAW monthly water flux summary

hy	Month	Precipitation P_G , (mm)	Evaporation E , (mm)	Transpiration E_t , (mm)	Runoff (mm)	Δ Storage (mm)
1999	Oct	95.2	23.4	10.9	0	60.6
	Nov	615	17.4	0	393.2	206.5
	Dec	526.3	-5.5	0	559.9	-24.7
	Jan	358.9	18	0	342.5	-1.7
	Feb	620.5	21.6	0.2	446.8	155.5
	Mar	168.4	27.9	7.7	315.8	-179.3
	Apr	22.7	14.9	28.3	61.5	-82.1
	May	130.6	38.6	32.3	42.9	18.5
	Jun	27.9	16.5	37	17.4	-42.2
	Jul	4.5	6.3	66.2	3.9	-71.5
	Aug	23.1	15.3	49.5	0	-41.7
Sep	3	5.3	45.6	0	-46.2	
	Total	2596.1	199.7	277.7	2183.9	-48.3
2000	Oct	174.9	16.8	17.4	0	141.3
	Nov	568.7	16.4	1.1	289.1	262.2
	Dec	450.7	5.1	0.4	540	-90
	Jan	402.1	23	0	174	203.7
	Feb	358.8	23.8	1.3	196.8	137.3
	Mar	166.1	36.9	8.1	427.5	-301.7
	Apr	94.8	39.8	27.4	64.4	-36.3
	May	138.5	44.8	33.7	81.5	-20.8
	Jun	99.7	19.8	60	47.5	-26.2
	Jul	0.2	3.7	68.2	12.2	-82.9
	Aug	2.9	4.6	68.4	0	-70.4
Sep	24.3	15.1	34.8	0	-27.8	
	Total	2481.7	249.8	320.8	1833	88.4

progressed, the climate at the WRCCRF became more continental as δ_e increased, and thereby increased the driving gradient for vapor transfer. This system was able to consistently transpire water under late summer conditions, hence β decreased. If the system were more water-limited and greater stomatal closure occurred, β would decrease at a slower rate, or might increase as observed in more arid canopies [Anthony *et al.*, in review]. These findings were consistent with comparisons of Bowen ratios between coniferous forests across a gradient from humid marine to continental environments [Jarvis *et al.*, 1976].

Runoff totals in Table 4.8 are the sum of deep percolation out of the soil profile and surface runoff, which only occurred during an uncommon soil freezing event from December 19 to 30, 1998. Simulated runoff ceased only during August through October during both years. Net water storage by the system occurred in October and November when the soil profile rewetted after the summer dry down, and during mid-winter months when the transient snowcover developed. Evaporation includes evaporation of intercepted water on the canopy and evaporation from the litter and soil layers, therefore evaporation can exceed P_G during some months. The monthly water flux summary indicates that simulated ET was 18.3 % and 23.9 % of P_G during the 1999 and 2000 hydrologic years, respectively. ET exceeded the monthly P_G during the months of April and June through September in 1999, and from July through September in 2000. During these months, transpiration decreased from an average maximum of 2.17 mm day^{-1} in July to a minimum of 1.34 mm day^{-1} in September.

The summary of the water balance components indicates how the system shifted from a water surplus to a water deficit between May and June. The timing of the

transition from water surplus to water deficit is particularly important, because it controls the amount of time that vegetation is dependent on stored soil water to meet evaporative demands. The timing and magnitude of mid-summer storms may also be an important source of water available for root uptake, however the storms must be of sufficient size and/or frequency to fully saturate the canopy and litter layer and result in infiltration into the soil.

The analysis discussed here helps in considering the implications of climate changes. PNW climate scenarios for the year 2025 generally indicate an increase in T_a for all months, but predictions for P_G changes are less consistent between models [Hamlet and Lettenmaier, 1999; Miles *et al.*, 2000]. For example, the Hadley Center GCM predicted precipitation increases of 22% for the summer months, whereas the Max Planck Institute GCM predicted a 9% decrease in summer precipitation for the region. When, and whether a decrease in precipitation occurs may have profound consequences for the hydrologic cycle and associated ecological processes due to the importance of the timing of the seasonal shift from surplus to deficit conditions.

4.5 Summary and Conclusions

Modifications to the SHAW model were presented for application in forested environments. Validation of individual hydrologic and physical processes simulated by the model exhibited reasonable agreement with measured values considering the potential sources of measurement error. Performance of the modified model was very similar for the 1999 calibration period, and for the uncalibrated 2000 hydrologic year. The relatively simple parameterization applied to this system indicated that hydrologic

processes can be reasonably simulated by assuming that all trees have similar physiological characteristics and have static biophysical properties (e.g. LAI, rooting depth) throughout a seasonal cycle.

The SHAW model is a powerful tool that can be used to investigate the impacts of climate variability and canopy characteristics on individual hydrological processes and on the seasonal variations of water and energy fluxes. The snowcover transition zone is particularly sensitive to climatic variation, because small increases in T_a will shift the system from a winter snow-dominated to rain-dominated regime, as exemplified by the 1999 winter. Similarly, shifts in the temporal transition from wet to dry conditions may result in late season reductions in transpiration, as a result of alterations in the onset of the seasonal drydown. The current parameterization could be used for additional simulations using perturbed climate data to estimate the range of potential impacts on the hydrologic cycle in the transition zone of the PNW.

The process study presented here focused on a particular old-growth forest, whereas the PNW region contains forests of a wide range of canopy ages and conditions. Additional studies focusing on detailed measurements and modeling of hydrological processes in other canopy types are needed to develop an improved understanding how mass and energy fluxes will respond to the coupled climate and vegetation variations in the PNW.

4.6 Acknowledgements

Support for this research was provided by the Western Regional Center (WESTGEC) of the National Institute for Global Environmental Change (NIGEC), the

U. S. Forest Service, and the Agricultural Research Service, Northwest Watershed Research Center. Office and computing facilities were provided by the U. S. Environmental Protection Agency, Western Ecology Division. Eddy covariance data were provided by Matthias Falk and Dr. Kyaw Tha Paw U (University of California, Davis). Sap flux data were provided by Dr. Nathan Phillips (Boston University) and Dr. Barbara Bond (Oregon State University).

5. CONCLUSIONS

5.1 Summary

The central question addressed in this investigation concerns how an old-growth seasonal temperate rainforest canopy interacts with climate to control hydrological fluxes. The general hydrologic and climatic characteristics of the site and spatial and temporal microclimate differences within the forest canopy were presented in Chapter 2, to provide background information for the detailed evaluation of hydrological processes presented in the following chapters. Chapter 3 presented a detailed analysis of the interception process and applied the Gash analytical model to this system. The results presented in Chapters 2 and 3 were then used to modify, parameterize and validate a detailed 1-dimensional process model of mass and energy transfer, discussed in Chapter 4.

The analysis of recent and historical climate data in Chapter 1 indicated that the climate during the 1999 and 2000 hydrologic years was characterized by average precipitation volumes, and above average winter temperatures. As a result, precipitation occurred mainly as rain, rather than snow, during the 1999 winter, and a spatially continuous snowcover never developed at the site, despite record snowpack conditions in the Pacific Northwest (PNW). Although a continuous snowcover did develop during the 2000 winter, the period of snowcover was shorter than the long-term average.

Relatively large microclimate differences were observed between the open field, above-canopy, and below-canopy sampling locations. The mean monthly air

temperature (T_a) values at the open station were slightly cooler (~ 0.6 °C on average) than the above-canopy location. Relative to the above canopy location, the open station exhibited larger diurnal T_a cycles that increased in magnitude throughout the summer. The larger diurnal variation was attributed to net radiation differences between the two landcovers and larger latent heat fluxes from the deeper rooted forest canopy during the driest periods of the year. Estimates of mean monthly potential evapotranspiration using the Penman-Monteith method indicated that use of the open site data as a proxy for above canopy microclimate may underestimate potential ET by 6% to 54%, with the larger errors associated with periods of low ET. The microclimate below the forest canopy exhibited cooler temperatures, higher relative humidity, low but consistent windspeeds, and a damped diurnal T_a cycle relative to the open site. Within-canopy conditions were similar to other observations of interior forest microclimates in this region.

The site hydrology was characterized by seasonally wet conditions. An ephemeral stream flowed from roughly November through May or June depending on the timing of the transition from wet to dry conditions. The shallow soil water content was spatially variable across the 4 ha stand, with maximum differences of 12% to 40% depending on the time of year. The northeastern quadrant had a high soil water content even during the driest part of the year. This observation implies that surface water fluxes may be spatially variable during summer. Consequently, eddy-covariance measurements may be atypical of the general area when the footprint encompasses the northeast quadrant of the stand. The depth to groundwater was very shallow during most of the year, ranging from 0.5 m to approximately 2.5 m below the

surface. The valley-bottom location of the site, and shallow water table suggest that moisture conditions at the site may not be representative of the higher relief areas in the western PNW, and therefore results from the WRCCRF should be extrapolated with caution to other sites.

Soil temperatures at 15 cm varied little between canopy gap and closed canopy areas despite large differences in the overlying canopy cover. These differences were due to small diurnal damping depths associated with high porosity, low bulk density soils, and a thick organic litter cover at the site.

The interception study presented in Chapter 3 indicated that canopy interception losses for the snow-free periods from roughly April through October were approximately 24% of the gross precipitation. The relatively large interception losses in this system resulted both from a large mean canopy storage capacity and from relatively high volumes of evaporation that occurred during extended rainfall events. Evaporation rates during saturated canopy conditions were found to be highly variable between events, and extremely sensitive to intermittent dry periods characterized by warmer air temperatures and decreased relative humidity. The mean canopy storage capacity was about 3.3 mm for the 2000 hydrologic year, and appeared to shift from ~3.1 mm in the spring and fall months to ~4.0 mm in the summer months, probably due to seasonal changes in the stand leaf area. The relatively high canopy storage volume may be attributed to the high leaf area index (LAI), deep, rough bark of the very old trees, and an abundant lichen and bryophyte community. Gash's analytical model for interception performed well when applied on an event basis, and when the Penman method was used to estimate evaporation during rainfall. Daily application of

the model was found to be inappropriate for the PNW environment because there were often extended periods of precipitation, that violated the key model assumption of only one canopy wetting and drying cycle per day.

Chapter 4 presented modifications to the Simultaneous Heat and Water (SHAW) model to more accurately simulate mass and energy fluxes in forested environments. The parameterization of the canopy interception characteristics was modified based on values derived from the analyses presented in Chapters 2 and 3. A simplified Jarvis-Stewart model to approximate the stomatal response to vapor pressure deficit (δe) and T_a was added to more accurately simulate transpiration at the beginning of the seasonal drydown when T_a , δe and soil water contents were relatively high. Parameters for the stomatal conductance model were derived from eddy-covariance measurements of ecosystem water flux completed during the preceding year. Within-canopy energy transfer processes were also improved by implementing a foliage clumping factor to more accurately simulate transmission of solar radiation through the canopy, and by including a formulation for free convection within the canopy air space.

The model parameterization was optimized for the 1999 hydrologic year and validated by applying it to the 2000 climate data without modification. Model performance statistics for the 0–30 cm soil water content and 15 cm soil temperature were very similar for the two years, and indicated excellent performance. The model also showed reasonable agreement for diurnal trends of within-canopy temperature and vapor density, timing of snowcover deposition and ablation, interception/throughfall volumes, soil water content at depth, and transpiration fluxes.

The largest differences between the simulated and measured values generally occurred during winter due to spatial variability or errors in the simulation of the transient snowcover. Analysis of simulated energy fluxes revealed that mean monthly Bowen ratios increased through the seasonal dry period because transpiration was relatively constant, supplied by stored soil water, despite extended periods without significant precipitation. During the seasonal dry months (July–September) of the 1999-2000 period, transpiration decreased from a mean maximum of 2.17 mm day^{-1} in July to a mean minimum of 1.34 mm day^{-1} in September. Dry soil conditions appeared to limit transpiration at the site, although not substantially, probably due to a large volume of root-extractable water, and shallow water table which maintains soil water at depth later in the dry season. These results also indicate that the site may be wetter than typical forested sites in the Cascades.

5.2 Future Directions

The results from this investigation indicate a number of directions for future research. Due to the cost and difficulty associated with collecting meteorological data above forest canopies, meteorological data for hydrological investigations in forests are frequently collected in clearcuts, or other open areas. The sensitivity of potential ET to microclimate data collected over an unmanaged grass and forest canopy suggest that use of data from open sites may introduce large errors into hydrological and ecological process models. The sensitivity analysis presented in Chapter 2 was completed for forest vegetation, assuming average canopy conductance values for well-watered conditions. The observed differences may increase or decrease if

feedbacks between environmental conditions and stomatal mechanics are considered. A comparison of the sensitivity to computed hydrologic fluxes should be completed with the SHAW model to gain a more accurate estimate of potential errors associated with data collected over non-representative vegetation covers. If estimated fluxes are significantly different, surface correction algorithms should be developed to correct meteorological data for landcover differences, since regional ET calculations often need to use data from open-site weather stations.

The interception study presented in Chapter 3 focused on defining the interception characteristics of the entire stand. The processes controlling interception are complex, and exhibit considerable variation in the horizontal and vertical dimensions. The interception analysis assumed that 6 hours were required for a saturated canopy to completely dry, but this threshold may vary depending on climatic conditions. The vertical variations of T_a and relative humidity presented in Chapters 2 and 4, suggest that drying of the deeper canopy layers may be limited by low radiation, T_a , δe and wind velocity, such that deeper layers may retain water between events, effectively reducing interception losses. The different canopy elements, such as lichens, bryophytes, leaves and bark have different resistances to vapor transport, and therefore may be expected to exhibit different water retention characteristics. Additional study of evaporation rates from different canopy elements and at different canopy depths should be completed to improve our understanding of interception dynamics during intermittent and closely-spaced precipitation events. Furthermore, the canopy saturation storage capacity is likely to be a dynamic quantity, dependent on precipitation intensity and wind velocity, and could be characterized in greater detail

with continued sampling. Additional research will improve the representation of the interception process in hydrological models, and could also be particularly beneficial for the simulation of leaf wetness duration for pathological investigations.

The SHAW model functioned very well on a seasonal basis, but variations were evident over shorter periods. A more detailed comparison of the measured and simulated vertical variations of T_a , vapor density, and wind speed within the canopy should be completed to further refine the SHAW model for forested systems. Improvement of simulated within-canopy scalar variations will enhance the simulation of fluxes between canopy layers, at finer temporal scales. Complete validation of the model at finer resolutions will increase the potential applications of the model, such as for determining wetness durations for individual canopy layers, as discussed above.

The largest divergences between the modeled and measured hydrologic variables occurred during periods characterized by snowfall or discontinuous snow covers. Although snow comprised a relatively minor component of the water balance during the 1999 and 2000 hydrologic years, slightly cooler conditions would have likely produced a deeper snowcover and longer snow season. Additional measurement and modeling studies of snowcover processes in the PNW during more typical winter conditions will improve our confidence in the ability of the SHAW model to simulate cold-season hydrological processes. Central to the improved simulation of snowcover processes in this transition zone will be a modified formulation to estimate the snow/rain precipitation threshold based on dew point, rather than air temperature, and reformulation of the model to handle mixed snow and rain events which frequently occur in this environment. Further research should also

focus on the development of techniques to simulate the complex processes of snow interception, melt and mass release from forest canopies. The development of methods to account for the spatial variability of deposition and ablation patterns will also improve the simulation of late-season snowcover dynamics, and more accurately simulate the timing of the rapid rise of T_g in the spring.

Although additional testing and validation of the SHAW model is warranted for cold-season processes in this environment, the model very effectively simulated the seasonal water and energy dynamics of the system, and could be used to examine the sensitivity of the system to projected climate changes. Simulations of future climates using General Circulation Models consistently predict temperatures to increase by approximately 2 °C by 2025, and generally predict precipitation to increase (Table 5.1). An increase in temperature is likely to shift the winter conditions (particularly

Table 5.1. Summary of the predicted changes in temperature and precipitation in the PNW, year 2025.

Model	Δ winter T_a	Δ summer T_a	Δ winter P_G (%)	Δ summer P_G (%)
CCCma	2.2	1.7	15	1
GFDL	1.8	1.9	-4	9
HC	2.0	1.5	20	22
MP1	1.9	2.2	3	-9

Table summarized from *Hamlet and Lettenmaier* [1999].

Model notation:

CCCma: Canadian Center for Climate Modeling and Analysis

GFDL: Geophysical Dynamics Laboratory

HC: Hadley Centre

MP1: Deutsches Klimarechenzentrum at the Max Planck Institute

for the 2000 test case) from a snow-dominated to a rain-dominated regime at the WRCCRF location. Future climate sensitivity analyses using the delta method, where an existing climate record is altered by a given mean amount, should be completed using the model parameterizations discussed in Chapter 4, to investigate the potential change in the timing and magnitude of hydrologic fluxes. Exploration of techniques to stochastically perturb climate records may help to identify the potential range of variability that might exist both in altered climate scenarios and in the absence of consistent climate change.

In addition to climate sensitivity, a complete sensitivity analysis of all system parameters should be completed. A sensitivity analysis such as this would help to identify how natural or anthropogenic changes to the canopy structure (e.g. management, pests, fire) might affect hydrologic fluxes. The analysis will also help to identify key parameters that the model is most sensitive to in forested environments, to suggest where site characterization efforts should focus for future investigations.

Ultimately forest hydrologists seek to understand the interactions of climate, vegetation, and human activities to develop an integrated understanding of hydrological processes at the basin, landscape and regional scales. This knowledge is particularly important in the PNW, where competing demands for forest products, water resources, species survival, and aesthetics, within a potentially changing climate require the effective management of natural resources. Integrated, interdisciplinary, intensive research sites such as the WRCCRF improve our knowledge of processes at the plot scale, which can be incorporated into increasingly sophisticated numerical models to enhance our understanding of processes at larger scales. Landcover in the

PNW is highly dynamic, with a wide variety of seral stages resulting from fires and timber harvest. Additional detailed process studies focusing on hydrological and ecological processes across a range of representative landcovers are needed to develop a quantitative understanding of how hydrological fluxes and ecological processes might change in response to altered climate and canopy characteristics.

BIBLIOGRAPHY

- Akima, H., A method of bivariate interpolation and smooth surface fitting for irregularly distributed data points, *ACM Transactions on Mathematical Software*, 4 (2), 148-159, 1978.
- Allen, R.G., Assessing integrity of weather data for reference evapotranspiration estimation, *J. Irr. Drain. Eng.*, 122 (2), 97-106, 1996.
- Asdak, C., P.G. Jarvis, P. van Gardingen, and A. Fraser, Rainfall interception loss in unlogged and logged forest areas of Central Kalimantan, Indonesia, *J. Hyd.*, 206, 237-244, 1998.
- Baldocchi, D., Flux footprints within and over forest canopies, *Boundary-Layer Meteorol.*, 85, 273-292, 1997.
- Baldocchi, D., E. Falge, L. Gu, R. Olson, D. Hollinger, S. Running, P. Anthoni, C. Bernhofer, K. Davis, R. Evans, J. Fuentes, A. Goldstein, G. Katul, B. Law, X. Lee, Y. Malhi, T. Meyers, W. Munger, W. Oechel, K.T. Paw U, K. Pilegaard, H.P. Schmid, R. Valentini, S. Verma, T. Vesala, K. Wilson, and S. Wofsy, FLUXNET: A new tool to study the temporal and spatial variability of ecosystem-scale carbon dioxide, water vapor and energy flux densities, *Bull. Amer. Met. Soc.*, in press.
- Bazzaz, F.A., *Plants in changing environments*, 320 pp., Cambridge University Press, Cambridge, U.K., 1996.
- Beschta, R.L., M.R. Pyles, A.E. Skaugset, and C.G. Surfleet, Peakflow responses to forest practices in the western cascades of Oregon, USA, *J. Hyd.*, 233, 102-120, 2000.
- Blanken, P.D., T.A. Black, P.C. Yang, H.H. Neumann, Z. Nesic, R. Staebler, G. den Hartog, M.D. Novak, and X. Lee, Energy balance and canopy conductance of a boreal aspen forest: Partitioning overstory and understory components, *J. Geophys. Res.*, 102 (D24), 28,915-28,927, 1997.
- Bond, B.J., and K.L. Kavanagh, Stomatal behavior of four woody species in relation to leaf-specific hydraulic conductance and threshold water potential, *Tree Physiol.*, 19, 503-510, 1999.
- Bowling, L.C., P. Storck, and D. Lettenmaier, Hydrologic effects of logging in western Washington, United States, *Wat. Resour. Res.*, 36 (11), 3223-3240, 2000.

- Brooks, S.M., and T. Spencer, Vegetation modification of rainfall characteristics: Implications for rainfall erosivity following logging in Sabah, Malaysia, *J. Trop. For. Sci.*, 7 (3), 435-446, 1995.
- Brown, T., Projecting U. S. fresh water withdrawals, *Wat. Resour. Res.*, 36 (3), 769-780, 2000.
- Calder, I.R., The measurement of water losses from a forested area using a 'natural' lysimeter, *J. Hyd.*, 30, 311-325, 1976.
- Calder, I.R., Do trees use more water than grass?, *Water Serv.*, 83, 11-14, 1979.
- Calder, I.R., Dependence of rainfall interception on drop size: 1 Development of the two-layer stochastic model, *J. Hyd.*, 185 (1 / 4), 363-378, 1996a.
- Calder, I.R., Rainfall interception and drop size--development and calibration of the two-layer stochastic interception model, *Tree Physiol.*, 16 (8), 727-732, 1996b.
- Calder, I.R., Water use by forests, limits and controls, *Tree Physiol.*, 18, 625-631, 1998.
- Calder, I.R., R.L. Hall, P.T.W. Rosier, H.G. Bastable, and K.T. Prasanna, Dependence of rainfall interception on drop size: 2. Experimental determination of the wetting functions and two-layer stochastic model parameters for five tropical tree species, *J. Hyd.*, 185 (1 / 4), 379-388, 1996.
- Calvet, J.-C., Investigating soil and atmospheric plant water stress using physiological and micrometeorological data, *Ag. For. Met.*, 103, 229-247, 2000.
- Campbell, G.S., *Soil physics with BASIC: Transport models for soil-plant systems*, 150 pp., Elsevier, New York, 1985.
- Chen, J., J.F. Franklin, and T.A. Spies, Contrasting microclimates among clearcut, edge, and interior of old-growth Douglas-fir forest, *Ag. For. Met.*, 63, 219-237, 1993.
- Chen, J., S.C. Saunders, T.R. Crow, R.J. Naiman, K.D. Brosofske, G.D. Mroz, B.L. Brookshire, and J.F. Franklin, Microclimate in forest ecosystem and landscape ecology, *BioSci.*, 49 (4), 288-297, 1999.
- Dawson, T.E., Hydraulic lift and water use by plants: implications for water balance, performance and plant-plant interactions, *Oecologia*, 95, 565-574, 1993.
- Dickinson, R.E., Modeling evapotranspiration for three-dimensional global climate models, in *Climate Processes and Climate Sensitivity*, *Geophys. Monogr.*, pp. 58-72, American Geophysical Union, 1984.

- Dingman, S.L., *Physical Hydrology*, 575 pp., Macmillan College Publishing Co., New York, 1994.
- Emerman, S.H., and T.E. Dawson, Hydraulic lift and its influence on the water content of the rhizosphere: an example from sugar maple, *Acer saccharum*, *Oecologia*, 108, 273-278, 1996.
- Flerchinger, G.N., J.M. Baker, and E.J.A. Spaans, A test of the radiative energy balance of the SHAW model for snowcover, *Hyd. Proc.*, 10, 1359-1367, 1996a.
- Flerchinger, G.N., K.R. Cooley, and Y. Deng, Impacts of spatially and temporally varying snowmelt on subsurface flow in a mountainous watershed: 1. Snowmelt simulation, *Hyd. Sci. J.*, 39 (5), 507-520, 1994.
- Flerchinger, G.N., C.L. Hanson, and J.R. Wight, Modeling evapotranspiration and surface energy budgets across a watershed, *Wat. Resour. Res.*, 32 (8), 2539-2548, 1996b.
- Flerchinger, G.N., W.P. Kustas, and M.A. Weltz, Simulating surface energy fluxes and radiometric surface temperatures for two arid vegetation communities using the SHAW model, *J. Appl. Met.*, 37, 449-460, 1998.
- Flerchinger, G.N., and F.B. Pierson, Modelling plant canopy effects on variability of soil temperature and water: Model calibration and validation, *J. Arid Env.*, 35, 641-653, 1997.
- Flerchinger, G.N., and K.E. Saxton, Simultaneous heat and water model of a freezing snow-residue-soil system I. Theory and development, *Trans. ASAE*, 32 (2), 565-571, 1989.
- Ford, E.D., and J.D. Deans, The effects of canopy structure on stemflow, throughfall and interception loss in a young Sitka Spruce plantation, *J. Appl. Ecol.*, 15, 905-917, 1978.
- Franklin, J.F., and T.A. Spies, Composition, function, and structure of old-growth Douglas-fir forests, in *Wildlife and vegetation of unmanaged Douglas-fir forests*, edited by L.F. Ruggiero, K.B. Aubry, A.B. Carey, and M.H. Huff, pp. 71-80, US Dept. of Ag. For. Serv., Portland, Oregon, 1991.
- Franklin, J.F., and R.H. Waring, Distinctive features of northwestern coniferous forest: Development, structure, and function, in *Ecosystem analysis*, pp. 59-86, Corvallis, Oregon, 1980.
- Garratt, J.R., and R.J. Francey, Bulk characteristics of heat transfer in the baroclinic atmospheric boundary layer, *Boundary-Layer Meteorol.*, 15, 399-421, 1978.

- Gash, J.H.C., An analytical model of rainfall interception by forests, *Quart. J. Roy. Met. Soc.*, 105, 43-55, 1979.
- Gash, J.H.C., C.R. Lloyd, and G. Lachaud, Estimating sparse forest rainfall interception with an analytical model, *J. Hyd.*, 170 (1 / 4), 79-86, 1995.
- Gash, J.H.C., and A.J. Morton, An application of the Rutter model to the estimation of the interception loss from Thetford forest, *J. Hyd.*, 38, 49-58, 1978.
- Gash, J.H.C., and J.B. Stewart, The evaporation from Thetford forest during 1975, *J. Hyd.*, 35, 385-396, 1977.
- Gash, J.H.C., I.R. Wright, and C.R. Lloyd, Comparative estimates of interception loss from three coniferous forests in Great Britain, *J. Hyd.*, 48, 89-105, 1980.
- Goulden, M.L., J.W. Munger, S.-M. Fan, B.C. Daube, and S.C. Wofsy, CO₂ exchange by a deciduous forest: response in interannual climate variability, *Science*, 271, 1576-1578, 1996.
- Gray, A.N., and T.A. Spies, Water content measurement in forest soils and decayed wood using time domain reflectometry, *Can. J. For. Res.*, 25, 376-385, 1995.
- Hall, R.L., I.R. Calder, E.R.N. Gunawardena, and P.T.W. Rosier, Dependence of rainfall interception on drop size: 3. Implementation and comparative performance of the stochastic model using data from a tropical site in Sri Lanka, *J. Hyd.*, 185 (1 / 4), 389-407, 1996.
- Hamlet, A.F., and D.P. Lettenmaier, Effects of climate change on hydrology and water resources in the Columbia River Basin, *J. Amer. Wat. Resour. Assn.*, 35 (6), 1597-1623, 1999.
- Hardy, J.P., R.E. Davis, R. Jordan, X. Li, C. Woodcock, W. Ni, and J.C. McKenzie, Snow ablation modeling at the stand scale in a boreal jack pine forest, *J. Geophys. Res.*, 102 (D24), 29,397-29,405, 1997.
- Harmon, M.E., K. Bible, S. Remillard, J. Sexton, B. Fasth, A. Priestley, J. Chen, and J. Franklin, Permanent plots surrounding the Wind River Canopy Crane, 1998.
- Harmon, M.E., K. Bible, M.J. Ryan, D. Shaw, H. Chen, J. Klopatek, and X. Li, Production, respiration, and overall carbon balance in an old-growth *Pseudotsuga/Tsuga* forest ecosystem, *Ecosystems*, in review.
- Harmon, M.E., S. Remillard, C.T. Dryness, and J. Norgren, Soils of the Thornton T. Munger RNA, US Forest Service, 1995.
- Harmon, M.E., and J. Sexton, Water balance of conifer logs in early stages of decomposition, *Plant and Soil*, 172, 141-152, 1995.

- Harr, R.D., Fog drip in the Bull Run Municipal Watershed, Oregon, *Water Resources Bulletin*, 18 (5), 785-789, 1982.
- Harr, R.D., W.C. Harper, J.T. Krygier, and F.S. Hsieh, Changes in storm hydrographs after road-building and clear-cutting in the Oregon Coast Range, *Wat. Resour. Res.*, 11 (3), 436-444, 1975.
- Harr, R.D., A. Levno, and R. Mersereau, Streamflow changes after logging 130-year-old Douglas fir in two small watersheds, *Wat. Resour. Res.*, 18, 637-644, 1982.
- Harr, R.D., and F.M. McCorison, Initial effects of clearcut logging on size and timing of peak flows in a small watershed in western Oregon, *Wat. Resour. Res.*, 15 (1), 90-94, 1979.
- Hicks, B.J., R.L. Beschta, and R.D. Harr, Long-term changes in streamflow following logging in western Oregon and associated fisheries implications, *Water Resources Bulletin*, 27, 217-226, 1991.
- Hillel, D., *Environmental Soil Physics*, 771 pp., Academic Press, San Diego, 1998.
- Hook, W.R., N.J. Livingston, Z.J. Sun, and P.B. Hook, Remote diode shorting improves measurement of soil water by time domain reflectometry, *Soil Sci. Soc. Am. J.*, 56 (5), 1384-1391, 1992.
- Hörmann, G., A. Branding, T. Clemen, M. Herbst, A. Hinrichs, and F. Thamm, Calculation and simulation of wind controlled canopy interception of a beech forest in Northern Germany, *Ag. For. Met.*, 79 (3), 131-148, 1996.
- Huber, L., and T.J. Gillespie, Modeling leaf wetness in relation to plant disease epidemiology, *Ann. Rev. Phytopathol.*, 30, 553-577, 1992.
- Hutchings, N.J., R. Milne, and J.M. Crowther, Canopy storage capacity and its vertical distribution in a Sitka spruce canopy, *J. Hyd.*, 104, 161-171, 1988.
- Hutjes, R.W.A., A. Wierda, and A.W.L. Veen, Rainfall interception in the Tai Forest, Ivory Coast: application of two simulation models to a humid tropical system, *J. Hyd.*, 114 (3 / 4), 259-275, 1990.
- Ishii, H., J.H. Reynolds, E.D. Ford, and D.C. Shaw, Height growth and vertical development of an old-growth *Pseudotsuga-Tsuga* forest in southwestern Washington State, U.S.A., *Can. J. For. Res.*, 30, 17-24, 2000.
- Jarvis, P.G., The interpretation of the variations in leaf water potential and stomatal conductance found in canopies in the field, *Phil. Trans. R. Soc. Lond. B.*, 273, 593-610, 1976.

- Jarvis, P.G., G.B. James, and J.J. Landsberg, Coniferous forest, in *Vegetation and the Atmosphere, Volume 2. Case Studies*, edited by J.L. Monteith, pp. 171-240, Academic Press, New York, 1976.
- Jetten, V.G., Interception of tropical rain forest: Performance of a canopy water balance model, *Hyd. Proc.*, 10, 671-685, 1996.
- Johnson, R.C., The interception, throughfall and stemflow in a forest in highland Scotland and the comparison with other upland forests in the U.K., *J. Hyd.*, 118, 281-287, 1990.
- Jones, H.G., *Plants and microclimate*, 428 pp., Cambridge University Press, New York, 1992.
- Jones, J.A., Hydrologic processes and peak discharge response to forest removal, regrowth, and roads in 10 small experimental basins, western Cascades, Oregon, *Wat. Resour. Res.*, 36 (9), 2621-2642, 2000.
- Jones, J.A., and G.E. Grant, Peak flow responses to clear-cutting and roads in small and large basins, western Cascades, Oregon, *Wat. Resour. Res.*, 32 (4), 959-974, 1996.
- Jones, J.A., and G.G. Grant, Comment on "Peak flow responses to clear-cutting and roads in small and large basins, western Cascades, Oregon: A second opinion" by R. B. Thomas and W. F. Megahan, *Wat. Resour. Res.*, 37 (1), 175-178, 2001.
- Kaduk, J., C.B. Field, J.A. Berry, T.E. Link, N. McDowell, M.E. Harmon, K. Bible, M. Falk, and T.S. King, Integrated land surface and carbon cycle modeling at the Wind River Canopy Crane Site, *J. Geophys. Res.*, in review.
- Kelliher, F.M., D. Whitehead, and D.S. Pollock, Rainfall interception by trees and slash in a young *Pinus radiata* D. Don stand, *J. Hyd.*, 131 (1 / 4), 187-204, 1992.
- Keppeler, E.T., and R.R. Ziemer, Logging effects on streamflow: Water yield and summer low flows at Caspar Creek in northwestern California, *Wat. Resour. Res.*, 26, 1669-1679, 1990.
- Klaassen, W., F. Bosveld, and E. de Water, Water storage and evaporation as constituents of rainfall interception, *J. Hyd.*, 212-213, 36-50, 1998.
- Klaassen, W., H.J.M. Lankreijer, and A.W.L. Veen, Rainfall interception near a forest edge, *J. Hyd.*, 185 (1 / 4), 349-361, 1996.

- Lankreijer, H.J.M., M.J. Hendriks, and W. Klaassen, A comparison of models simulating rainfall interception of forests, *Ag. For. Met.*, 64 (3 / 4), 187-199, 1993.
- Law, B.E., S. Van Tuyl, A. Cescatti, and D.D. Baldocchi, Estimation of leaf area index in open-canopy ponderosa pine forests at different successional stages and management regimes in Oregon, *Ag. For. Met.*, 108, 1-14, 2001.
- Lee, X., On micrometeorological observations of surface-air exchange over tall vegetation, *Ag. For. Met.*, 91, 39-49, 1998.
- Lewis, J., S.R. Mori, E.T. Keppler, and R.R. Ziemer, Impacts of logging on storm peak flows, flow volumes and suspended sediment loads in Caspar, Creek, California, pp. 76, 2000.
- Leyton, L., E.R.C. Reynolds, and F.B. Thompson, Rainfall interception in forest and moorland, in *International Symposium on Forest Hydrology*, edited by W.E. Sopper, and H.W. Lull, pp. 163-168, Pergamon Press, New York, 1967.
- Link, T.E., and D. Marks, Point simulation of seasonal snow cover dynamics beneath boreal forest canopies, *J. Geophys. Res.*, 104 (D22), 27,841-27,857, 1999.
- Link, T.E., D. Marks, and M.H. Unsworth, Climate and canopy conditions at the Wind River Canopy Crane Research Facility, 1998-2000, *J. Hydromet.*, in review-a.
- Link, T.E., D. Marks, and M.H. Unsworth, The interception dynamics of a seasonal temperate rainforest, *J. Hydromet.*, in review-b.
- Little, E.L.J., Atlas of United States trees, volume 1, conifers and important hardwoods, pp. 200, U.S. Department of Agriculture, 1971.
- Llorens, P., and F. Gallart, A simplified method for forest water storage capacity measurement, *J. Hyd.*, 240, 131-144, 2000.
- Lloyd, C.R., J.H.C. Gash, W.J. Shuttleworth, and A.D.O. Marques, The measurement and modelling of rainfall interception by Amazon rain forest., *Ag. For. Met.*, 43, 277-294, 1988.
- Lloyd, C.R., and F.A.d.O. Marques, Spatial variability of throughfall and stemflow measurements in Amazonian rainforest, *Ag. For. Met.*, 42, 63-73, 1988.
- Loustau, D., P. Berbigier, and A. Granier, Interception loss, throughfall and stemflow in a maritime pine stand. II. An application of Gash's analytical model of interception, *J. Hyd.*, 138, 469-485, 1992a.

- Loustau, D., P. Berbigier, A. Granier, and F.E.H. Moussa, Interception loss, throughfall and stemflow in a maritime pine stand. I. Variability of throughfall and stemflow beneath the pine canopy, *J. Hyd.*, 138 (3 / 4), 449-467, 1992b.
- Mahfouf, J.F., and B. Jacquemin, A study of rainfall interception using a land surface parameterization for mesoscale meteorological models, *J. Appl. Met.*, 28 (12), 1282-1302, 1989.
- Maidment, D.R., *Handbook of Hydrology*, McGraw Hill, Inc., New York, New York, 1993.
- Marks, D., J. Domingo, D. Susong, T. Link, and D. Garen, A spatially distributed energy balance snowmelt model for application in mountain basins, *Hyd. Proc.*, 13, 1935-1959, 1999.
- Marks, D., J. Kimball, D. Tingey, and T.E. Link, The sensitivity of snowmelt processes to climate conditions and forest cover during rain-on-snow: A case study of the 1996 Pacific Northwest flood, *Hyd. Proc.*, 12, 1569-1587, 1998.
- Massman, W.J., The derivation and validation of a new model for the interception of rainfall by forests, *Ag. Met.*, 28, 261-286, 1983.
- McCabe, G.J., and Wolock, David M., General-circulation-model simulations of future snowpack in the western United States, *J. Amer. Wat. Resour. Assn.*, 35 (6), 1473-1484, 1999.
- McCune, B., K.A. Amsberry, F.J. Camacho, S. Clery, C. Cole, C. Emerson, G. Felder, P. French, D. Greene, R. Harris, M. Hutten, B. Larson, M. Lesko, S. Majors, T. Markwell, G.G. Parker, K. Pendergrass, E.B. Peterson, E.T. Peterson, J. Platt, J. Proctor, T. Rambo, A. Rosso, D. Shaw, R. Turner, and M. Widmer, Vertical profile of epiphytes in a Pacific Northwest old-growth forest, *NW Sci.*, 71 (2), 145-152, 1997.
- McMinn, R.G., Water relations and forest distribution in the Douglas fir region of Vancouver Island, Div. Forest Biol., Dept. Agr. Can., 1960.
- Mencuccini, M., and J. Grace, Hydraulic conductance, light interception and needle nutrient concentration in Scots pine stands and their relations with net primary productivity, *Tree Physiol.*, 16, 459-468, 1996.
- Miles, E.L., A.K. Snover, A.F. Hamlet, B. Callahan, and D. Fluharty, Pacific Northwest Regional Assessment: The impacts of climate variability and climate change on the water resources of the Columbia River Basin, *J. Amer. Wat. Resour. Assn.*, 36 (2), 399-420, 2000.

- Miller, D.J., and J. Sias, Deciphering large landslides: linking hydrological, groundwater and slope stability models through GIS, *Hyd. Proc.*, 12, 923-941, 1998.
- Monteith, J.L., and M.H. Unsworth, *Principles of Environmental Physics*, 291 pp., Edward Arnold, New York, 1990.
- Mosley, M.P., The effect of a New Zealand beech forest canopy on the kinetic energy of water drops and on surface erosion, *Earth Surf. Proc. Land.*, 7, 103-107, 1982.
- National Research Council, *Environmental Issues in Pacific Northwest Forest Management*, 259 pp., National Academy Press, Washington, D.C., 2000.
- NCDC, National Climatic Data Center, 2001.
- Neal, C., A.J. Robson, C.L. Bhardwaj, T. Conway, H.A. Jeffery, M. Neal, G.P. Ryland, C.J. Smith, and J. Walls, Relationships between precipitation, stemflow and throughfall for a lowland beech plantation, Black Wood, Hampshire, southern England: findings on interception at a forest edge and the effects of storm damage, *J. Hyd.*, 146 (1 / 4), 221-233, 1993.
- Nobel, P.S., *Physicochemical and environmental plant physiology*, 635 pp., Academic Press, San Diego, 1991.
- Ogink-Hendriks, M.J., Modelling surface conductance and transpiration of an oak forest in The Netherlands, *Ag. For. Met.*, 74 (1-2), 99-118, 1995.
- Parker, G.G., M.E. Harmon, M.A. Lefsky, J. Chen, R. Van Pelt, S.B. Weiss, S.C. Thomas, W.E. Winner, D.C. Shaw, and J.F. Franklin, Three dimensional structure of an old-growth *Pseudotsuga-Tsuga* forest and its implications for radiation balance, microclimate, and atmospheric exchange of carbon dioxide, *Ecosystems*, in review.
- Paw U, K.T., Y. Brunet, S. Collineau, R.H. Shaw, T. Maitani, J. Qiu, and L. Hipps, On coherent structures in turbulence above and within agricultural plant canopies, *Ag. For. Met.*, 61, 55-68, 1992.
- Paw U, K.T., T.H. Suchanek, S.L. Ustin, J. Chen, W. Winner, S. Thomas, T. Hsiao, R. Shaw, T. King, M. Falk, D. Pyles, and D. Matista, Carbon dioxide exchange between an old growth forest and the atmosphere, *Ecosystems*, to appear, in review.
- Pearce, A.J., and L.K. Rowe, Rainfall interception in a multi-storied, evergreen mixed forest: estimates using Gash's analytical model, *J. Hyd.*, 49, 341-353, 1981.

- Putuhena, W.M., and I. Cordery, Estimation of interception capacity of the forest floor, *J. Hyd.*, 180, 283-299, 1996.
- Roberts, J., Forest transpiration: A conservative hydrological process?, *J. Hyd.*, 66, 133-141, 1983.
- Robins, P.C., A method of measuring the aerodynamic resistance to the transport of water vapour from forest canopies, *J. Appl. Ecol.*, 11, 315-325, 1974.
- Rothacher, J., Net precipitation under a Douglas-fir forest, *For. Sci.*, 9 (4), 423-429, 1963.
- Rowe, L.K., Rainfall interception by an evergreen beech forest, Nelson, New Zealand, *J. Hyd.*, 66, 143-158, 1983.
- Rupp, D.E., R.F. Keim, M. Ossiander, M. Brugnach, and J.S. Selker, A scale-dependent random cascade model of temporal rainfall with periodicity, *Wat. Resour. Res.*, in review.
- Rutter, A.J., K.A. Kershaw, P.C. Robins, and A.J. Morton, A predictive model of rainfall interception in forests, 1. Derivation of the model from observations in a plantation of Corsican pine, *Ag. Met.*, 9, 367-384, 1971.
- Rutter, A.J., and A.J. Morton, A predictive model of rainfall interception in forests III. Sensitivity of the model to stand parameters and meteorological variables, *J. Appl. Ecol.*, 14, 567-588, 1977.
- Rutter, A.J., A.J. Morton, and P.C. Robins, A predictive model of rainfall interception in forests II. Generalization of the model and comparison with observations in some coniferous and hardwood stands, *J. Appl. Ecol.*, 12 (1), 367-380, 1975.
- Scatena, F.N., Watershed scaled rainfall interception on two forested watersheds in the Luquillo Mountains of Puerto Rico, *J. Hyd.*, 113 (1 / 4), 89-102, 1990.
- Schellekens, J., F.C. Scatena, L.A. Bruijnzeel, and A.J. Wickel, Modelling rainfall interception in a lowland tropical rain forest in northeastern Puerto Rico, *J. Hyd.*, 225, 168-184, 1999.
- Sellers, P.J., F. Hall, H. Margolis, B. Kelly, D. Baldocchi, G.d. Hartog, J. Cihlar, M.G. Ryan, B. Goodison, P. Crill, K.J. Ranson, D. Lettenmaier, and D.E. Wickland, The Boreal Ecosystem-Atmosphere Study (BOREAS): An overview and early results from the 1994 field year, *Bull. Amer. Met. Soc.*, 76, 1549-1577, 1995.
- Sellers, P.J., F.G. Hall, G. Asrar, D.E. Strelbel, and R.E. Murphy, An overview of the First International Satellite Land Surface Climatology Project (ISLSCP) Field Experiment (FIFE), *J. Geophys. Res.*, 97 (D17), 18,345-18,371, 1992.

- Sellers, P.J., D.A. Randall, G.J. Collatz, J.A. Berry, C.B. Field, D.A. Dazlich, C. Zhang, G.D. Collelo, and L. Bounoua, A revised land surface parameterization (SiB2) for atmospheric GCMs. Part I: Model Formulation, *J. Clim.*, 1996.
- Shaw, D.C., J.F. Franklin, J. Klopatek, E. Freeman, K. Bible, T. Newton, S. Greene, and J. Wade-Murphy, Ecological setting of the Wind River old-growth forest, *Ecosystems*, to appear, in review.
- Stewart, J.B., Modelling surface conductance of pine forest, *Ag. For. Met.*, 43, 19-35, 1988.
- Tanner, B.D., Automated weather stations, *Remote Sens. Rev.*, 5 (1), 73-98, 1990.
- Thomas, R.B., and W.F. Megahan, Peak flow responses to clear-cutting and roads in small and large basins, western Cascades, Oregon: A second opinion, *Wat. Resour. Res.*, 34 (12), 3393-3403, 1998.
- Thomas, R.B., and W.F. Megahan, Reply, *Wat. Resour. Res.*, 37 (1), 181-183, 2001.
- Thomas, S.C., and W.E. Winner, Leaf area index of an old-growth Douglas-fir forest estimated from direct structural measurements in the canopy, *Can. J. For. Res.*, 30, 1922-1930, 2000.
- Topp, G.C., J.L. Davis, and A.P. Annan, Electromagnetic determination of soil water content: Measurements in coaxial transmission lines, *Wat. Resour. Res.*, 16 (3), 574-582, 1980.
- U.S. Army Corps of Engineers, Snow hydrology: Summary report of the snow investigations, North Pacific Division, Portland, OR, 1956.
- Unsworth, M., H., N. Phillips, T. Link, B. Bond, M. Falk, M. Harmon, T. Hinckley, D. Marks, and K.T. Paw U, Components and controls of water flux in an old growth Douglas fir/western hemlock ecosystem, *Ecosystems*, in review.
- Viville, D., P. Biron, A. Granier, E. Dambrine, and A. Probst, Interception in a mountainous declining spruce stand in the Strengbach catchment (Vosges, France), *J. Hyd.*, 144, 273-282, 1993.
- Waring, R.H., and S.W. Running, *Forest Ecosystems: Analysis at Multiple Scales*, 370 pp., Academic Press, New York, 1998.
- Weaver, H.L., A mechanistic model of evapotranspiration from saltcedar (*Tamarix chiniensis*), Doctoral thesis, Washington State University, Pullman, Washington, 1984.
- Wigmosta, M.S., L.W. Vail, and D.P. Lettenmaier, A distributed hydrology-vegetation model for complex terrain, *Wat. Resour. Res.*, 30 (6), 1665-1679, 1994.

- Williams, M., B.J. Bond, and M.G. Ryan, Evaluation different soil and plant hydraulic constraints on tree function using a model and sap flow data from ponderosa pine, *Plant Cell Env.*, 24, 679-690, 2001.
- Williams, M., Y. Malhi, A.D. Nobre, E.B. Rastetter, J. Grace, and M.G.P. Pereira, Seasonal variation in net carbon exchange and evapotranspiration in a Brazilian rain forest: a modelling analysis, *Plant Cell Env.*, 21, 953-968, 1998.
- Wilm, H.G., Determining net rainfall under a conifer forest, *J. Ag. Res.*, 67 (12), 501-512, 1943.
- Wilson, K.B., P.J. Hanson, P.J. Mulholland, D.D. Baldocchi, and S.D. Wullschleger, A comparison of methods for determining forest evapotranspiration and its components: sap-flow, soil water budget, eddy covariance and catchment water balance, *Ag. For. Met.*, 106, 153-168, 2001.
- WMO, Guide to meteorological instruments and methods of observation, World Meteorological Organization, Geneva, Switzerland, 1996.
- WRCC, Western Regional Climate Center, 2001.
- Wright, K., K.H. Sendek, R.H. Rice, and R.B. Thomas, Logging effects on streamflow: Storm runoff at Caspar Creek in northwestern California, *Wat. Resour. Res.*, 26, 1657-1667, 1990.
- Zeng, N., J.W. Shuttleworth, and J.H.C. Gash, Influence of temporal variability of rainfall on interception loss. Part I. Point analysis, *J. Hyd.*, 228, 228-241, 2000.
- Ziemer, R.R., Storm flow response to road building and partial cutting in small streams of northern California, *Wat. Resour. Res.*, 17, 907-917, 1981.
- Zinke, P.J., Forest interception studies in the United States, in *International Symposium on Forest Hydrology*, edited by W.E. Sopper, and H.W. Lull, pp. 137-161, Pergamon Press, New York, 1967.